2023

Ecosystem Transitions And State Changes Rapidly Alter The Coastal Carbon Landscape: Evidence From The Chesapeake Bay Region

Alexander Jason Smith
College of William and Mary - Virginia Institute of Marine Science, andersmith19@gmail.com

Ecosystem transitions and state changes rapidly alter the coastal carbon landscape: evidence from the Chesapeake Bay region

A Dissertation

Presented to

The Faculty of the School of Marine Science

William & Mary

In Partial Fulfillment

of the Requirements for the Degree of

Doctor of Philosophy

by

Alexander Jason Smith

May 2023

APPROVAL PAGE

This dissertation is submitted in partial fulfillment of

the requirements for the degree of

Doctor of Philosophy

Alexander Jason Smith

Approved by the Committee, April 2023

Matthew L. Kirwan, Ph.D.
Committee Chair / Advisor

Elizabeth A. Canuel, Ph.D.

Christopher J. Hein, Ph.D.

David S. Johnson, Ph.D.

J. Patrick Megonigal, Ph.D.
Smithsonian Environmental Research Center
Edgewater, MD, U.S.A.

This Ph.D. is dedicated to my brother, Bryan Smith, who taught me how to be unfailing curious and courageous in the face of the unknown. I wish you could see how every part of my life is a result of growing up with you. I miss you every day.

Table of Contents

Acknowledgements

To my committee, Drs. Liz Canuel, Chris Hein, David Johnson, and Pat Megonigal: thank you for your guidance and for pushing me beyond my marsh view to think of bigger and broader contexts. You all have made me a better, more creative researcher and scientist and thank you for asking easy questions during my qualifying exams.

To my advisor, Dr. Matt Kirwan: thank you so much for believing in me. I can't count the number of ways in which you have influenced and improved my life and skills. I think back to when we met in the lobby of a NC State conference hall almost 6 years ago and I'm blown away by how different I am now thanks to you. Not only am I a better scientist, writer, and researcher (hopefully), but your encouragement has fundamentally changed my future. You are an excellent mentor and advisor and I look forward to being your colleague and friend.

To my lab members: thank you for your blood, sweat, and (I don't think there were many) tears in the field, guidance during random office drop-ins, necessary distractions provided throughout the work day, and amazing insight into problems I couldn't tackle alone. You all are not just wonderful collaborators, but fantastic scientists and even better friends.

To my friends: thank you for not talking about science with me. Your capacity for friendship, support, and love and all you have graciously given has been critical for my mental and physical well-being. I look forward to more late nights, board games, beach days, vacations, and phone calls with all of you. Thank you especially to my friends from VIMS who have studied, sweat, and panicked with me along the way.

To my family, especially my parents Bob and Peggy Smith: you have provided and cared for me my entire life, through my most fragile moments when I didn't even know I needed your love. You have taught me how to be a kind person, hard worker, and someone with somewhat common sense. I don't tell you enough how much your quiet, constant support means to me and how important it is in my life.

To my partner, Devin Rogers: thank you for loving and supporting me throughout this journey. Having you believe in me and my dreams from the start constantly uplifts me. Knowing that I have you (and your cooking) to rely on has fostered me in uncountable ways. We're building a life and future together full of love, happiness, and laugher. Thank you and I love you.

Abstract

The coastal landscape is a naturally shifting mosaic of distinct ecosystems that are rapidly migrating with climate change. While directional changes in climate, such as warming and sea level rise, are fundamentally reorganizing the coastal landscape, ecosystem function, especially carbon storage, is affected to an unknown degree. This dissertation presents four chapters that examine the role of ecosystem transitions in coastal carbon dynamics across a range of spatial scales – within individual ecosystems, between two ecosystems, and at the landscape between an array of ecosystems. Ghost forests, or the marsh-forest ecotone, serves as an ideal example of a migratory ecotone. As sea levels rise, terrestrial forests die-off from salt water intrusion and are replaced by salt-tolerant marsh species. While this transition is widely seen and studied, we present the first field study that quantifies carbon loss during this transition (**Chapter 1**). Significantly, we find that the loss of carbon during marsh migration can be replaced by the accumulating marsh soils, but the timescale for this replacement is at the scale of centuries. Warming, a co-occurring climate stressor, is expected to affect carbon storage to an unknown degree as it affects both antagonistic properties to soil carbon storage: production and decomposition. In a whole-ecosystem soil warming experiment, we find that moderate amounts of warming consistently maximized root growth, marsh elevation gain, and belowground carbon accumulation (**Chapter 2**). However, our work indicates nonpermanent benefits as global temperatures continue to rise and elevated temperatures exacerbate marsh elevation and carbon loss. At the landscape scale, we see that while climate change can drastically reduce or increase the extent of coastal habitats, compensatory mechanisms largely maintain individual ecosystem extents (**Chapter 3**). However, coastal squeeze in some environments still reduce extents of ecosystem critical to regional carbon storage. Blue carbon habitats that comprise the coastal zone are able to compensate this loss in less time than it takes to accrue that loss. These findings reveal unique functional compensatory mechanisms at the landscape scale that quickly absorb carbon losses and could facilitate increased regional carbon storage in the face of accelerating climate change. Finally, we concentrate on ecosystem vulnerability of salt marshes, an ecosystem with a critical role in global and local carbon dynamics. By leveraging decadal SET data, we are able to identify early warning signals of marsh collapse in the changing microtopography of the marsh surface (**Chapter 4**). Increasing microtopographic heterogeneity in degrading salt marshes mirrored trends in a diverse array of systems with alternative stable states – indicating that early warning signals of marsh drowning and ecosystem transition are observable at small-spatial scales prior to runaway ecosystem degradation. Congruence between traditional and novel metrics of marsh vulnerability indicate that microtopographic metrics can be easily applied to existing SET records to identify hidden vulnerability before widespread marsh degradation

Ecosystem transitions and state changes rapidly alter the coastal carbon landscape: evidence from the Chesapeake Bay region

The following introduction serves to describe dynamics of ecotone migration, a concept that underlies all chapters of this dissertation, and is adapted from a perspective article written by Alexander J. Smith and Emily M. Goetz and published in ***Landscape Ecology****. Full citation available in the References section.*

Introduction

Ecotones, confined transitional boundaries between two distinct ecosystems whose overlap results in a unique ecological community, are relatively dynamic and unstable zones compared to their neighboring ecosystems and are frequently characterized by a change in abiotic stressors (Longhurst, 2006; Wasson, Woolfolk and Fresquez, 2013; Wang *et al.*, 2019). Relatively high stress at the ecotone reduces the competitive dominance of species from the less-stressed adjacent ecosystem and forces the establishment of a community comprised of species from both adjacent ecosystems as well as unique species that are competitively dominant under increased stress (Lloyd *et al.*, 2000) or facilitated by novel species interaction (Maher, Germino and Hasselquist, 2005). The littoral zone of a lake serves as a model ecotone (van der Maarel, 1990). The boundary between dry and submerged benthos at the littoral zone changes seasonally: high water levels in winter months inundate the area, and low water levels in summer months expose the area to both oxygen and heat. These seasonal changes create drastically different environmental conditions in the intertidal than in either of the adjacent ecosystems, leading to the establishment of a unique biological community and a distinct ecosystem. Although ecotones exist at a variety of spatial scales, from biomes to soil-plant interactions (Gosz, 1993), here we focus on ecotones at the landscape scale (~1-100m) because of the climatic factors that drive landscape dynamics.

Like its biological community, an ecotone's structure and function are derived from the adjacent systems but remain unique from either ecosystem. The unique combination of habitat features may create a larger diversity of niches and, consequently, higher species richness than in the adjacent ecosystems (Horváth, March and Wolf, 2001; Ribalet *et al.*, 2010); however, this is not universal (Delcourt and Delcourt, 1992; Risser, 1995; Senft, 2009) and may be limited to large ecotones (Smith *et al.*, 1997). Similarly, ecosystem functions may be enhanced within some ecotones, as seen with the increased sedimentation and organic matter preservation in wetlands (Kolasa and Zalewski, 1995). Conversely,

ecotones may limit the movement of species, materials, or drivers (e.g., wind) from crossing to an adjacent ecosystem (Naiman *et al.*, 1988; Johnston, 1991; Forman and Moore, 1992). The movement, or lack thereof, of species or material across the ecotone may contribute to feedback loops that either shift or maintain the position of the ecotone and adjacent ecosystems (Kolasa and Zalewski, 1995), leading to dynamism and variation in ecosystem function across the ecotone transition.

Ecotones can be classified based on their long-term stability and direction of movement as stationary, shifting, or directional (Peters *et al.*, 2006). Stationary ecotones occur where abiotic controls over an ecotone's location are inherent, reinforced by strong biotic feedbacks, and, consequently, stable over time, as seen in ecosystem transitions at abrupt elevation or geomorphological gradients (Körner, 1998; Peters *et al.*, 2006; Figure 1a). Shifting ecotones are more dynamic and, while they maintain a relatively constant location over time, they exist in an unstable equilibrium and periodically move laterally into adjacent ecosystems (Figure 1b). Shifting ecotones occur where varying environmental conditions allow for dominance by either ecosystem to shift at the boundary. For example, at the grassland-shrubland ecotone, increased drought or winter precipitation may cause the ecotone boundary to shift farther into grassland (i.e., grassland converts to shrubland), whereas, during a rainy period, movement of the ecotone may reverse direction and migrate into adjacent shrubland (Peters, 2002; Shiponeni *et al.*, 2011; Moreno-de las Heras, 2016). Short-term assessments of ecotone position may indicate that the ecotone is moving unidirectionally; however, the net movement of a shifting ecotone's position over many years is minimal because of the periodic reversals in movement and overall bidirectionality of ecotone movement. Conversely, directional ecotones move unidirectionally over time (Figure 1c). Typically, positive feedbacks on the leading end of the directional ecotone stabilize the encroaching ecotone and spur advancement into the adjacent ecosystem (in Figure 1c, ecosystem II). The trailing edge of the ecotone is then converted into the adjacent encroaching ecosystem (in Figure 1c, ecosystem I), leading to net movement of the ecotone over time. This is seen at the boundary between salt marsh and forest, where sea-level rise causes forest dieback and marsh encroachment, and the marsh-

upland ecotone moves inland (Smith, 2013; Wasson, Woolfolk and Fresquez, 2013; Schieder, Walters and Kirwan, 2018).

While the effects of directional climate change on individual species and populations have been studied extensively (Goldblum and Rigg, 2005; Caputi *et al.*, 2013; Martínez-Soto and Johnson, 2020), the effects of climate change on the directional movement of ecotones at the ecosystem scale is a developing field of research (Deaton, Hein and Kirwan, 2017; Theuerkauf and Rodriguez, 2017; Smith and Kirwan, 2021), despite the longstanding theory that ecotones are reactive to and indicative of climate change (Noble, 1993; Wasson, Woolfolk and Fresquez, 2013; Saintilan *et al.*, 2014). Previous work has demonstrated that ecotones may be especially sensitive to changing conditions because species therein are nearing abiotic limits (Goldblum and Rigg, 2005; Wasson, Woolfolk and Fresquez, 2013) and that ecotones are useful study systems because they can be readily tracked over time (Kupfer and Cairns, 1996). Thus, observing changes in ecotone dynamics may provide insight into climate change impacts on both ecotones and their adjacent ecosystems. Past ecotone studies have focused on the movement patterns of a single ecotone type, especially the acceleration of directional ecotone movement (Kupfer and Cairns, 1996; Schieder and Kirwan, 2019) and the latitudinal migration of biomes (Gonzalez *et al.*, 2010; Coldren *et al.*, 2018). We uniquely propose that climate-driven changes in ecotone movement may extend beyond existing directional ecotones to include changes in the movement patterns and classification of previously shifting ecotones. In this review, we present three landscape ecotone case studies in marine, terrestrial, and the interfacing environments to demonstrate how climate change is impacting historically shifting and directional ecotones. We further discuss how changes in ecotone dynamics may affect ecotone function and call for future work documenting changes in ecotone dynamics.

LANDSCAPE ECOTONE CASE STUDIES

Shifting Ecotone: deep chlorophyll layer (DCL) ecotone

Formation of the deep chlorophyll layer (DCL), the subsurface depth layer in both freshwater and marine aquatic systems that contains the maximum concentration of chlorophyll, is dependent on light attenuation depth and the nutricline (Fee, 1976; Abbott *et al.*, 1984). While light is abundant in surface waters, low nutrient availability limits the amount of primary production. Deeper in the water column, attenuation reduces the availability of light, but nutrient availability increases. These inverse environmental gradients establish the DCL at the overlapping zone between lit, nutrient-depleted surface waters and dark, nutrient-rich deep waters (Cullen, 1982). While community composition of the DCL varies geographically, the DCL tends to have more flagellated planktons, pennate diatoms, and cryptophytes compared to the centric diatom-dominated surface communities (Kimor, Berman and Schneller, 1987; Barbiero and Tuchman, 2004). The DCL supports a unique community of species adapted to low-light conditions through development of accessory pigments or vertical migration to surface waters (Pollehne, Klein and Zeitzschel, 1993; Cullen, 2015). This unique assemblage of species establishes the DCL as an ecotone.

The concentration of chlorophyll at depth has multiple important functions for the aquatic ecosystem. Because of the relatively high concentration of planktonic organisms, there is an increased presence of both mixotrophic and heterotrophic protozoans at the DCL (Bird and Kalff, 1989). The rate of energy movement and grazing velocity is higher at the DCL, as is secondary organic matter export through sloppy heterotrophic feeding and sinking fecal pellets (Pollehne, Klein and Zeitzschel, 1993; Macías, Stips and Garcia-Gorriz, 2014). Compared to adjacent ecosystems, bacteria biomass is ten times greater at the DCL, and microbial diversity is similarly found to be higher (Auer and Powell, 2004; Junior *et al.*, 2015). The DCL creates an environment with enhanced ecological functioning and biodiversity compared to the light-rich, nutrient-poor surface waters and the light-poor, nutrient-rich deep waters that border the system on either side.

Directional movement of the DCL ecotone

Oscillations in phytoplankton concentrations at the DCL are driven by the balance between vertical mixing and nutrient sinking (Huisman *et al.*, 2006), where seasonal variation in nutrient availability, as controlled by the upwelling of deep, nutrient-rich waters, determines primary production throughout the year. Therefore, the location of the DCL varies based on short-term environmental conditions and weather, but its overall position remains relatively unmoved on a longer time scale, which is characteristic of a shifting ecotone (Estrada *et al.*, 1993; Letelier *et al.*, 2004; Figure 2a). Prior research indicates that the DCL, despite its interannual variations in depth, is relatively stable in the water column over the course of years to decades (Cullen, 1982; Estrada *et al.*, 1993). Developments in phytoplankton modeling and observation, however, challenge this notion and indicate that phytoplankton communities in DCLs can have sustained fluctuations in population density over long-term timescales (Letelier *et al.*, 2004; Huisman *et al.*, 2006). As global temperatures rise and surface ocean waters are heated, vertical stratification increases and, consequently, vertical mixing decreases (Bopp *et al.*, 2001), limiting nutrient availability to phytoplankton. As a result, low phytoplankton densities at the DCL become more frequent and long lasting (Huisman *et al.*, 2006). Sustained shifts to a warmer climate have led to increased stratification and, consequently, the depletion of the DCL and the overall directional movement of the DCL ecotone into shallower water depths in non-polar regions (Figure 2b).

DCLs in lakes similarly indicate climate-induced directional ecotone movement, but, instead of decreasing densities corresponding with warmer waters and shallower depths, DCL chlorophyll concentrations in lakes are increasing as surface temperatures increase (Barbiero and Tuchman, 2004; Reinl, Sterner and Austin, 2020). While open-ocean DCLs are limited by decreased nutrient concentrations from decreased vertical mixing, increased temperatures in lakes are associated with increased productivity and higher phytoplankton concentrations at the DCL (Reinl, Sterner and Austin, 2020). As waters continue to warm, the DCL in lakes may also become shallower as the increased concentration of smaller phytoplankton cells increases the scattering of light and decreases light attenuation (Yvon-Durocher *et al.*, 2011). From this, warming waters in lakes may lead to higher

chlorophyll concentrations in DCLs at shallower depths, as opposed to the reduced chlorophyll concentrations seen in open-ocean DCLs (Figure 2c). Although lake and open-ocean DCLs have similar directional movements—both are shoaling—climate changes induce opposite effects on chlorophyll concentration and ecosystem function in these systems, indicating that, while climate change is driving ecotone migration, local conditions and ecosystem type can influence ecotone function (Figure 2b, 2c).

Shifting Ecotone: grassland-shrubland ecotone

Grassland and shrubland ecosystems, located throughout the world in arid and semi-arid biomes, are characterized by frequent drought intervals, fires, and livestock grazing—disturbances that create heterogeneous habitat patches and form the highly dynamic grassland-shrubland ecotone (Anderson, 2006; Fuhlendorf *et al.*, 2006; McGranahan *et al.*, 2012; Connell, Scasta and Porensky, 2018). This heterogeneity in vegetation structure influences biodiversity and habitat use among ecotone residents (Connell, Scasta and Porensky, 2018). Spatial patches in the ecotone may act as habitat islands for species supported by the adjacent ecosystems (Sanchez and Parmenter, 2002; Schooley, Bestelmeyer and Campanella, 2018), but the ecotone also supports species distinct from those occupying adjacent ecosystems (Jorgensen, Demarais and Monasmith, 2000). The mosaic of grass and shrub patches at the ecotone thus forms a distinct ecosystem that supports a unique community.

Terrestrial ecotones are typically identified by changes in vegetation communities at the landscape scale (Risser, 1995), which are determined by abiotic characteristics, disturbance, and species-environment feedback (D'Odorico *et al.*, 2010; Porensky *et al.*, 2016; Archer *et al.*, 2017). Grassland and shrubland ecosystems are alternative stable states, meaning that either unique ecosystem can exist in the same area, with the same climate (Vetter, 2009; Ratajczak *et al.*, 2014). Because grassland and shrubland species coexist and compete for dominance at the ecotone, the biotic and abiotic factors that determine competitive advantage between these systems determine the position and movement of the ecotone (Peters, 2002; Peters *et al.*, 2006). Changes in environmental conditions can lead to abrupt lateral

movement in the shifting ecotone and transformation of an area from one state into the alternate state (Vetter, 2009).

Grass and shrub species possess competitive advantages under different precipitation patterns: grasses outcompete shrubs with frequent summer rains, and shrubs have a competitive advantage during prolonged drought and winter rain (Peters, 2002; Shiponeni *et al.*, 2011). Shrubs may act as "resource islands" that limit water accessibility to grasses and make it difficult for them to grow back after die-off (Duniway, Snyder and Herrick, 2010; Pockman and Small, 2010). Additionally, shrubs may perpetuate their own survival and expansion by warming surface air temperatures in winter, preventing lethal freezes that are typically followed by grassland encroachment (D'Odorico *et al.*, 2010), and by providing habitat for grass-grazing herbivores at the ecotone (Bestelmeyer, Khalil and Peters, 2007). Conversely, grass species may outcompete shrubs during years with frequent summer rains or regular fire disturbance, due to their deeper root structure and regrowth (Novellie and Bezuidenhout, 1994; Peters, 2002; Shiponeni *et al.*, 2011). These differences in competitive advantage contribute to their coexistence in a shifting ecotone under fluctuating and seasonal climatic conditions.

Directional movement of the grassland-shrubland ecotone

While grassland-shrubland boundaries are theoretically shifting ecotones, global patterns of shrub encroachment over the past century (Naito and Cairns, 2011; Archer *et al.*, 2017) indicate that the grassland-shrubland boundary has become a directional ecotone (but see Masubelele *et al.*, 2014). This pattern of movement, also called "desertification", is driven by a suite of interacting biotic and abiotic factors that favor shrubland over grassland, including livestock grazing (increased consumption of grasses), fire suppression (reduced shrub disturbance), and prolonged drought (decreased grass growth), the last of which is predicted to increase with future climate change (Roux, 1966; Vetter, 2009; Rutherford, Powrie and Husted, 2012). Drought is the primary climactic driver of shrub encroachment (Novellie and Bezuidenhout, 1994; O'Connor and Roux, 1995) and also amplifies the effects of secondary impacts, such as livestock grazing, on grassland to shrubland conversion (Vetter, 2009).

Ultimately, unidirectional changes in climate may thus disrupt the oscillating equilibrium previously held at the shifting grassland-shrubland ecotone, leading to dominance of shrubland within the ecotone and continued directional encroachment of shrubland into grassland.

Directional Ecotone: salt marsh-upland ecotone

In marshes, the transition between salt marsh and coastal forest forms a unique ecotone, sometimes referred to as the "ghost forest", defined by a rapid change in species composition across an elevation and salinity gradient (Wasson, Woolfolk and Fresquez, 2013; Santelmann *et al.*, 2019). Vegetation composition varies across the transition from marsh to forest based on differences in inundation, soil salinity, moisture, and competition (Pennings and Callaway, 1992). Germination of the upland species in the marsh-upland ecotone tends to be limited by salinity, such that the lower limit of upland vegetation zones is determined by abiotic constraints (Muñoz-Rodríguez *et al.*, 2017). The upper limit of marsh vegetation zones, however, is determined by competition, where marsh species are outcompeted by more freshwater-reliant, terrestrial species, such as *Myrica cerifera* (wax myrtle) or *Phragmites australis* (common reed) (Veldkornet, Adams and Potts, 2015). This distinct zonation enables the ecotone to support high levels of vegetative complexity and biodiversity niches within a relatively small area (Traut, 2005).

Accelerated directional movement of the marsh-upland ecotone

Shifting environmental gradients drive the lateral movement of the marsh-upland ecotone while maintaining species composition within the ecotone (Figure 3). Where sea levels are rising, the marsh-upland ecotone exhibits directional migration into upland systems (Smith, 2013; Schieder, Walters and Kirwan, 2018). The chronic press of saline intrusion into forests limits forest regeneration, and acute storm pulses kill mature, salinity-resistant trees (Fagherazzi *et al.*, 2019). Together, these processes facilitate the inland migration of marsh vegetation, a process often referred to as marsh migration. With this unidirectional ecotone movement, vegetative structure is preserved within the directional ecotone as

persistent zones of marsh and ecotone habitat encroach into upland forests concurrently (Wasson, Woolfolk and Fresquez, 2013). The ecotone itself is typically dominated by snags left over from the retreating upland forest and grass species from the encroaching salt marsh, along with ecotone-specific species (Kirwan and Gedan, 2019).

Although the directional movement of the marsh-upland ecotone has been a naturally occurring process throughout the Holocene (Horton *et al.*, 2018), anthropogenic climate change processes have intensified the drivers of ecotone movement (Donnelly and Bertness, 2001). As the global rate of sea-level rise and the frequency of storms has increased, the directional movement of the marsh-upland ecotone has also accelerated, where possible (Schieder and Kirwan, 2019).

DISCUSSION

Climate change and ecotone dynamics

In the case studies reviewed, we see the manifestation of global changes in ecotone dynamics on the ecosystem level. From these examples, we find evidence that changing climates at both the local and global scales can propel directional ecotones by manipulating the abiotic conditions that determine the width and position of shifting ecotones (deep chlorophyll layer), limiting reversals in shifting ecotones (grassland-shrubland), and directly accelerating the drivers of directional ecotones (marsh-upland). Local and global climate changes have caused ecotone dynamics to change in a variety of landscapes, but we find evidence for a general shift toward directional ecotone movement as abiotic gradients are modified by changes in global climate drivers.

In the deep chlorophyll layer (DCL) case study, shifts in environmental conditions caused by global climate changes—specifically warming-induced stratification—disrupt the previously shifting ecotone. In response to warming, the DCL reaches a shallower depth and either increases or decreases its chlorophyll concentration depending on the local conditions of the system. Warming surface waters in lakes increase phytoplankton productivity, albeit at shallower depths, whereas increased ocean

stratification and reduced vertical mixing diminish productivity and shrink the DCL in open-ocean ecosystems (Bopp *et al.*, 2001; Huisman *et al.*, 2006; Reinl, Sterner and Austin, 2020). These differences emphasize that local conditions interact with climate to determine the effect of directional ecotone movement on ecosystem function.

The grassland-shrubland and salt marsh-upland ecotone case studies demonstrate more uniform directional movement of ecotones, driven by a changing climate in two distinct ways. The grassland-shrubland ecotone typically acts as a shifting ecotone under stable or equally oscillating climate conditions (Peters *et al.*, 2006; Shiponeni *et al.*, 2011). Due to directional changes in climate, however, the shifting ecotone dynamics driven by variable abiotic and biotic conditions (e.g., precipitation patterns, grazing intensity) are suppressed, and the resulting climate conditions favor shrubland dominance (Duniway, Snyder and Herrick, 2010; Pockman and Small, 2010). As grassland and shrubland ecosystems endure more prolonged droughts, conditions become more favorable for shrubland species, thereby disrupting the equilibrium of the shifting ecotone, amplifying the effects of disturbance at the transition, and promoting directional movement of the ecotone into grasslands. Here, directional movement is not directly spurred by a shifting abiotic gradient, such as salinity or light. Instead, reduced variations in climate disrupt the equilibrium inherent to a shifting ecotone and prevent the expected reversals that maintain the long-term position of the ecotone.

Conversely, rising sea levels caused by global climate changes drive the accelerating migration of salt marshes into upland ecosystems (Schieder, Walters and Kirwan, 2018). As saltwater rises and moves inland, the salinity gradient that spans from salt marsh to coastal forest also shifts inland, creating an environment favorable for migration of salt marsh species into the forest (Smith, 2013; Muñoz-Rodríguez *et al.*, 2017). As opposed to the grassland-shrubland and deep chlorophyll layer case studies, where an equilibrium is disturbed, the accelerated directional movement of the marsh-upland ecotone results from the acceleration of a preexisting pattern of movement within an existing environmental gradient.

Ecotones occur over a broad spectrum of temporal and spatial scales and are therefore subject to scale-dependent constraints and drivers. Although constraints at multiple scales are simultaneously driving ecotone dynamics (Gosz, 1993), ecotone dynamics at broad spatial scales (biome and landscape ecotone) are dominated by changes in climate and topography, as compared to smaller spatial scale ecotones (population and plant-soil ecotones), which are controlled by interspecies interactions and soil chemistry. Therefore, the strongest representations of climate change's influence on ecotone dynamics will be observed at the landscape scale and above. Temporally, changes in climate—especially anthropogenic changes—manifest over the decadal to centennial. Meaningful examinations of the effects of climate on ecotone movement, and ecotone dynamics more generally, therefore necessitate a broad spatial scale and a multi-decadal or centennial temporal scale. Smaller-scale observations may exhibit patterns that are not representative of the long-term impacts of climate changes on ecotone movement. For example, short-term observations of variable ecotone position may indicate shifting movement at an ecotone that is actually moving directionally when examined over the decadal time scale. From this, it is evident that spatial and temporal scales of ecotone observation must align with the questions being asked and the drivers and constraints of ecotone dynamics being examined.

Ecotone and adjacent ecosystem function

In the presented case studies, changes in ecotone dynamics have the potential to reduce overall ecosystem function, though the mechanism of this reduction varies. As shifting ecotones become directional, the direction and rate of their movement, the encroaching ecosystem functionality, and the retreating ecosystem functionality will determine the change in ecosystem function at the landscape scale. The DCL case study emphasizes that, as ecotones become more variable in both ecotone area and presence, ecosystem functions—namely primary production—within these zones can diminish (Huisman *et al.*, 2006).

The ecosystem function of a directional, migrating ecotone is likely to decrease as a mature system is replaced with a young ecosystem, which may require time for process rates to increase to those

seen in mature systems (Greiner *et al.*, 2013; Smith and Kirwan, 2021). Additionally, directional ecotone movement can cause an overall reduction of functionality at the landscape scale when a low-functioning system replaces a high-functioning system, such as when seagrasses are replaced by bare sediment (Trevathan-Tackett *et al.*, 2018). The transition from a low- to high-carbon burial system seen during directional mangrove encroachment emphasizes that net ecosystem functionality under novel landscape changes is dependent on both of the ecotones' adjacent ecosystems (Yando *et al.*, 2016).

Because directional ecotones are constantly migrating and being displaced, the unique ecotone system must continually re-establish. The rate of migration thus determines the ability of the new ecotone to mature and reach its previous functionality. A slowly migrating ecotone is afforded time to mature, whereas rapid ecotone movement provides limited time to reach maturity before conversion to the adjacent ecosystem. Therefore, with accelerating rates of directional movement, such as those seen at the marsh-upland ecotone, mature ecotone functionality may never be reached before the ecotone is again displaced (Smith and Kirwan, 2021).

Directional ecotone migration also differs based on the structure, community composition, and land use of the retreating ecosystem on which it is encroaching. Ecotones with developed boundaries on one side, such as armored shorelines in the case of the marsh-upland ecotone, tend to be truncated or absent, with minimal opportunity for ecotone migration (Wasson, Woolfolk and Fresquez, 2013; Gehman *et al.*, 2018). For ecotones without anthropogenic or morphological boundaries, land use in the adjacent ecosystem still affects community composition of the resulting ecotone (Anisfeld, Cooper and Kemp, 2017; Gedan and Fernández-Pascual, 2019). Because movement on the encroaching side of a directional ecotone is persistent, the upland boundary of the ecotone may influence areal extent and community composition as the ecotone migrates, possibly resulting in reductions in ecotone area or connectivity between adjacent ecosystems over time. Furthermore, invasive species, which often benefit from disturbance (Minchinton and Bertness, 2003; Smith, 2013), may prevent an ecotone from maintaining its structure and functionality as it migrates.

As shown in the case studies explored in this paper, ecotones are unique environments that rely on controlling factors imposed by both neighboring ecosystems and global changes. Because ecotones are unique environments distinct from the surrounding, adjacent ecosystems, they warrant their own assessments and exploration of ecosystem functions, especially in dynamic ecotones where climate changes alter movement patterns. The deep chlorophyll layer and grassland-shrubland case studies exemplify the increased net ecotone movement and local changes in ecotone function that may result from climate change. Likewise, the marsh-upland case study demonstrates the potential for faster directional ecotone movement with climate change. If the demonstrated effects of climate change on ecotone movement extend beyond the included case studies to more ecotones, it will be important to consider functions within all ecosystems involved—including not only the adjacent ecosystems, but changes at the ecotone itself. Additionally, ecotone shifts due to climate changes call for future studies to consider interactive effects between traditional ecotone disturbances, local conditions, and broader controlling factors, such as global climate, as well as influences of the secondary effects of climate change (e.g., changing wind patterns, seed dispersal, and animal migration).

In response to directional climate change (e.g., sea-level rise or precipitation changes), ecotone movement patterns may change, although this response is not uniform for all ecotones (Neilson, 1993; Noble, 1993). When environmental conditions fall out of equilibrium and one adjacent ecosystem outcompetes the other, shifting ecotones may become directional ecotones. Further, shifts in environmental gradients may cause directional ecotones to exhibit accelerated landscape-scale migration (Allen and Breshears, 1998; Wasson, Woolfolk and Fresquez, 2013; Gedan and Fernández-Pascual, 2019; Kirwan and Gedan, 2019). Observing changes in ecotone dynamics may thus provide insight into the extent of climate change impacts on both ecotones and their adjacent ecosystems.

In the ecotone literature, studies in multiple environments—including aquatic, terrestrial, and ecosystems at the marine-terrestrial interface—show developing changes in ecotone movement at the landscape scale. Patterns of movement within the deep chlorophyll layer, grassland-shrubland, and salt

marsh-upland ecotones suggest that climate change may drive changes in the movement patterns of ecotones, specifically shifting ecotone dynamics toward greater and more directional movement. This may occur through increases in climate variability (e.g., greater annual temperature variation) that change the seasonal dynamics of ecotones, unidirectional climate shifts (e.g., prolonged drought) that reduce reversals in shifting ecotone movement, or directional movement of abiotic gradients (e.g., salinity) that propagates accelerated directional ecotone movement. Future studies should consider this pattern in additional ecotones and as caused by additional climate drivers not discussed here. Future work should also examine ecosystem function in ecotones and their adjacent ecosystems, as increased directional movement may lead to changes in function, and predicted climate changes will likely accelerate ecotone displacement.

*Adapted from an article published in **Geophysical Research Letters**. Full citation is available in the References section.*

Chapter 1

Sea-level Driven Marsh Migration Results in Rapid Net Loss of Carbon

Authors

Alexander J. Smith[1]*, Matthew L. Kirwan[1]

[1]Virginia Institute of Marine Science, College of William and Mary, Gloucester Point, VA, USA.

Abstract

Sea level rise alters coastal carbon cycling by driving the rapid migration of coastal ecosystems, salinization of freshwater systems, and replacement of terrestrial forests with tidal wetlands. Wetland soils accumulate carbon (C) at faster rates than terrestrial soils, implying that sea level rise may lead to enhanced carbon accumulation. Here, we show that carbon stored in tree biomass greatly exceeds carbon stored in adjacent marsh soils so that marsh migration reduces total carbon stocks by approximately 50% in less than 100 years. Continued marsh soil carbon accumulation may eventually offset forest carbon loss, but we estimate that the time for replacement is similar to estimates of marsh survival (i.e. centuries), which suggests that forest C may never be replaced. These findings reveal a critical C source not included in coastal C budgets driven by migrating ecosystems and rapidly shifting allocations between carbon stored in soils and biomass.

Introduction

Coastal wetlands are thought to disproportionally influence the global carbon (C) budget because of C accumulation rates (CAR) 1 to 2 orders of magnitude greater than terrestrial

systems (Chmura *et al.*, 2003; Mcleod *et al.*, 2011). Salt marshes, mangroves, and seagrasses account for approximately 50% of C buried in the ocean despite covering <2% of the ocean's surface (Duarte, Middelburg and Caraco, 2005). However, sea level rise, reduced sediment supply, and other anthropogenic stressors threaten the persistence and strength of the coastal carbon sink (Kirwan and Megonigal, 2013; Saintilan *et al.*, 2020). Extensive historical loss of coastal ecosystems (Kirwan and Gedan, 2019) suggests that coastal wetlands are simultaneously valuable yet vulnerable C sinks (Hopkinson, Cai and Hu, 2012; Nahlik and Fennessy, 2016; Theuerkauf and Rodriguez, 2017), making it imperative to understand how the coastal C sink will respond to global change (Ward, 2020).

For more than a decade, blue carbon research has focused on quantifying C stored in the soils of single ecosystems, often at single points within an ecosystem (Chmura *et al.*, 2003; Duarte, Middelburg and Caraco, 2005; Mcleod *et al.*, 2011; Ward, 2020). However, climate change limits the applicability of this traditional blue carbon approach by altering the position of ecotones, the relative spatial extents of ecosystems within the coastal landscape, and the partitioning of C between soils and vegetation (Kirwan and Megonigal, 2013; Smith, 2013; Kirwan, Walters, *et al.*, 2016; Osland *et al.*, 2017; Krauss *et al.*, 2018). For example, sea level rise (SLR) is leading to the widespread migration of wetlands into retreating upland forests across the Atlantic coast of North America (Schieder, Walters and Kirwan, 2018; Kirwan and Gedan, 2019), where coastal ecosystems and their carbon pools are expected to change rapidly (i.e. at decadal time scales) (Enwright, Griffith and Osland, 2016; Krauss *et al.*, 2018; Schieder and Kirwan, 2019; Wang *et al.*, 2019). Following conventional blue carbon approaches focusing on soil C, this transgression should increase coastal C by replacing a low C burial system (upland forest) with a high C burial system (salt marsh) (Elsey-Quirk *et al.*, 2011; Mcleod *et al.*, 2011;

Morris *et al.*, 2016; Wang *et al.*, 2019). Yet, this traditional approach largely ignores the contribution of C stored in biomass, which is known to be important in other systems. For example, living biomass accounts for approximately 30% of C stored in mangroves and nearly half of C stored in the world's forests (Pan, 2011; Hamilton and Friess, 2018). In contrast to terrestrial systems that exhibit positive carbon-climate feedbacks (Melillo, 2017), work in coastal wetlands points to a potentially negative carbon-climate feedback, where marsh soil carbon accumulation rate (CAR) increases with warming-driven sea level rise (Kirwan and Mudd, 2012; Doughty *et al.*, 2016). However, we show here that tree biomass rather than soil organic matter dominates C stocks in rapidly migrating marsh-forest ecotones, so that sea-level driven marsh migration leads to a century scale loss of C that is unaccounted for in our conceptual understanding of coastal C cycling.

Methods

Approach and Study Area

We measured biomass and soil C stocks across the forest-marsh ecotone at four rapidly transgressing sites in the Chesapeake Bay region of Maryland and Virginia in the United States of America (Figure 4). The Chesapeake Bay serves as a model region for studying the C implications of sea-level driven land conversion because rates of relative SLR (between 3 and 6 mm yr^{-1}) are twice as fast as eustatic rates (~2 mm yr^{-1}) and the gently sloping, rural coast allows for many opportunities for marsh migration. Approximately 100,000 acres of salt marsh have migrated into retreating coastal forests since the mid-19th century in the Chesapeake Bay, and rates of forest retreat are accelerating in parallel with relative SLR (Schieder, Walters and Kirwan, 2018; Schieder and Kirwan, 2019). Regional conditions in the Chesapeake Bay create

rapid, widespread landscape changes that exemplify the slower, yet eventual, ecosystem shifts that salinization drives across the coastal landscape.

Within the Chesapeake Bay region, we studied sites at Goodwin Island (GI), Phillips Creek (PC), Monie Bay (MB), and Moneystump Swamp (MS). At each site, four transects starting in salt-unaffected forest and ending in young salt marsh that was once upland forest were established perpendicular to the marsh-forest ecotone. We identified and delineated five unique vegetation zones along the transects according to vegetation and forest health: high forest, mid forest, low forest, transition zone, and high marsh (Figure 4). The high forest is defined as a forest unaffected by salt intrusion displaying a mixed aged structure of both coniferous and hardwood trees. The mid forest displays early signs of salt stress and exhibits 100% hardwood tree mortality, but conifer seedling regeneration is present in the understory and the canopy has a predominantly healthy, mixed age structure. The low forest is defined by relatively higher salt stress, as indicated by a lack of conifer regeneration, increased standing conifer tree mortality, and the expansion of shrub species in the understory. The transition zone has approximately 50% mortality in all standing trees with an understory dominated by *Phragmites australis* and herbaceous species typical of high marsh. The high marsh, dominated by herbaceous marsh grasses *Distichlis spicata*, *Spartina alterniflora*, and *Spartina patens*, has no living canopy and is the completed phase of marsh migration. This general vegetation pattern (from forest to shrub/*P. australis* to salt marsh) is observed in retreating coastal forests throughout the Atlantic Coast (Brinson, R. and K, 1995; Gardner and Reeves, 2002; Williams, M. and Sternberg, 2003; Smith, 2013; Langston, Kaplan and Putz, 2017; Kirwan and Gedan, 2019; Smart *et al.*, 2020), suggesting that our sites are broadly representative of the sea-level driven conversion of upland forest to marsh throughout the Atlantic Coast. As discussed below, simple projections of

topography and sea level rise suggest that these spatial gradients in vegetation type correspond to the temporal evolution of the coastal landscape, where complete conversion of forest to marsh occurs in less than 100 years on average at our sites (t_{mig}, SI Table 1).

Field Methods

Within each vegetation zone along each transect, we established a 100 m^2 plot within which we surveyed vegetation and quantified C stocks. To estimate the total amount of C present within a plot, we estimated C within three distinct C stocks (woody C, herbaceous C, and soil C). Woody C includes the above- (stem wood, bark, and branches) and belowground biomass of the trees and shrubs, and was estimated from allometric estimations of biomass. For trees, we used species-specific allometric equations to predict above and belowground biomass from diameter at breast height (1.37 m) measurements of all trees within the plot (Clark and Schroeder, 1985; Ter-Mikaelian and Korzukhin, 1997; Martin *et al.*, 1998; Norris *et al.*, 2001; Jenkins *et al.*, 2003; McElligot and Bragg, 2013; Chojnacky, Heath and Jenkins, 2014). Aboveground shrub biomass of all shrubs within the 100 m^2 plot was approximated from allometric equations as a function of basal diameter and belowground shrub biomass was approximated using a 1.098 root to shoot ratio for marsh shrubs (Mokany, Raison and Prokushkin, 2006; Conti, 2019). Herbaceous C comprises C within aboveground macrophytes in the understory. Macrophyte aboveground biomass within six randomly distributed 0.25 m^2 plots nested within each 100 m^2 plot was destructively harvested during peak biomass (July-August 2019), separated into live and dead fractions, and dried to a constant weight.

Soil C was quantified by collecting three soil samples within each plot using a hand turn, 4-inch soil mud auger in the forest zones and a Russian peat corer in the transition zone and high marsh. The soil C stock includes all organic C beneath unincorporated detritus and forest litter.

To compare sediment samples from different vegetation zones that had variable depths, soil samples were portioned into two depth intervals: 0 to 10 cm (hereafter referred to as "shallow soils"), which was present among all vegetation zones, and 10 cm to parent material ("deep soils"), where the parent material is defined as the point of resistance into inorganic clay or sand (SI Table 1). Both deep and shallow soils were analyzed for dry bulk density (DBD) and percent organic matter (%OM) using loss-on-ignition methods. To measure soil C accumulation rates, larger diameter (15cm) cores were taken at two of the high marsh plots at each site for ^{210}Pb gamma emission dating. Elevation relative to a benchmark at each site was measured at the center, highest, and lowest point of the plot using a laser level. The average value of each plot was then referenced to NAVD88 using an RTK GPS at the benchmark location, and mean higher high water (MHHW) using interpolated tide gauge data summarized in Holmquist et al. (2006).

Lab and Analytical Methods

Biomass was converted to C using species specific conversion ratios (~40-50%), which were available for dominant coniferous vegetation, *Pinus taeda* and *Juniperus virginiana* (Norris *et al.*, 2001; McElligot and Bragg, 2013) or using a general 50% biomass to C conversion, for mixed herbaceous macrophytes, shrub, and deciduous tree biomass. Following the general approach of C. B. Craft, Seneca, and Broome 1991, we converted the organic content of soils to total organic C (TOC) by constructing an empirical relationship for our sites and vegetation zones. Eight dried soil samples within each vegetation zone were selected to represent the range of organic matter contents from the vegetation zones. We then measured TOC by packaging approximately 3 mg of homogenized sediment in tin capsules, treating it with aerosolized 6 mol HCl for 12 hours, drying the sample for an additional 12 hours, and processing the sample in a CHN analyzer (Thermo Electron Corporation FlashEA 1112, NC Soil Analyzer). The CHN

analyzer was calibrated using acetanilide standards (71.09% C, 10.36% N). The relationship between organic matter (OM) and C was consistent across vegetation zones, so one collective relationship was used to estimate soil C content across all zones ($TOC=0.0033(\%OM)^2+0.2967(\%OM)+8.4341$, $R^2=0.73$) (SI Figure 1). Statistical differences of similar stocks across the vegetation zones were calculated using a one way ANOVA using the statistical computing software R with a 95% confidence interval, which was applied to average stock values from the four sites.

We measured soil salinity by preparing 1:5 soil to water suspensions (adding approximately 50 ml of distilled water to ~10 g of oven-dried soil samples) from the top 10 cm of soil collected from three points in each plot (Hardie and Doyle, 2012). The suspensions and containers were shaken for 1 minute by hand every 30 minutes over two hours (Rhoades, 1992). Samples were undisturbed and settled for 18 hours then filtered through a 20 micron filter to obtain extracts (He *et al.*, 2012). The conductivity of the extracts was measured using a FieldScout EC 450 Meter conductivity probe. To determine soil C accumulation rates in the high marsh sediment cores, we measured Pb^{210} activities down core using gamma spectrometry. We then applied the constant initial concentration (CIC) model, which approximates an average sediment accumulation rate, on dated sediment cores from the high marsh, with Cs^{137} as an independent chronometer (Appleby and Oldfield, 1978; Sanchez-Cabeza and Ruiz-Fernandez, 2012) (SI Figure 2). C accumulation rates were obtained by measuring DBD and the concentration of C in dated sediments and multiplying them by the accumulation rates derived from the CIC model (Arias-Ortiz, 2018).

Results and Discussion

Shifting C allocations in marsh-forest ecotones

The total C stock averaged across sites decreased by approximately 50% from the high forest (17.44 +/- 2.9 kg C m^{-2}) to the high marsh (9.73 +/- 1.59 kg C m^{-2}). Total C was maximized in the mid forest (22.1 +/- 0.63 kg C m^{-2}), though total C in the mid forest and high forest were not statistically different (Figure 5a, SI Figure 3-6, p=0.33). Total C stocks increased with increasing elevation (R^2=0.21, p=0.05) and decreasing salinity (R^2=0.57, p<<0.05) (Figure 5e, Figure 5f); both trends were consistent across all sites (Figure 5e). Based on a regionally averaged rate of sea level rise (4.46 mm y^{-1}) and the difference in elevation between high forest and high marsh, we estimate that our chronosequence represents less than a century (t_m=ΔElevation/SLR), though this simple approach ignores pulse events and any dynamic feedbacks that could accelerate or mediate the transgression process (Figure 5e; SI Table 1).

The average C stock of living woody vegetation decreased from 13.2 +/- 4.0 kg C m^{-2} in the high forest to 0.18 +/- 0.02 kg C m^{-2} in the high marsh. Specifically, tree carbon decreased from 12.7 kg C m^{-2} to 0.09 kg C m^{-2} and shrubs decreased from 0.62 kg C m^{-2} to 0.09 kg C m^{-2}. Shrub density was maximized in the mid forest (6.22 kg C m^{-2}, p<<0.05) where it accounted for 38% of C stored in woody biomass, but across every forest zone, C stored in trees was found to be greater than C stored in shrubs (Figure 5b, p<<0.05). All of the forest zones were consistently dominated by above ground, woody C in living biomass rather than herbaceous or soil C (p=0.06). Herbaceous C increased from the high forest (0.03 +/- 0.01 kg C m^{-2}) to the high marsh (0.34 +/- 0.03 kg C m^{-2}) (Figure 5c). Herbaceous C was maximized in the transition zone at each site (p=0.08) where *Phragmites australis* presence increased the herbaceous C stock by an average of 57% (Figure 5c, p<<.05), except for at Moneystump Swamp where *P. australis* has historically been removed (Figure 5c, SI Figure 4). The transition zone and high marsh had far smaller biomass C stocks, but had substantial contributions from soil C stocks. Deep soil C

increased by an order of magnitude along the forest (0.11 kg C m^{-2}) to marsh (6.4 kg C m^{-2}) gradient while shallow soil C decreased slightly. Overall, soil C approximately doubled across the forest to marsh gradient and deep soil C contributed 70.3% of the total C stock in the high marsh (Figure 5d, Figure 5a, SI Figure 5). Using the CIC model, the average vertical accretion rate across the high marsh zones of four sites was 2.35 +/- 0.84 mm y^{-1} and ranged from 1.44 to 3.11 mm y^{-1} (SI Figure 1, SI Table 1). CAR calculated from dry bulk density, total organic carbon, and the CIC derived sedimentation rates varied between 0.036 and 0.065 kg C $m^{-2}y^{-1}$ (SI Table 1). Nevertheless, forest zones were consistently dominated by above ground biomass C rather than herbaceous or soil C.

Upland transgression decreases C stocks

For the last two decades, the paradigm in blue carbon research has maintained that vegetated intertidal systems disproportionately affect the global C cycle because rates of soil C burial far exceed those of terrestrial systems (Chmura *et al.*, 2003; Duarte, Middelburg and Caraco, 2005; Mcleod *et al.*, 2011). By inference, sea-level driven conversion of terrestrial forests to tidal marshes would be expected to lead to increased rates of C burial and consequently increased soil C stocks over time (Elsey-Quirk *et al.*, 2011; Morris *et al.*, 2012; Wang *et al.*, 2019). Our finding that the magnitude of C stored in marsh soils is greater than coastal forest soils is consistent with this paradigm (Figure 5d). However, we also find that C stored within the living biomass of terrestrial, coastal forests far exceeds the total amount of C stored in adjacent marshes (Figure 5a). This observation suggests that sea-level driven land conversion could lead to substantial losses of C that are not considered in current conceptual models of coastal C cycling.

The total C stock in forested zones was dominated by C stored in living trees, and tree mortality drove the decrease in total C across the forest-marsh ecotone (Figure 5a). We observed a strong, significant relationship between increasing soil salinity and decreasing total C (Figure 5f), which is consistent with previous work that identifies salinity as a primary driver of tree mortality and forest retreat (Brinson, R. and K, 1995; Williams, M. and Sternberg, 2003). Our measures do not directly account for dead yet present vegetation in the form of litterfall, logs, or standing dead trees, suggesting that we potentially overestimate the gradient in C stocks across the forest zones, and underestimate the gradient between stressed forest and high marsh. However, previous work suggests that dead woody vegetation comprised approximately 9% of the aboveground C stock and large living trees were still dominant in the aboveground C stock (Krauss *et al.*, 2018). Additionally, our finding that the biomass of live trees is much greater than the carbon stored in adjacent marsh soils suggests that most of the carbon stored in live trees does not persist in marsh soils, perhaps driven by rapid decomposition rates (Kozlowski, 1997) and elevated tree methane fluxes near the marsh-forest boundary (Norwood *et al.*, 2020). The expansion of shrubs and *P. australis* and increasing soil organic matter thickness may all be expected to contribute to C accumulation in migrating forest-marsh ecotones (Craft, 2000; Elsey-Quirk *et al.*, 2011; Smith, 2013; McTigue, 2019) (Figure 5a). However, we find that these processes only partially offset tree mortality and that the net total C stock decreases by approximately 50% with the conversion of forest to marsh (Figure 5a).

Previous work in other transgressing coastal ecosystems suggest that sea level rise and saltwater intrusion may lead to decreased total C stocks more generally. Ecosystem transgression in many regions of the U.S. is characterized by the replacement of wetland forests rather than the upland forests considered here (Brinson, R. and K, 1995; Doyle, 2010). Wetland forests typically

have organic rich soils whereas the studied terrestrial forests are dominated by mineral soils. Nevertheless, decreased aboveground biomass associated with tree mortality has been reported in a number of tidal freshwater systems where marshes replace forested wetlands (Ken W. Krauss et al. 2018; Brinson, R., and K 1995; Brinson, D., and Jones 1985; K.W. Krauss, L., and Creech 2007). Like our findings for the Chesapeake Bay, biomass in coastal forests exceeds biomass of adjacent marshes in the Albemarle and Pamlico Sounds (NC) (Smart *et al.*, 2020). In other systems, salinization and salt water intrusion into tidal freshwater systems has been shown to reduce C fixation (GA tidal freshwater marsh) (Herbert, J. and Craft, 2018), increase soil respiration (FL freshwater wetland) (Chambers, R. and Z, 2011), and lead to peat collapse (FL everglades) (Chambers, 2014), resulting in decreased soil C stocks. Salt water intrusion is further shown to reduce belowground biomass while also enhancing greenhouse gas efflux after prolonged exposure (FL everglades, NC tidal freshwater forested wetland) (Ardón, Helton and Bernhardt, 2018; Wilson, 2018). These observations from mostly freshwater systems offer mechanistic insight into the processes that lead to decreases in specific carbon stocks, and suggest that the patterns of loss we observe may apply more generally to other types of transgressing coastal systems.

Timescales of C replacement

Although we find that marsh migration consistently leads to a net loss of total carbon (Figure 5a, SI Figure 6), our finding that soil C stocks increase across the marsh-forest ecotone (Figure 5d) suggest that C stored in marshes may increase through time and perhaps eventually offset C lost from forest mortality. C stored in marsh soils increases through time as belowground organic matter accumulates in newly flooded, anaerobic soils (Craft *et al.*, 1999; Stagg, 2016). Sediment cores taken from our study sites in much older sections of the marsh

display deeper, organic rich soils reflecting larger carbon stocks typical of mature salt marshes (Thomas, 2004; Schieder and Kirwan, 2019; Dontis *et al.*, 2020). CAR would also be expected to increase with increasing tidal inundation associated with accelerated SLR (Kirwan and Mudd, 2012; Gonneea *et al.*, 2019; McTigue, 2019; Rogers *et al.*, 2019). Thus, the size of the C stock in marshes and its ability to offset C loss due to forest mortality depends on marsh age.

Given the high CAR in marsh soils and the high soil C content of older marshes (Elsey-Quirk *et al.*, 2011; Holmquist *et al.*, 2018; Krauss *et al.*, 2018), salt marshes may eventually offset C that is lost during marsh migration. We estimate the "time to replacement" of forest C at each site as:

$$t_r = \frac{\Delta C_f}{CAR_m} \quad (1)$$

where ΔC_f is the total amount of C lost from the forest during transgression (kg m^{-2}), CAR_m is the C accumulation rate in the adjacent high marsh (kg m^{-2} y^{-1}), and t_r is the time (y) needed to replace the forest C lost with marsh soil C. The inheritance of carbon from terrestrial systems into the migrating marsh soils is unknown and beyond the scope of this paper. Therefore, we calculate C_f in two ways. First, we assume that all C in the forest is lost during the transgression process so that $\Delta C_f = C_f$, where C_f is the total forest C stock observed in the mid or high forest. This calculation represents the maximum time to replacement ($t_{r,\max}$) as it assumes no preservation of forest C in soils. Alternatively, we assume that a substantial fraction of C measured in the high marsh soils is C that has been preserved from forests, so that $\Delta C_f = C_f - C_m$ where C_m is the measured marsh C stock, representing the minimum total C stock during marsh migration. This calculation represents a minimum time to replacement ($t_{r,\min}$) as it includes refractory C in forest soils that has been preserved in soils during transgression, and assumes that

any forest C in the high marsh soil will continue to be preserved in the future. Based on measured values of C_f, C_m, and CAR_m at each of our sites, eqn. 1 predicts that it will take approximately 130 to 760 years for marsh soil C to replace forest C lost during transgression (SI Table 1). This approach intentionally compares rates of C accumulation in one system with C stocks in another system, allowing us to calculate replacement timescales associated with migrating ecosystem boundaries in a manner that is easily applicable across ecosystems and spatial scales.

Our proposed replacement time metric leads to a conceptual model of changing carbon stocks that may be relevant to a variety of migrating ecosystems (Figure 6). In our system, the initial total C stock in the upland forests ($\boldsymbol{C_f}$) decreases with the onset of salt water intrusion (**a**). Progressive forest mortality leads to C loss until the total C stock is minimized ($\boldsymbol{C_m}$) when forests are first replaced by marshes (**b**), but developing marsh soils increase the total C stock through time and the system begins to partially offset lost C. As the marsh ages, soil C stocks increase with sea level rise and salt water intrusion as developing marsh soils accumulate carbon until submergence (**c**), potentially compensating for or even exceeding the lost forest carbon (**d**). However, in the studied Chesapeake Bay region, marshes submerge or erode on timescales ($\mathbf{c_1}$, $\mathbf{c_2}$; Hussein 2009; Schieder, Walters, and Kirwan 2018; Kirwan, Temmerman, et al. 2016) that overlap with estimated times of carbon replacement (**d**, 130-760 years) (SI Table 1), suggesting that complete replacement of forest carbon is tenuous. Moreover, salt intrusion can lead to forest die-off without marsh migration (Taylor *et al.*, 2020), leading to a large loss of aboveground C with little to no replacement in accumulating soil C stocks.

While the conceptual model is potentially generalizable across systems, the magnitude and rate of change would be expected to vary. For example, rapidly decreasing aboveground

biomass and increasing belowground carbon stock is likely a common response to inundation and salinization, though rates would be determined by particular species tolerance and biogeochemical settings (Field, Gjerdrum and Elphick, 2016; Flester and Blum, 2020). In contrast to our reported long timescales of replacement, we expect t_r to be relatively short in sequences beginning as freshwater wetlands or agricultural fields due to low values of ΔC_f from initial high soil C stocks or limited aboveground biomass, respectively (Krauss *et al.*, 2018; Van de Broek *et al.*, 2018). The general framework we present is intentionally simplistic, thereby allowing for its application to larger scale landscape models parameterized with spatially variable terms or to other transgressing ecosystems with site specific information.

Broader Implications

The traditional focus on wetland soils leads to an important and unique negative carbon-climate feedback proposed for the coastal zone, where accelerated sea level rise drives faster soil C accumulation (Kirwan and Mudd, 2012; Rogers *et al.*, 2019; Wang *et al.*, 2019). In contrast, our finding that C stored in the biomass of woody vegetation is far greater than the C stored in young, adjacent marshes (Figure 5) implies that sea level rise will lead to a net loss of C that cannot be predicted on the basis of wetland soil C stocks alone. Furthermore, our simple estimates of time to replacement suggest that the loss of C from forests following marsh migration will work against the proposed negative carbon-climate feedback in marsh soils at the scale of centuries (SI Table 1). Together, these findings help broaden the scope of traditional blue carbon research by connecting adjacent ecosystems, identifying a C source not considered in our current conceptual understanding of coastal carbon-climate feedbacks, and demonstrating that sea level rise will lead to fundamental changes in C allocation between soils and biomass at the coastal interface.

*Adapted from an article published in **Global Change Biology**. Full citation is available in the References section.*

Chapter 2

Temperature Optimum for Marsh Resilience and Carbon Accumulation Revealed in a Whole Ecosystem Warming Experiment

Authors

Alexander J. Smith*[1], Genevieve L. Noyce[2], J. Patrick Megonigal[2], Glenn R. Guntenspergen[3], Matthew L. Kirwan[1]

1 Virginia Institute of Marine Science, College of William and Mary, Gloucester Point, 23062, Virginia, USA

2 Smithsonian Environmental Research Center, 647 Contees Wharf Road, Edgewater, 21037, Maryland, USA

3 U.S. Geological Survey, Eastern Ecological Science Center, 12100 Beech Forest Road, Laurel, MD 20708-4035

Abstract

Coastal marshes are globally important, carbon dense ecosystems simultaneously maintained and threatened by sea-level rise. Warming temperatures may increase wetland plant productivity and organic matter accumulation, but temperature-modulated feedbacks between productivity and decomposition make it difficult to assess how wetlands and their thick, organic rich soils will respond to climate warming. Here, we actively increased aboveground plant-surface and below-ground soil temperatures in two marsh plant communities, and found that a moderate amount of warming (1.7°C above ambient temperatures) consistently maximized root growth, marsh elevation gain, and below-ground carbon accumulation. Marsh elevation loss

observed at higher temperatures was associated with increased carbon mineralization and increased microtopographic heterogeneity, a potential early warning signal of marsh drowning. Maximized elevation and below-ground carbon accumulation for moderate warming scenarios uniquely suggest linkages between metabolic theory of individuals and landscape-scale ecosystem resilience and function, but our work indicates nonpermanent benefits as global temperatures continue to rise.

Introduction

Marshes are highly valuable ecosystems providing a range of ecosystem services from storm protection to carbon accumulation, but accelerating rates of sea-level rise threaten to drown them and eliminate these services (Mcleod *et al.*, 2011; Shepard, Crain and Beck, 2011; Kirwan and Megonigal, 2013; Jankowski, Törnqvist and Fernandes, 2017). Warming simultaneously accelerates sea-level rise and alters *in situ* process rates that regulate marsh elevation and vulnerability to drowning, namely production, decomposition, and vertical accretion. Vertical accretion maintains marsh elevation relative to sea level through autochthonous root production and the capture of allochthonous sediments and organic matter (Kirwan and Megonigal, 2013; Morris *et al.*, 2016). As increased damming and management practices decrease suspended sediment available for capture, temperature sensitive biogenic controls to vertical accretion, such as production and decomposition, become increasingly important (Temmerman *et al.*, 2003; Peteet *et al.*, 2018). Above- and belowground production increase with temperature, which is expected to accelerate both vertical accretion and carbon inputs to the soil (Charles and Dukes, 2009; Gedan and Bertness, 2009; Coldren *et al.*, 2016). Therefore, warming could increase vertical accretion rates and contribute to a negative carbon-climate feedback by increasing soil carbon storage (Kirschbaum, 1995; Najjar *et al.*, 2000;

Rogers *et al.*, 2019). However, this conceptual framework largely neglects temperature driven increases in decomposition, which can reduce marsh stability and potentially offset benefits from increased productivity (Kirschbaum, 1995; Kirwan and Blum, 2011; Kirwan, Guntenspergen and Langley, 2014).

Global climate models project mean global temperature increases of 2.6-5.0 °C by the end of the 21st century (IPCC, 2021). Some studies have attempted to replicate these temperatures experimentally in salt marshes using aboveground heating lamps or passive heating systems (Charles and Dukes, 2009; Gedan and Bertness, 2009; Coldren *et al.*, 2016; Zhong *et al.*, 2019). While these designs have successfully simulated increased temperatures at the marsh surface, these methods fail to increase temperature at deep soil depths (~1 meter) that are expected to warm under future climate conditions (Phillips, 2020). Given the large, deep stores of organic material that have accumulated in marshes over time, these passive, surficial warming designs neglect to warm a significant portion of soil organic material that will experience warming in the future. Additionally, studies reliant on passive warming typically feature a single, low magnitude temperature treatment and therefore cannot account for non-linear warming responses that may occur as the climate continues to warm. Therefore, experimental warming of just surface sediments and vegetation fails to accurately simulate whole-scale ecosystem warming, and its cascading impacts on marsh resilience and function.

To address uncertain marsh response and resilience to future temperatures, the Salt Marsh Accretion Response to Warming Experiment (SMARTX) actively warmed entire marsh ecosystems, from plant canopy to a soil depth of approximately 1.5 m, using heating lamps at the surface and subterranean cables to achieve four discrete temperature treatments (ambient, 1.7, 3.4, and 5.1 °C above ambient temperatures) in two brackish marsh plant communities that are

dominated by either C_3 or C_4 plant species (SI Figure 1) (Noyce *et al.*, 2019). The C_3 site is dominated by the C_3 sedge *Schoenoplectus americanus* (93% of aboveground biomass) (Lynch, Hensel and Cahoon, 2015) and is relatively wet due to lower elevation and more frequent tidal flooding while the C_4 site is dominated by *Spartina patens* and *Distichlis spicata* (76% of aboveground biomass) (Lynch, Hensel and Cahoon, 2015) and is relatively elevated and dry. We measured marsh surface elevation in response to whole-ecosystem warming at annual and seasonal time scales and found that while marsh resilience is optimized under moderate degrees of warming, further warming led to decreased rates of carbon accumulation, early signs of marsh collapse, and increased vulnerability to sea-level rise.

Materials and Methods

Site Description and Experimental Design

The Salt Marsh Accretion Response to Temperature Experiment (SMARTX) was conducted in the Kirkpatrick Marsh, part of the Smithsonian's Global Change Research Wetland (GCReW) (Noyce *et al.*, 2019). Kirkpatrick Marsh is a 22-ha brackish high marsh located in the United States on a microtidal subestuary of the Chesapeake Bay (38°53′ N, 76°33′ W). The site is characterized by C_4 plant communities, dominated by *Spartina patens* and *Distichlis spicata*, and C_3 plant communities, dominated by the C_3 sedge *Schoenoplectus americanus*. The marsh platform is 40-60 cm above daily mean low water level and is inundated during approximately 28% of high tides. The average elevation of C_4 communities at this site range on average between 0.234 and 0.255 m while the average elevation of the C_3 marsh dominated by *Schoenoplectus americanus* is 0.214 m (Jordan and Correll, 1991). Soils at the site are organic-rich (>80%) to a depth of approximately 5 m (Jordan and Correll, 1991; Rietl *et al.*, 2021). Soil bulk densities range from 0.079 to 0.180 g cm^3 in the upper 60 cm of soil indicating that the soil

profile reflects historic uniform organic matter deposition. While there are abiotic and biotic differences between C_3 and C_4 plant communities (e.g., elevation, inundation frequency, organic matter content, vegetation composition, and shoot density), experimental transects were established in portions of the marsh with distinct C_3 and C_4 communities so that variance within sites is relatively low. The high organic matter content of the marsh soils allows us to assume that changes in marsh elevation are analogous to changes in the soil carbon stock due to a lack of mineral sedimentation and allochthonous carbon influx (Morris *et al.*, 2016). The Kirkpatrick Marsh is within a regional hotspot of late 20^{th} century sea-level rise, driven by geologic conditions along the mid-Atlantic seaboard of the United States (Sallenger, Doran and Howd, 2012), and the long-term mean sea-level rise trend for the past 50 years in this region is 3.8 mm yr^{-1} (NOAA, 2021).

Six replicate transects within the Kirkpatrick Marsh, three in each of the dominant plant communities, were established in 2016. A heating gradient consisting of an ambient temperature plot and heated plots raised to +1.7, +3.4, and +5.1 °C above ambient temperatures was established along each transect. Transects were designed to have similar plant community compositions along the entire transect. All plots are 2 by 2 meters with a 0.2 m buffer between plots to mitigate an edge effect. Heating was achieved aboveground using infrared heaters while vertical resistance cables heated soils down to 1.5 m, a depth not reached using passive warming techniques. Temperatures were maintained using an integrated microprocessor based feedback control to create a fixed temperature differential from the ambient temperature for each plot. Ambient temperature plots have dummy equipment to emulate site disturbance without manipulating temperature. Temperature variation is assessed via thermocouples embedded in

acrylic plates in the plant canopy and in the surface soils. Heating began in June of 2016 and is applied year-round.

Elevation Trends

Soil surface elevations were tracked using surface elevation tables (SETs). SETs were installed in each plot to measure soil surface elevation. Elevation benchmarks were installed outside of the experimental plot in June 2016 by driving a series of stainless-steel rods through the entire soil profile to "refusal" (approximately 12.5 meters, but ranging from 6 to 13.5 meters) and then permanently anchored (Lynch, Hensel and Cahoon, 2015). SET benchmark vertical stability over time was assessed by periodically surveying them relative to each other with a Trimble S5 Total Station and no significant differences in elevation were found. Elevation measurements were collected from approximately 60 "pins" that are 4.5 mm apart and measure the distance from a parallel bar attached to the anchored benchmark to the ground surface, and recorded to the nearest millimeter. This resulted in high-precision measurements of soil surface elevations relative to the base of the benchmark. Measurements were taken every June, August, and January since warming began on June 1, 2016. In addition to this, measurements were taken more frequently (every two months from March 2019 to February 2020) to examine inter-annual variability in marsh elevation.

To determine long term trends, marsh surface elevation was regressed against time for each individual SET pin resulting in approximately 60 estimates of linear elevation trends for each plot. Pin linear regressions across replicate plots (~180 linear regressions per treatment) were then averaged together to estimate the average long-term change in elevation at the treatment level. Treatments were compared using paired t-tests. To examine the effect of an installation effect (the loss of elevation driven by compaction and disturbance during the

installation of a SET), we similarly analyzed elevation trends omitting the August 2016 measurement and found general trends to be unaffected and statistically insignificant differences in long-term rates of elevation change. In addition to long term and annual elevation trends, we used SET data to calculate two metrics of microheterogeneity (random roughness ($\sqrt{\frac{\sum(x_i - x_\mu)}{n-1}}$) and tortuosity ($(\sum\sqrt{((x_2 - x_1)^2 + (y_2 - y_1)^2 + (z_2 - z_1)^2)})/l$)), in an effort to quantify marsh surface breakup (Moser, Ahn and Noe, 2007; Karstens *et al.*, 2016). As an additional metric of microheterogeneity, we quantified the number of holes, defined as locations with an elevation difference between that exceeded 20 mm. Spatial dependence between pins was calculated using a gamma autocorrelation metric as well as the number of pins away from one pin where pin height becomes independent (similar to van Belzen *et al.*, 2017; SI Table 2). Low levels of autocorrelation within plots indicate a lack of dependence between pins within plots, especially beyond pins more than 27 mm from one another, and negligible dependence between plots.

Annual above- and belowground productivity was measured as described in Noyce et al (2019). Aboveground productivity was determined by tracking the height and width of 653 stems from Apr to Nov 2019 and converting to biomass using allometric equations. For belowground productivity, root ingrowth cores were installed in November 2018 and removed a year later, after which the dry weight of fine roots in the core was determined. Methane emissions were measured as described in Noyce and Megonigal (2021) using static chambers and a Los Gatos Research Ultraportable Greenhouse Gas Analyzer. Water level was derived from one water level sensor (AquaTROLL 200) located in each plant community, which was then corrected to water level above marsh surface (m) using three averaged RTK elevation measurements from each plot. To examine the effect of productivity, decomposition, and water level on seasonal elevation trends, an ANOVA and multiple paired t-tests were applied.

Results and Discussion

Moderate warming optimizes marsh resilience and carbon accumulation

We measured marsh surface elevation response across warming gradients in C_3 and C_4 plant communities over a 4-year period (June 2016 to February 2020). Marsh surface elevation was regressed against time for each individual surface elevation table (SET) pin (Lynch, Hensel and Cahoon, 2015), resulting in derived rates of elevation gain and loss, but more generally marsh surface elevation increased through time in the C_3 community and decreased through time in the C_4 community (Figure 7a, 7b). Despite these contrasting elevation trends, both communities responded similarly to warming treatments, where elevation gain was optimized at 1.7 °C above current ambient conditions (Figure 7c). This optimal temperature treatment increased elevation gain by approximately 2.1 mm y^{-1} and 2.5 mm y^{-1} in the C_3 and C_4 communities, respectively (SI Table 1), but elevation gain was still less than the 3.8 mm yr^{-1} mean sea-level rise trend for the past 50 years in this region (NOAA, 2021). Warming beyond the temperature optimum reduced this positive effect and resulted in a 0.8 mm y^{-1} and 0.9 mm y^{-1} loss of elevation at the +5.1 °C treatment (Figure 7c), a rate equivalent to or less than ambient rates of elevation gain. Root production was also optimized at +1.7 °C in our experiment driven by optimum allocation of growth to belowground biomass in response to nitrogen limitation; above 1.7 °C increased nitrogen mineralization reduces plant nitrogen demand and root productivity (Noyce *et al.*, 2019). Therefore, belowground organic matter production drives the long-term elevation response to warming, with a consistent temperature optimum for root productivity and elevation change in both plant communities (Figure 7c).

Carbon accumulation rates were also maximized at moderate warming treatments. Carbon accumulation rates were calculated as the product of elevation change in each

experimental plot (ranging from 2.5 to -0.9 mm yr^{-1}) and the average carbon density of all C_3 (104.8 kg C m^{-3}) and all C_4 plots (238.8 kg C m^{-3}). These estimates assume that elevation change is driven predominately by organic matter accumulation at our sites, as evidenced by high soil organic matter content (~90%), limited allochthonous input of mineral sediment (Morris *et al.*, 2016; Rietl *et al.*, 2021), and accretion rates that are tightly controlled by root zone processes (Langley *et al.*, 2009; Rietl *et al.*, 2021). The C_3 community carbon accumulation rate was maximized at +1.7 °C (262 g C m^{-2} y^{-1}) and minimized at the control and +5.1 °C treatments (25 and -71 g C m^{-2} y^{-1} respectively). The C_4 carbon accumulation rate was also maximized at +1.7 °C (24 g C m^{-2} y^{-1}), but with a net loss of carbon storage in the control and +5.1 °C treatments (-249 and -296 g C m^{-2} y^{-1} respectively) (SI Figure 2). Our finding that the more flood-tolerant C_3 community responses to warming are more positive than less-flood tolerant C_4 responses offer empirical support to numerical modeling that suggests the positive impacts of temperature on marsh carbon accumulation are maximized at high sea-level rise rates (Couto *et al.*, 2014), but also highlights that warming-induced gains in one part of the system (C_3) may be offset by losses elsewhere (C_4).

Warming responses have traditionally been interpreted in the context of an optimal temperature for metabolism, where rates of productivity increase up to a point of typical summer temperatures and then decline with further warming (Long, Incoll and Woolhouse, 1975; Giurgevich and Dunn, 1979; Seneca and Blum, 1984; O'sullivan *et al.*, 2017). The photosynthetic optimum of *Spartina*, a common C_4 salt marsh genus, is approximately 2.2 to 7.2 °C above the mean high temperature during summer days at our study site (~28°C) (Giurgevich and Dunn, 1979; Kirwan, Guntenspergen and Morris, 2009). This, and decreased net primary production observed during elevated regional summer temperatures (Noyce *et al.*, 2019),

indicates that moderate amounts of warming in the region are likely elevating temperatures closer to or above this metabolic optimum. Although some studies have indicated that marsh grasses can acclimate leaf respiration and photosynthetic capacity to increasing temperatures (Wang *et al.*, 2020; Sturchio *et al.*, 2021), the warmest treatment likely exceeds the metabolic temperature optimum during warm summer days leading to a reduction in marsh elevation, analogous to the hump-shaped relationships between temperature and productivity proposed for *S. alterniflora* more globally (Rogers, Wilton and Saintilan, 2006; Więski and Pennings, 2014; Liu *et al.*, 2016, 2020). Our observations of consistent treatment optima, where root production, elevation change, and carbon accumulation rates in two disparate plant communities were maximized at +1.7 °C, suggest that the qualitative patterns are applicable beyond our particular study area, but that the exact temperature optimum may vary around +1.7 °C (Figure 7c). Moreover, because autochthonous, plant-mediated mechanisms drive these consistent optima, this suggests that metabolic temperature optima for individual plants or communities can cascade up to whole-marsh elevation change dynamics, thereby uniquely linking metabolic theory to ecosystem resilience and function.

Interactions between productivity and decomposition drive seasonal elevation trends

From March 2019 to February 2020, we measured marsh elevation every two months to quantify the potential influence of temperature over seasonal timescales (Figure 8a). Surprisingly, we found seasonal variations in relative marsh elevation that ranged from 8.75 to 13.25 mm, approximately 10 times greater than the long-term accretion rates observed in this study (Figure 8a, 8b). Seasonal variation was maximized in the +1.7 °C treatment in both the C_3 and C_4 community, closely following patterns in annual elevation gain and root productivity (Figure 8b). Marsh elevations were consistently maximized in the early spring (March to May)

prior to increased sedge and grass productivity and were minimized in the fall (August to December).

While multiple factors are known to influence seasonal marsh elevation change, we attribute it largely to seasonal changes in organic matter accumulation, expressed as the temperature-modulated balance between decomposition and production. Previous work links seasonal elevation change to declines in water level associated with evapotranspiration and drought during warm periods (Friedrichs and Perry, 2001; Cahoon *et al.*, 2011; Bashan *et al.*, 2013), but we found that water level fluctuations were only loosely correlated with fluctuations in seasonal elevation patterns ($p=0.10$) and could not explain variation between treatments ($p=0.54$). Previous work in mineral-rich systems suggests that seasonal elevation change can be driven by changes in plant growth and its effect on sediment trapping (Palinkas and Engelhardt, 2019; Noyce and Megonigal, 2021), but at our site, seasonal elevation change is inversely correlated with productivity (Figure 8a). Instead, seasonal elevation patterns correspond to organic matter decomposition inferred from methane emissions measured at our study site. In particular, methane emissions correlate closely with temperature (Darby and Turner, 2008) and inversely with marsh elevation ($p=0.01$), signifying increased organic matter preservation in the winter and increased decomposition in the summer. Warming is known to increase both organic matter productivity (Connor and Chmura, 2000; Crosby *et al.*, 2016) and decomposition (Najjar *et al.*, 2000; Kirwan, Guntenspergen and Langley, 2014; Mueller, Jensen and Megonigal, 2016; Hanson *et al.*, 2020) separately, but the observed summer elevation loss uniquely indicates that the balance between these processes is largely negative, with higher rates of decomposition dominating productivity and reducing organic matter storage. Though counterintuitive, the loss of elevation during the most productive portions of the growing season could be explained by

soil priming effects, where root growth delivers oxygen and organic carbon to anaerobic soils and enhances decomposition (Dakos *et al.*, 2008; Mueller *et al.*, 2020; Rietl *et al.*, 2021). The amplitude of seasonal marsh elevation variability (Figure 8b) mirrors interannual trends in marsh elevation under manipulated warming treatments (Figure 7c). Therefore, at both the seasonal and annual timescales, marsh resilience and carbon storage are decreased at high temperatures (Figure 7c, Figure 8a).

Increasing heterogeneity in microtopography: evidence for decreasing resilience

Ecosystems often respond to stressors with increased spatial variability, such as increased autocorrelation and variance, which can signal an approaching critical threshold and imminent state change (Kéfi *et al.*, 2007; Veraart *et al.*, 2012; Kefi *et al.*, 2014; van Belzen *et al.*, 2017), but few spatial indicators have been tested as early indicators of state change in coastal wetlands (Ganju *et al.*, 2017; Martinez, 2021). Over the duration of this three year study, we observed an increase in the number of elevation measurements that were greater than 20 mm different than adjacent pin measurements in the C3 community as the marsh degraded. These observations inspired us to examine the effect of temperature and plant community on spatial variability using three metrics of microtopography heterogeneity (tortuosity, random roughness, and number of holes, with holes defined as differences in elevation between adjacent SET pin measurements greater than 20 mm) that may predict proximity to state change. Microtopographic heterogeneity decreased through time in the C_4 community, and increased through time in the C_3 community (Figure 9). This pattern could be expected given that the high elevation C_4 marsh is higher in the tidal frame than the C_3 marsh and is therefore farther from an extinction threshold (Rietl *et al.*, 2021). Additionally, we found that heterogeneity increased sharply in the warmest treatments in the C_3 community, as evidenced by a tripling in the number of holes formed in the +5.1 °C

treatment (Figure 9a) and a sharp increase in tortuosity and random roughness in the +5.1 °C treatment (Figure 9b), suggesting a threshold response to warming at high temperatures. Previous work examines heterogeneity at landscape scales, including the development and/or recovery of unvegetated ponds in salt marshes (Temmerman *et al.*, 2003; Ganju *et al.*, 2017). However, our finding that microtopographic heterogeneity is increasing faster in a drowning, low elevation marsh suggests that early signs of ecosystem transition are visible at far smaller spatial scales that precede landscape transitions. Integrating vertical and lateral metrics of marsh vulnerability is critical to understanding the fate of marshes (Ganju *et al.*, 2017; van Belzen *et al.*, 2017), and we find that the warmest temperature treatments amplify both vertical (i.e. elevation change) and spatial (i.e. microtopographic heterogeneity) metrics of marsh vulnerability.

Implications for coastal marsh survival

Coastal carbon pools are simultaneously threatened and maintained by sea-level rise (Najjar *et al.*, 2000; Rogers *et al.*, 2019), and the limits of soil organic matter accumulation help determine the resilience of the microtidal, sediment-deficient marshes most vulnerable to sea-level rise (Mudd, D'Alpaos and Morris, 2010; Kearney and Turner, 2016; Kirwan, Temmerman, *et al.*, 2016). Temperature warming is well known to increase rates of both soil organic matter production (Kirwan, Guntenspergen and Morris, 2009; Gedan and Bertness, 2010) and decomposition (Kirschbaum, 1995; Kirwan and Blum, 2011; Kirwan, Guntenspergen and Langley, 2014) which are opposing processes that affect elevation gain in opposite directions. However, the balance between these processes, and their impact on marsh resilience, has been difficult to isolate and quantify (Figure 10). Previous experiments that rely solely on passive warming generally find positive increases in productivity and elevation change (Charles and Dukes, 2009; Gedan and Bertness, 2009; Kirwan, Guntenspergen and Morris, 2009; Baldwin,

Jensen and Schönfeldt, 2014; Coldren *et al.*, 2016, 2019), but the warming these experiments achieve is relatively modest aboveground and negligible below the soil surface, limiting the ability to influence decomposition. In contrast, our whole-ecosystem soil warming experiment reveals a prominent link between productivity and decomposition expressed over seasonal timescales (i.e. Figure 8) that leads to a consistent temperature optimum of +1.7 °C for marsh resilience and carbon accumulation in two disparate plant communities. Our observation of a distinct temperature optimum helps rectify observations of elevation loss in response to warming at low latitudes (Coldren *et al.*, 2019) with the more general positive responses observed in mid and high-latitude warming experiments (Charles and Dukes, 2009; Gedan and Bertness, 2009; Baldwin, Jensen and Schönfeldt, 2014), thereby indicating a latitudinal increase in resilience (Figure 10). However, our observations also suggest that positive responses will likely diminish through time with further warming, as marshes approach and surpass their temperature optima (Figure 7; Figure 10). Temperature increases of 2 °C have been identified as tipping points for mass coral bleaching and mortality, increased mortality and reproductive failure for intertidal barnacles and mussels, and the expansion of tropical mangroves into temperate wetlands (Hoegh-Guldberg *et al.*, 2007; Helmuth *et al.*, 2010; Cavanaugh *et al.*, 2019). Here, we quantify a distinct and consistent temperature optimum (+1.7 °C) for U.S. mid-Atlantic marsh resilience and soil carbon accumulation. Our work uniquely connects metabolic theory to ecosystem resilience to identify a potential temperature optimum for coastal wetland resilience and therefore contributes to the growing body of evidence that continued warming will negatively impact many coastal and marine ecosystems.

*Adapted from a manuscript in review at **Ecosystems**.*

Chapter 3

Compensatory Mechanisms Absorb Regional Carbon Losses within a Rapidly Shifting Coastal Mosaic

Authors

Alexander J. Smith[1], Karen McGlathery[2], Yaping Chen[1], Carolyn J. Ewers Lewis[2], Scott C. Doney[2], Keryn Gedan[3], Carly K. LaRoche[2], Peter Berg[2], Michael L. Pace[2], Julie C. Zinnert[4], Matthew L. Kirwan[1]

[1]Department of Physical Sciences, Virginia Institute of Marine Science, College of William and Mary, Gloucester Point, Virginia

[2]Department of Environmental Sciences, University of Virginia, Charlottesville, Virginia

[3]Department of Biological Sciences, George Washington University, Washington, DC

[4]Department of Biology, Virginia Commonwealth University, Richmond, Virginia

Abstract

Coastal landscapes are naturally shifting mosaics of distinct ecosystems that are rapidly migrating with sea-level rise. Previous work illustrates that transitions among individual ecosystems have disproportionate impacts on the global carbon cycle, but this cannot address non-linear interactions between multiple ecosystems that potentially cascade across the coastal landscape. Here, we synthesize carbon stocks, accumulation rates, and regional land cover data over 36 years (1984 and 2020) for a variety of ecosystems across a large portion of the rapidly transgressing mid-Atlantic coast. The coastal landscape of the Virginia Eastern Shore consists of

temperate forest, salt marsh, seagrass beds, barrier islands, and coastal lagoons. We find that rapid losses and gains within individual ecosystems largely offset each other, resulting in relatively stable areas for the different ecosystems, and a 4% (196.9 Gg C) reduction in regional carbon storage. However, new metrics of carbon replacement times indicate that it will take only ~7 years of carbon accumulation in surviving ecosystems to compensate this loss. Our findings reveal unique compensatory mechanisms at the scale of entire landscapes that quickly absorb losses and facilitate increased regional carbon storage in the face of accelerating climate changes.

Introduction

The ability of ecosystems, communities, and populations to absorb environmental change and reorganize so as to retain structure and function has been a hallmark of resilience and compensation research (Folke *et al.*, 2004; Ghedini, Russell and Connell, 2015). Compensatory dynamics, occurring when an environmental change stimulates a counteracting response that reestablishes equilibrium, are expected to be an important stabilizing mechanism through which communities respond to environmental change (Gonzalez and Loreau, 2009; Ghedini, Russell and Connell, 2015). While compensatory dynamics have a long history in community and population ecology (Gonzalez and Loreau, 2009), this framework can also provide insights into the mechanisms that potentially stabilize ecosystem extent and function, a growing concern in the face of accelerating changes in global climate (MacArthur, Diamond and Karr, 1972; Houlahan *et al.*, 2007; Loreau and Mazancourt, 2013; Ghedini, Russell and Connell, 2015). This presents the opportunity to expand the traditional application of compensatory mechanisms to explore the novel concepts of spatial and functional compensation, processes necessary for stabilizing entire ecosystems and landscapes in a rapidly changing climate.

Spatial compensation, an expansion of compensation theory, occurs where losses and gains of an individual ecosystem in different locations offset each other, thereby maintaining ecosystem area within the broader region. The preservation of area in migrating ecotones, such as the sea-level driven upland transgression of marshes, poleward expansion of subarctic forests, and upslope migration of alpine ecoclines, are all examples of the principles of spatial compensation across a variety of environmental settings (Gamache and Payette, 2005; Maher, Germino and Hasselquist, 2005; Schieder, Walters and Kirwan, 2018). Functional compensation is independent of spatial compensation and is defined by the preservation of an ecosystem function, despite reductions in process rates within ecosystem subunits (i.e. subregions or habitats) due to environmental change (Schulze and Mooney, 2012). These compensations may be realized as heterogenous responses to environmental changes across the landscape, such as when salt marsh interiors accumulate increased carbon under elevated rates of sea-level rise despite losing carbon through sea-level mediated edge erosion (Herbert, Windham-Myers and Kirwan, 2021). Climate change affects both ecosystem extent and function, often simultaneously, which allows spatial and functional compensation to be used as theoretical frameworks to examine the legacy effect of climate change on landscape dynamics.

Climate change is forcing transitions between coastal ecosystems at an increasing rate that can lead to large-scale ecosystem degradation and loss (Doney *et al.*, 2012; Bernhardt and Leslie, 2013). For example, accelerating rates of sea-level rise are leading to increased marsh erosion and degradation as well as the burial of back-barrier marshes beneath transgressing barrier islands (Theuerkauf and Rodriguez, 2017; FitzGerald and Hughes, 2019; Fagherazzi *et al.*, 2020). Co-occurring climate drivers, such as increasing temperatures and elevated atmospheric CO_2 concentrations, further threaten coastal ecosystems by exceeding the biological

limits of foundational species (Noyce *et al.*, 2019; Smith *et al.*, 2022). Anthropogenic effects, such as alterations to sediment budgets, eutrophication, and urbanization, can further accelerate habitat degradation (Hartig *et al.*, 2002; Kirwan and Megonigal, 2013). There is widespread evidence that direct and indirect anthropogenic influences have changed the distribution, extent, and function of habitats that comprise the coastal landscape mosaic (e.g. Ewers Lewis et al. 2019), but these simultaneous changes to ecosystem structure and function have unclear effects on regional functions, including carbon storage. Moreover, impacts have rarely been examined at the scale of the landscape, rather than that of an individual ecosystem, where inter-ecosystem spatial and functional compensatory mechanisms can emerge.

As the coastal landscape changes, carbon rich ecosystems, such as seagrass meadows and salt marshes, are often replaced with unvegetated sediments that should reduce regional carbon storage in the absence of compensatory mechanisms and other landscape-scale interactions between ecosystems (Mcleod *et al.*, 2011; Garrard and Beaumont, 2014; Trevathan-Tackett *et al.*, 2018; Aoki *et al.*, 2021). Studies have attempted to look at the impact of degraded blue carbon habitat (i.e. marshes, seagrass meadows, mangroves, etc.) on regional and global carbon storage (Siikamäki *et al.*, 2013; Macreadie *et al.*, 2017; Ewers Lewis *et al.*, 2019), but many of these studies neglect to consider functional or spatial gains in distal areas of the coastal landscape. For example, while marshes drowning under sea-level rise reduce marsh area and release stored carbon, increasing sea-level rise drives simultaneous increases in carbon accumulation in the marsh interior (Guimond *et al.*, 2020; Herbert, Windham-Myers and Kirwan, 2021). Furthermore, sea-level rise creates new marsh at the upland boundary additionally compensating for the spatial and functional losses at the seaward edge (Schieder, Walters and Kirwan, 2018; Smith and Kirwan, 2021). At the same time, there is substantial amount of carbon

lost from dying tree biomass during the upland transgression of marshes into forested land (Smart *et al.*, 2020; Smith and Kirwan, 2021). Therefore, solely examining carbon dynamics in specific carbon-rich ecosystems is unsatisfactory in understanding how coastal carbon dynamics are changing regionally. While similar studies that estimate regional carbon storage may concentrate on changes in specific boundaries (He *et al.*, 2016; Fryer and Williams, 2021), the non-linear, non-uniform, and co-occurring nature of ecosystem transitions within the coastal zone requires the examination of the entire coastal landscape mosaic inclusive of the many terrestrial, intertidal, benthic, and epipelagic habitats that comprise it.

Here, we synthesize nearly 40 years of carbon and landcover data across a rapidly transgressing coastal landscape to show that rapid spatial and functional compensatory mechanisms maintain both ecosystem extents and regional carbon storage despite sometimes substantial ecosystem losses. We used land cover data from Landsat images between 1984 and 2020 to quantify increases, decreases, and net changes in ecosystem extent. Multiplying ecosystem extents by area-specific carbon stocks produced landscape-scale carbon stocks for both 1984 and 2020. Using the change in regional carbon stocks and ecosystem-scale carbon burial rates, we then calculated the 'time to replacement' at the regional scale, which is an estimate of the time required for all of the carbon accumulating environments in the landscape to replace the carbon that was lost between 1984 and 2020. Our analysis shows that compensatory mechanisms largely maintain the spatial extent of the most dynamic ecosystems (i.e., barrier islands and salt marshes), but that declines in forest and marsh area led to a small decrease in landscape-scale carbon storage. We calculate that surviving ecosystems compensate for the decadal loss of carbon storage rapidly, suggesting that compensatory mechanisms quickly restore functionality at the landscape scale despite accelerating climate stressors.

Methods

Study Area

We quantified land cover changes, carbon stocks, and carbon accumulation rates for a variety of ecosystems along the Virginia Atlantic coast, a known hotspot for sea-level rise and ecosystem transgression (Chen and Kirwan, 2022; Mariotti and Hein, 2022). The VCR was established in 1970 by the Nature Conservancy and is the site of the VCR Long-Term Ecological Research (LTER) project. The coastal landscape includes 14 undeveloped barrier and marsh islands, intertidal marshes, tidal flats, bays, and lagoons that make up the eastern side of the Delmarva Peninsula along the Virginia Atlantic Coast (Figure 11a, 11b). With a spatial extent >14,000 ha, this is the largest undeveloped barrier system along the U.S. Atlantic Coast and, consequently, provides a unique opportunity to study landscape transformations in the absence of direct human alteration (Hayden *et al.*, 1991). Our study area is bounded on the east by nine barrier islands, which range from 3-12 km long and 0.1-1.0 km wide and are located 2.0-13.5 km offshore (Deaton, Hein and Kirwan, 2017). The back-barrier landscape is a heterogenous mosaic of salt marshes, tidal flats, and subtidal seagrass meadows surrounded by open water with an average depth of 1 m and a tidal range of ~1.2 m (Figure 11a, 11b; Safak et al. 2015; McLoughlin et al. 2015). This region experiences some of the highest rates of relative sea-level rise along the U.S. Atlantic Coast (5.37 ± 0.7 mm yr^{-1} from 1978 to 2019) (Sallenger, Doran and Howd, 2012; Flester and Blum, 2020). Consequently, relatively rapid rates of marsh migration into coastal forests (up to 4.0 m y^{-1} lateral migration) and barrier island retreat (up to 40 m yr^{-1}) are quickly reorganizing the coastal landscape (Figure 11c-e; (Fenster, Dolan and Smith, 2016; Deaton, Hein and Kirwan, 2017; Flester and Blum, 2020). Additionally, the study area includes the largest recovery of an eelgrass ecosystem to date (Orth and McGlathery, 2012; McGlathery

et al., 2013; Orth *et al.*, 2020). Not only do long-term data collected show that the VCR is the most dynamic coastal barrier island landscape on the U.S. Atlantic seaboard (May, Dolan and Hayden, 1983; Morton, 2008; Fenster, Dolan and Smith, 2016), but the extensive catalog of long-term monitoring data available through past research at the VCR makes this one of the most studied undeveloped coastal barrier systems in the U.S..

Landcover Change

To quantify climate-driven landcover change in a shifting coastal mosaic, we gathered Landsat imagery covering the study area between 1984 and 2020 with cloud cover <60% from the USGS EarthExplorer collected by Landsat-5 TM and Landsat-8 OLI. All images were processed using the ancillary Quality Assessment dataset to mask out pixels associated with clouds, cloud shadows, and ice. We restricted our land cover analysis to the portion of the landscape between sea-level and elevations of 2 m above sea-level (NAVD88) according to the high-resolution topobathymetric digital elevation model of the Eastern Shore, which has a horizontal resolution of 1 m and a vertical resolution of 1 cm (Faunce and Rapp, 2020). This elevation range excluded deep, permanent waters within inlet channels and seaward of barrier islands while including the majority of coastal forests influenced by sea-level rise in the region (Molino *et al.*, 2021; Chen and Kirwan, 2022). Imagery was further clipped to our region of interest (i.e. the VCR-LTER) before mapping with random forest classifier. Specifically, we classified the area of interest into five landcover types following the phenology-based algorithm described in detail by Chen and Kirwan (2022): Water, Sand, Marsh, Forest, and lands used by humans (abbreviated in this manuscript to Human). The resulting landcover maps in 1984 and 2020 were thoroughly validated with high-resolution imagery (≤ 1m) acquired from the U.S.

Bureau of Land Management and National Agriculture Imagery Program across the study region that suggest an overall classification accuracy of 94-96% within the VCR-LTER (SI Table 2).

Seagrass extent was quantified separately using seagrass extent data in 2017 collected by the SAV Monitoring and Restoration group at the Virginia Institute of Marine Science (vims.edu/research/units/programs/sav/reports/index.php). In 1984, the seagrass extent was assumed to be zero due to extirpation within the VCR (Orth and McGlathery, 2012; Orth *et al.*, 2020). The spatial extent of barrier islands, not an explicit class in this paper's landcover classification scheme, was calculated manually delineating island extents from high-resolution (≤ 1 m) aerial photographs acquired around 1984 (Aerial Photo Single Frames, the U.S. Bureau of Land Management and USGS EarthExplorer) and 2020 (the National Agriculture Imagery Program, NAIP). Using the resulting maps, we estimated the spatial extent of each of the seven land cover types in 1984 and 2020, and quantified the areal change between 1984 and 2020 for each land cover across the study region (Table 2). We then conducted pixel-wise analysis using the differenced land cover map between 1984 and 2020 in ArcGIS (v10.7) to locate areas undergoing land cover transition and to record the land cover information associated with these transitions (Table 1).

Estimates of Regional Carbon Storage

Regional carbon storage was estimated by synthesizing carbon stocks reported in previous work, with an emphasis on datasets specific to the Virginia Coastal Reserve ranging from 1990 to 2021 (SI Table 1). Our study focused on four vegetated systems (forests, marshes, seagrasses, and barrier islands) known to contribute significant amounts of carbon to regional and global carbon storage (Mcleod *et al.*, 2011). Unvegetated tidal flats and bare underwater sediments were excluded from this analysis because of limited data on spatial extents and limited

influence to coastal carbon storage, respectively. Our reported carbon stocks for these systems represent the carbon stored in soils and living aboveground and belowground biomass. A majority of the datasets reported both above- and belowground carbon stocks, except for barrier islands where a species-specific root-to-shoot ratio was used to approximate belowground biomass. Biomass was then converted to carbon using respective above- or belowground species-specific conversion factors for marsh grass and seagrass vegetation. When a conversion factor was unavailable or the species not listed (e.g. barrier island vegetation, some marsh and forest species), biomass was converted to carbon using a standard 50% conversion. Soil carbon measurements for seagrasses and some marsh sites were quantified directly while soil carbon in barrier islands, forests, and some marsh sites were inferred from a general or site-specific percent organic matter (%OM) to carbon relationship. To similarly scale all ecosystems to a spatially explicit carbon density (g C m^{-2}), soil %OM and carbon stock measurements deeper than 1 m, such as those in salt marshes, were excluded. For ecosystems with organic matter depths shallower than 1 m, soil beneath the deepest measurement was assumed to have no carbon (SI Table 1). Once the carbon stock was determined for a specific ecosystem type, it was multiplied by the spatial extent of the corresponding ecosystem in both 1984 and 2020 to estimate the regional carbon stock of each vegetated ecosystem. Carbon accumulation rates were calculated from datasets that used cesium-137 (^{137}Cs) in salt marshes and barrier islands, and lead-210 (^{210}Pb) in seagrasses. In salt marshes, the average soil carbon accumulation rate was 78.4 g C m^{-2} y^{-1}, in seagrass meadows the average was 40.0 g C m^{-2} y^{-1}, and in barrier islands the average was 21.9 g C m^{-2} y^{-1}.

In addition to these vegetated systems, we considered carbon stored in the water column as dissolved inorganic carbon (DIC). DIC in the water column was approximated using the

CO2SYS MATLAB 1.1 package and total alkalinity (TA), pCO_2, temperature, and salinity data (Orr, Epitalon, and Gattuso 2015; Orr et al. 2018; Lewis and Wallace 1998; van Heuven et al. 2011). Hourly water column pCO_2, temperature, and salinity data were collected in April and June in South Bay in the VCR (Berg *et al.*, 2019). TA was calculated using Cai et al.'s (2010) linear regression, TA = 670.6 + 46.6 S ± 12.3 μmol kg^{-1}, for the Mid-Atlantic Bight, where S is salinity. The average VCR volume, 979.7 ± 126 million cubic meters (Mm^3), was calculated by multiplying area by average depth in 14 bays and summing the resulting volumes (Safak *et al.*, 2015). The average water-column DIC concentration was multiplied by the seawater mass of the VCR lagoon system, 1 Pg, which had been calculated from average seawater density and the average volume (Safak *et al.*, 2015).

Results

Landcover Changes and Carbon Dynamics

The landcover change analyses revealed that over 80% of the study area, the Virginia Coast Reserve (VCR), remained the same class in 1984 and 2020 (Figure 11a-b, Figure 12, Table 1). The stable portion of the landscape with respect to total area is comprised mostly of temperate salt marsh rather than the more dynamic landscape features, such as barrier islands and seagrass. The VCR coastal landscape was dominated by marsh (70% and 67%), forest (12% and 11%), and open-water (6% and 12%) in both years (1984 and 2020, respectively, Table 2). The proportion of sand landcover class remained relatively stable at the landscape scale (7%), and human areas remained <5% of the landscape in 1984 and 2020 (Table 2). The areas of individual ecosystems all decreased except for seagrass and water, which nearly doubled from 26.7 to 53.0 km^2. Forest area decreased by 5.5% (54.0 to 51.0 km^2) and marsh area decreased by 4.0% (318 to 305 km^2). Both sand and human area decreased by ~18% (Table 2). The largest landcover

change observed was seagrass, which increased from ~0 to 29.3 km^2 (increased from ~0% to 6.4% of landscape cover) in response to widespread restoration efforts beginning in 2000 that returned seagrass populations that had been extirpated from the coastal lagoons following marine disease and hurricane disturbance in the 1930s (Orth and McGlathery, 2012). Conversion of water and marsh to sand were the dominant contributors to sand creation (39.9% and 56.3% of sand creation, respectively) and can be best explained by barrier island rollover and migration (Figure 11e, Figure 12). The dominant driver of forest loss was marsh migration (64.8%) followed by the elimination of forested areas on barrier islands (23.9%) (Figure 12). Despite large increases in marsh area near adjacent upland edges (6.6 km^2), losses of marsh at the seaward side (14.3 km^2) offset these gains leading to a 4% net loss of marsh area (Table 2). This approach does not account for any temporary transitions between classification years.

Area-specific carbon storage ranged from 13.9 ± 4.6 (SE) kg C m^{-2} in marshes to 0.30 ± 0.8 kg C m^{-2} in seagrass within the VCR (SI Table 1). A landscape-scale analysis indicates that a majority of carbon within the VCR region is stored in the salt marsh (81% in 1984 and 82% in 2020) (Figure 13). Forest carbon was the second largest contributor to regional carbon storage (17% and 16%) while carbon in the water column, seagrasses, and barrier islands all contributed <3% to the regional carbon storage (Figure 13). Carbon stored in anthropogenic dominated environments (agricultural fields, residential housing, and urbanized areas) were not included in regional carbon estimates, but are expected to contribute negligibly to regional carbon storage given the limited extent within the studied coastal domain (Figure 11a, 11b). Regional carbon storage decreased by 4%, from 4563.9 in 1984 to 4366.9 Gg C in 2020 (Table. 2; Figure 14). This landscape-scale loss of 196.9 Gg C occurred despite large increases in carbon storage in seagrass, which recolonized in the VCR during the study period. The dominant driver of this loss

was the reduction of marsh and forested land, which together accounted for over 95% of the carbon lost between 1984 and 2020 (Figure 13; Figure 14). These changes in regional carbon storage are driven by changes in spatial extent as our estimates do not consider changing environmental factors that could impact the carbon density of an ecosystem, such as temperature, precipitation, atmospheric CO_2, age, or sea-level (Smith and Kirwan, 2021).

Landscape-scale Time to Replacement

Following Smith and Kirwan (2021), the "time to replacement" metric, t_r, can be used to estimate the time required for ecosystem carbon accumulation rates, *CAR*, to replace losses in carbon stocks, C_L (i.e. $t_r = C_L/CAR$). In past applications of the metric, it has been used to look at the carbon lost and replaced over time at a fixed location (i.e. during the transition from forest to marsh at a given point in space). Below, we extend the application of time to replacement to the ecosystem and landscape scales to estimate the amount of time it takes entire carbon accumulating ecosystems within the coastal landscape of the VCR to replace the carbon that was lost from 1984 to 2020.

A meter-scale time to replacement, t_r^{meter} (yr), can be defined as the amount of time that the carbon stock from the loss of a 1 m^2 of ecosystem *x*, C_x (g C m^{-2}), could be replaced by a spatially explicit carbon accumulation rate, CAR_y (g C m^{-2} y^{-1}), of ecosystem *y* where the areas of carbon loss and carbon accumulation are equivalent:

Eq. 1: $$t_r^{meter}(x, y) = \frac{C_x}{CAR_y}$$

where *x* and *y* can be the same or different ecosystems. For example, the large carbon stock in 1 m^2 of forest, C_{forest} = 13,295 g C m^{-2}, would take 169.6 yr to be replaced by 1 m^2 of marsh, CAR_{marsh} = 78.4 g C m^{-2} y^{-1} (SI Table 1).

Similarly, an ecosystem-scale time to replacement, t_r^{eco} (y), can be defined as:

Eq. 2: $$t_r^{eco}(x,y) = \frac{C_x \Delta A_x}{CAR_y A_y}$$

where ΔA_x is the observed change in ecosystem area from 1984 to 2020 (36 yr) for ecosystem *x*, and A_y is the time averaged area of ecosystem *y*. For the forest to marsh example considered above, the ecosystem-scale time to replacement (1.7 yr) is less than the meter-scale time to replacement, because of the small area of lost forest (3.0 km^2) relative to the extant marsh (305 km^2).

This exercise can be done for the sum of all the carbon accumulating ecosystems, called the landscape-scale time to replacement, t_r^{land}:

Eq. 3: $$t_r^{land}(x,\Sigma) = \frac{C_x \Delta A_x}{\sum_i CAR_i A_i}$$

where $\sum_i CAR_i A_i$ is the total carbon accumulation rate of all of the ecosystems within the coastal landscape. The landscape time to replacement for this carbon loss is 1.6 yr, which is relatively similar to the previous calculation due to the dominance of salt marshes within the coastal environment.

Finally, to encapsulate multiple simultaneous changes in ecosystem carbon storage within the landscape, the modified form of a landscape time to replacement can be expressed as:

Eq. 4: $$t_r = \frac{C_{land}}{\sum_i CAR_i A_i}$$

where C_{land} (g) is the net carbon lost at the landscape scale across all ecosystems, $\sum(CAR_i * A_i)$ is the carbon accumulation rate (CAR_i, g C m^{-2} y^{-1}) of all of the ecosystems (*i*) within the coastal landscape multiplied by the respective ecosystem area (A_i, m^2). Using data derived from our

study site (shown in Table 2; C_{land}=196.9 ± 3.2 Gg C; $\sum(CAR_i * A_i)$=25.7 ± .02 Gg C y^{-1}), we find that it takes approximately 7.42 ± 0.75 years to replace the carbon that was lost from 1984-2020 (36 years).

Discussion

Coastal ecosystems are rapidly migrating in response to sea-level rise, leading to a fundamental reorganization of the coastal landscape (Doody, 2013; Deaton, Hein and Kirwan, 2017; FitzGerald *et al.*, 2018; Kirwan and Gedan, 2019). Despite visible differences in land cover (Figure 11c-e), the total spatial extent for individual ecosystems changed very little between 1984 and 2020 (Figure 11a-b, Figure 12, Table 1). We attribute this spatial compensation to widespread but equivalent gains or losses in individual ecosystems (Table 1, Table 2). This indicates that despite significant changes in the location of individual ecosystems, spatial compensation largely maintains the total extent of each ecosystem (Table 1, Table 2), which is consistent with observations from a number of other coastal and terrestrial ecosystems (Turner, 2010; Smith and Goetz, 2021) and for the VCR from 1972-2001 (McGlathery *et al.*, 2013). For example, barrier islands tend to migrate landward while maintaining relative area (Deaton, Hein and Kirwan, 2017), and marsh erosion is compensated by marsh migration regionally (Schieder, Walters and Kirwan, 2018). While spatial compensation can be observed within at least some individual ecosystems of the VCR (Flester and Blum, 2020; Burns, Alexander and Alber, 2021), this represents one of the first studies to examine spatial compensation across multiple ecosystems at the landscape scale.

The shifting mosaic steady-state concept suggests that the overall ecosystem composition is maintained in a landscape despite shifts in ecosystem location (Bormann and Likens, 2012; Forman, 2014). Although our observations of spatial compensation within salt marshes are

consistent with the shifting mosaic steady-state theory, some ecosystems did not maintain consistent spatial extents. We observed significant decreases in forested land and sand and increases in seagrass that were not compensated elsewhere in the landscape (Table 2). Marsh migration into retreating forests was not compensated for by migration of forests into adjacent uplands due to topography and anthropogenic land uses, resulting in coastal squeeze of forested ecosystems (Figure 12) (Pontee, 2013; Torio and Chmura, 2013). Similarly, the net decrease of sand within the landscape is driven by erosion and colonization of barrier island overwash fans that was not compensated by back-barrier spit elongation (Figure 12). However, in similar studies, changes in barrier island extent observed over two different time frames (from 1984 to 2011 and from 1984 to 2016) were drastically different, a 29% reduction and a 11% increase in spatial extent respectively, which emphasizes that temporal scale and the timing of measurements can dictate apparent spatial patterns (Zinnert *et al.*, 2016, 2019).

The lack of spatial compensation in forested land compounds with reduced blue carbon storage to increase the observed reduction in regional carbon storage (Figure 14, Figure 15, Table 2). Area-specific carbon storage ranges within the VCR from 11.7 kg C m^{-2} in marshes to 0.30 kg C m^{-2} in seagrass (SI Table 1). Marsh carbon storage, 11.7 kg C m^{-2}, was found to be smaller than the average carbon storage in marshes of the conterminous United States (27.0-28.0 kg C m^{-2}), Europe (26.1 kg C m^{-2}), and Southeastern Australia (25.3 kg C m^{-2}), but within the range of measured soil carbon stocks (Kelleway *et al.*, 2016; Nahlik and Fennessy, 2016; Holmquist *et al.*, 2018; Van de Broek *et al.*, 2018). Although seagrass meadows can store significant amounts of carbon (Fourqurean *et al.*, 2012), the juvenile stocks in the VCR (<20 years old) contain shallow belowground organic carbon profiles, with organic-rich sediments in the top 3-6 cm that have accumulated since seagrass restoration, far shallower than organic

matter depths in salt marshes, which can extend more than a meter deep (Oreska, McGlathery and Porter, 2017). This results in a smaller spatial carbon density that integrates carbon stored in the top 1 meter despite relatively dense carbon in shallow seagrass soils. If seagrasses accumulated soil carbon stores at comparable depths to the other blue carbon systems, the landscape scale carbon storage of seagrass would approximately triple (SI Table 1, Figure 14). Together, we find that positive changes in the carbon stocks of seagrasses did not compensate for the loss of carbon from forests and the other blue carbon habitats, resulting in a landscape-scale reduction in carbon stocks (Figure 15, Table 2). Coastal forests are not typically placed in a blue carbon context, but studies that examine non-wetland coastal forest stocks find similarly high magnitude carbon storage (Smart *et al.*, 2020, 2021; Aguilos *et al.*, 2021; Smith and Kirwan, 2021). The scale of carbon loss observed between 1984 and 2020 (196.9 Gg C) is on a similar scale to other studies that examine the loss of carbon due to overwash, urbanization, or wildfire in other systems (Zhang *et al.*, 2012; Theuerkauf and Rodriguez, 2017; Sirin *et al.*, 2020). While the propagation of dominant landscape features through time mirrors the shifting mosaic steady-state concept, the reduction in regional carbon storage indicates that landscape-scale compensatory functions are temporarily reduced (Figure 14).

Blue carbon ecosystems are well known to be vulnerable to a variety of climate and anthropogenic stressors that threaten the persistence of individual ecosystems and their carbon pools (Mcleod *et al.*, 2011). However, the broader coastal landscape is uniquely positioned to potentially replace carbon lost from individual points within the landscape because of rapid carbon accumulation rates across a diverse suite of ecosystems. Where ecosystems are lost, high carbon accumulation rates in surviving ecosystems may be able to mediate carbon loss (Figure 15, Elsey-Quirk *et al.*, 2011; Mcleod *et al.*, 2011; Holmquist *et al.*, 2018; Smith and Kirwan,

2021). For example, despite loss in barrier island volume, the expansion of highly productive shrubs into barrier island grasslands have compensated for carbon loss (Zinnert *et al.*, 2016, 2019; Woods, Tuley and Zinnert, 2021). Although the time to replacement metric has been largely used to look at the carbon lost and replaced over time at a fixed location (Smith and Kirwan, 2021), the extension of the metric to estimate the time required for an entire landscape to replace lost carbon reveals small landscape scale legacy affects. Specifically, we find that it takes approximately 7 years to replace the 4% reduction in landscape carbon storage observed over 36 years. This metric suggests that surviving ecosystems quickly replace the amount of carbon lost during decadal-scale ecosystem transitions.

The carbon loss for minor reductions in ecosystem extents can be replaced by the entire VCR landscape in a matter of seconds (Figure 16a), but larger scale ecosystem reductions can have a legacy effect on regional carbon storage that last longer than centuries (Figure 16b). As the carbon stock of the lost ecosystem increases, so does the time to replacement and the legacy effect of that carbon loss; carbon lost from 1 m^2 of forest loss takes two orders of magnitude longer to be replaced than carbon lost from 1 m^2 of barrier island (Figure 16a). However, the magnitude of the legacy effect of carbon loss is not only reliant on the magnitude of loss, but also the rate at which it is replaced. Barrier islands are shown to have the slowest regional soil carbon accumulation rate leading to the slowest compensatory mechanisms in the VCR (Figure 16b).

Similarly, the area over which carbon is replaced can greatly affect the rate of recovery. For example, 1 m^2 of forest loss was estimated to have a legacy effect of 169.6 years when being replaced by 1 m^2 of marsh (eq. 1; Smith and Kirwan, 2021). The legacy effect decreases to ~20 seconds when 1 m^2 of forest loss is replaced by the cumulative area of all the marshes within the

VCR (Figure 16a; eq.2: 13.9 kg C/25.7 Gg C y^{-1}=17.7 seconds). Not only does this indicate that times to replacement will increase with marsh loss, but it also indicates that functional compensation may be scale dependent with weak compensation at local scales and stronger compensation at larger scales. However, as spatial scales increase, so does uncertainty in carbon loss. A global application of the time to replacement metric could reveal compensatory mechanisms across a range of spatial scales, but accounting for changes in carbon storage and accumulation across multiple spatial and temporal scales remains complex.

To project the legacy effect of complete ecosystem loss on the landscape, we apply the time to replacement metric to approximate the amount of time required to replace carbon lost from entire landscape-scale ecosystem collapse (Figure 16b). While this scale of collapse is rare, climate change and urbanization can often result in relatively rapid and irreversible ecosystem loss seen in deforestation and seagrass extirpation (Zhang *et al.*, 2012; Arias-Ortiz *et al.*, 2018). For example, in the VCR, seagrass became locally extinct due to a combination of hurricane disturbance and an outbreak of seagrass wasting disease in the 1930's (Orth and McGlathery, 2012; Orth *et al.*, 2020). Within the VCR, if all current seagrass was to experience a similar die-off and the soil carbon stocks were not preserved within the landscape, our analysis indicates that the system would be in a carbon deficit for less than half a year (Figure 16b; eq.4: 8.66 Gg C/25.7 Gg C y^{-1}=0.34 years). Similarly, if forests were suddenly lost, due to wildfire or disease for example, the entire coastal landscape would require approximately 30 years to replace the lost carbon (Figure 16b; eq.4: 754 Gg C/25.7 Gg C y^{-1}=29.3 years). This emphasizes that the coastal landscape is resilient even to rapid, large-scale changes in the carbon dense ecosystems that comprise it.

These time to replacement calculations are based on observed carbon accumulation rates and carbon stocks across a variety of coastal ecosystems, and are therefore inherently simplistic. They do not include dynamic aspects of preservation and decomposition following ecosystem loss, interacting facets of climate change, temporal variability during ecosystem recovery, or couplings and exchanges between ecosystems. Organic matter preservation between systems following ecosystem transition may reduce time to replacement estimates in highly connected landscapes: organic matter produced in marshes contribute to seagrass soil carbon stocks and salt marsh soils can incorporate eelgrass detritus (Greiner *et al.*, 2013; Oreska, McGlathery and Porter, 2017; Prentice *et al.*, 2020; Ward *et al.*, 2021; Krause *et al.*, 2022)**.** However, the preservation and connectivity of organic matter between ecosystems in the coastal environment is highly variable. On the other hand, recovering seagrass meadows require a decade for carbon accumulation rates to be equivalent to mature ecosystems (Greiner *et al.*, 2013; McGlathery *et al.*, 2013), which could substantially increase the time to replacement in seagrass meadows. However, because marshes rather than seagrasses dominate carbon storage and dynamics within this study area, accounting for this lag time in functionality still results in decadal landscape-scale times to replacement. While the refinement of these caveats will improve the accuracy of time to replacement estimates, the rapid replacement of even large-scale carbon reductions implies a functional resilience in the coastal landscape capable of absorbing climate driven reductions in carbon storage.

Conclusions and Implications

While compensatory mechanisms have traditionally been examined in the context of how populations and communities reorganize following environmental change, our work expands the scope of compensatory mechanism theory to encompass abiotic processes at the scale of entire

landforms (i.e. spatial and functional compensation). From 1984 to 2020, we found that the landscape composition of a rapidly migrating coastal mosaic remained relatively constant because a majority of landscape losses were compensated by gains elsewhere in the landscape (Table 2, Figure 12). Contrary to this apparent stability, there was a slight reduction in regional carbon storage across the landscape as critical mature ecosystems were unable to spatially compensate losses (Figure 12, Figure 14, Figure 15).

As an immature ecosystem ages, the functionality of the entire system is expected to increase, but accelerating rates in sea-level rise and resulting ecosystem transitions could prevent recovery before net gains in carbon storage are achieved (Smith and Kirwan, 2021). In terrestrial forested ecosystems, enhanced woody biomass growth following wildfires can result in functional compensation of lost carbon pools (Kashian *et al.*, 2006; Smithwick *et al.*, 2009), but only if the system recovers before the next disturbance (Smithwick *et al.*, 2009; Brown and Johnstone, 2011). In contrast to these findings, the short timescales calculated for the replacement of coastal carbon suggest compensatory mechanisms in the coastal landscape are uniquely suited to maintaining functional rates that exceed ecosystem rates of carbon loss. However, when ecosystems with high carbon accumulation rates are converted to ecosystems with low carbon sequestration, landscape-scale carbon accumulation is reduced. While spatial compensation in this study conserved ecosystem area, rapid loss of area in high carbon accumulating systems, such as the conversion of mangroves to shrimp farms or seagrasses to bare mud, results in decreased regional carbon accumulation, in addition to the initial carbon stock loss (Aoki *et al.*, 2021; Merecí-Guamán *et al.*, 2021). Therefore, even if the landscape was able to quickly replace the large magnitude of lost carbon, the reduction of blue

carbon ecosystems leads to slower accumulation of long-term carbon stocks in the coastal landscape.

We estimated that it will take less than 8 years for the coastal landscape to compensate for the loss of carbon associated with the landscape changes observed over 36 years (Figure 16). The pace of ecosystem transition and loss of local carbon stocks are fundamentally linked to rates of sea-level rise in barrier islands, marshes, and coastal forests (Theuerkauf and Rodriguez, 2017; Smith and Kirwan, 2021; Mariotti and Hein, 2022), suggesting that accelerating sea-level rise rates will further lengthen the time for carbon pools to recover. Although disturbances associated with climate, storms, and anthropogenic stressors are ubiquitous in coastal landscapes, our estimates of short replacement timescales suggest that functional compensation is possible despite potentially rapid moments of carbon loss. Together with our observations of maintained ecosystem extent, these results suggest that spatial and functional compensation are achieved rapidly at the scale of entire landscapes, and that fast-acting compensatory dynamics may quickly compensate for the carbon lost in rapidly transitioning ecosystems.

*Adapted from a manuscript in review at **Estuaries and Coasts**.*

Chapter 4

Microtopographic Variation as an Early Indicator of Ecosystem State Change and Vulnerability in Coastal Marshes

Authors

Alexander Smith[1], Glenn Guntenspergen[2], Joel Carr[2], David Walters[2], Matthew Kirwan[1]

[1]Virginia Institute of Marine Science, William & Mary, Gloucester Point, VA, 23062, USA

[2]Eastern Ecological Science Center, U.S. Geological Survey, Laurel, MD, 20708, USA

Abstract

As global climate change alters the magnitude and rates of environmental stressors, predicting the extent of ecosystem degradation becomes increasingly urgent. At the landscape scale, disturbances and stressors can increase spatial variability and heterogeneity – indicators that can serve as potential early warnings of declining ecosystem resilience. Increased spatial variability in salt marshes at the landscape scale has been used to quantify the propagation of ponding in salt marsh interiors, but ponding at the landscape scale follows a state change rather than predicts it. Here, we suggest a novel application of commonly collected Surface Elevation Table (SET) data and explore millimeter-scale marsh surface microtopography as a potential early indicator of ecosystem transition. We find an increase in spatial variability using multiple metrics of microtopographic heterogeneity in vulnerable salt marsh communities across the North American Atlantic seaboard. Increasing microtopographic heterogeneity in degrading salt marshes mirrored trends in a diverse array of systems with alternative stable states – indicating that early warning signals of marsh drowning and ecosystem transition are observable at small-

spatial scales prior to runaway ecosystem degradation. Congruence between traditional and novel metrics of marsh vulnerability indicate that microtopographic metrics can be easily applied to existing SET records to identify hidden vulnerability before widespread marsh degradation.

Introduction

Salt marshes provide critical ecosystem services, but are threatened by sea level rise and diminishing sediment availability that together lead to erosion and marsh submergence (Hopkinson, Cai and Hu, 2012; Temmerman *et al.*, 2013; Kirwan and Megonigal, 2013). Regional and global assessments predict that sea level rise (SLR) alone could lead to the loss of 20-50% of marshes by the end of the century (Craft *et al.*, 2009; Kirwan, Temmerman, *et al.*, 2016). On the other hand, feedbacks between vegetation, inundation, and sediment transport allow some marshes to persist with sea level rise as stable ecosystems for millennia (Kirwan and Megonigal, 2013). Predicting the fate of marshes to sea level rise is hotly debated (Kirwan et al., 2016; Schuerch et al., 2018; Tornqvist et al., 2021; Saintilan *et al.*, 2022), driven in part by the realization that early warning signals are difficult to detect in systems with non-linear or "catastrophic" transitions (Wilson and Agnew, 1992; Scheffer *et al.*, 2001).

The collapse of marshes is often expressed through the runaway growth of unvegetated ponds, that consist of shallow depressions filled with standing water, and occur within the marsh interior (Mariotti, 2016). The transition between stable, vegetated marsh and unvegetated pond is abrupt, commonly irreversible, and driven by positive feedbacks that separate them into two alternative states (Wang and Temmerman, 2013) Once ponds form, positive biophysical and biochemical feedbacks expand the ponded area, which potentially leads to permanent marsh loss (Stevenson, Kearney and Pendleton, 1985; DeLaune, Nyman and Jr., 1994; Mariotti and Fagherazzi, 2013; Mariotti, 2016; Himmelstein et al., 2021). As ponds proliferate in the marsh

landscape, extensive pond networks decrease wetland stability through enhanced sediment export and reduced sediment trapping (Stevenson, Kearney and Pendleton, 1985; Ganju, Nidzieko and Kirwan, 2013; Ganju et at al., 2017).

Salt marsh vulnerability assessments often rely on comparisons between the rate of sea level rise and point-based measurements of marsh elevation change or vertical accretion rates (Reed, 1995; Raposa *et al.*, 2016). While these traditional methods capture vertical stability, they underestimate spatio-temporal variability and neglect lateral processes, such as ponding, erosion, and lateral migration, across the landscape (Kirwan, Temmerman, *et al.*, 2016; Ganju *et al.*, 2017). Recent modelling indicates that these neglected lateral dynamics are especially important as biophysical feedbacks maintain marsh stability in the vertical direction, but not the lateral direction (Mariotti and Fagherazzi, 2013; Mariotti and Carr, 2014). Therefore, these traditional metrics of wetland vulnerability neglect spatial dynamics that may be more representative of whole-ecosystem resilience, and offer clues to impending ecosystem transitions.

The Surface Elevation Table (SET) method is a global standard for assessing wetland vulnerability to SLR through the monitoring of vertical elevation change (Webb *et al.*, 2013; Cahoon *et al.*, 2006; Webb *et al.*, 2013; Raposa *et al.*, 2016; Jankowski, Törnqvist and Fernandes, 2017; Saintilan *et al.*, 2022). The method measures elevation change relative to a stable benchmark and is typically paired with an artificial marker horizon (consisting of feldspar, clay, or sand) to capture the suite of biophysical processes contributing to the gain (subsidence) and loss (accretion) of marsh elevation change through time (Callaway, Cahoon and Lynch, 2013). SET stations are used extensively; from 1997 to 2017 at least 985 SETs were installed within Louisiana (Covington, 2020) and over 1,000 SET stations on the mid-Atlantic U.S. coast were affected by Hurricane Sandy in 2012 (Yeates *et al.*, 2020).

SET stations have been utilized in numerous field studies (Baustian, Mendelssohn and Hester, 2012; Lovelock *et al.*, 2015; Blum *et al.*, 2021), coordinated wetland monitoring networks (Raposa *et al.*, 2016; Jankowski, Törnqvist and Fernandes, 2017), and global reviews to quantify wetland vulnerability (Saintilan *et al.*, 2022). However, the collected data is underutilized by focusing on solely the vertical component. Although the SET method explicitly includes measurements of elevation at multiple discrete points within the same local area, the full set of collected data is seldom utilized or even analyzed (Smith *et al.*, 2022). Because SET stations measure elevation at multiple discrete points within the same local area through time, these stations additionally capture changes in the microtopography of the marsh surface. However, this data is seldom utilized or even analyzed (Smith *et al.*, 2022). While the focus on the vertical component of SET records follows traditional understandings of marsh vulnerability to SLR, analyzing changes to the spatial variation of SET records likely aids in detecting early warning signals of wetland degradation prior to ecosystem state change.

Microtopography in wetland ecosystems is driven by numerous abiotic and biotic drivers as well as the interactions between them (Figure 17a; Diamond *et al.*, 2021). While these numerous drivers create a spatially complex surface microtopography, climate change imparts directional changes on these drivers to have cascading changes to microtopography (Figure 17a). Similar dynamics can be seen at the landscape scale, where accelerating rates of SLR are homogenizing not just the landscape diversity of marshes, but also the topography (Mariotti, 2020; Mariotti *et al.*, 2020; Schepers, Brennand, *et al.*, 2020). As ponds dominate the landscape, average elevation of the landscape falls because ponds exist as a stable alternative state at lower elevations (Watson *et al.*, 2017; Schepers, Brennand, *et al.*, 2020). However, the distribution of landscape-averaged elevation is heteroscedastic as the elevation variance of the landscape

initially increases during the transition period between alternative stable states (Schepers, Brennand, *et al.*, 2020; Wang *et al.*, 2021). We hypothesize that prior to pond formation, wetland microtopographic variation will similarly increase as the system degrades (Figure 17b). Uniquely, while this variance is likely to follow the same pattern during the "catastrophic", non-linear transition between alternative states (Wilson and Agnew, 1992; Scheffer *et al.*, 2001), increasing microtopographic variation may serve as an early warning signal of ecosystem state change.

To examine this novel early indicator of ecosystem state change in coastal marshes, we analyzed changes in multiple metrics of microtopographic variation across ~14 years of SET data from 20 SET stations across the U.S. mid-Atlantic coast. Here, we show that multiple metrics of changing microtopographic variation correlate with traditional metrics of wetland vulnerability and that these metrics may be an early warning indicator of state change in wetlands that are likely to be vulnerable to future rates of SLR.

Methods

Approach

Eight tidal salt marshes along the Atlantic Coast of the United States ranging across Virginia at the southern extent and Maine at the northern extent, were selected for study. Specifically, we examined salt marshes within Saxis Wildlife Management Area (SX) in Virginia, Fishing Bay Wildlife Management Area (FB8), Blackwater National Wildlife Refuge (BW7), the Smithsonian Environmental Research Center at Hogs Island (HI), and Eastern Neck National Wildlife Refuge (EN) in Maryland, Bombay Hook National Wildlife Refuge (BH) in Delaware, Great Meadows National Wildlife Refuge (GM) in Connecticut, and Rachel Carson

National Wildlife Refuge (RC) in Maine (Figure 18). Within this extent, often referred to as the mid-Atlantic, the 50-year averaged rates of SLR ranged from 4.00 mm y^{-1} in Virginia (SX), where rates are twice as high as eustatic rates (~ 2 mm y^{-1}), to 1.90 mm y^{-1} in Maine (RC) (Table 3). Porewater salinity at these sites range between 8.9-19.9 ppt without a clear latitudinal gradient (Table 3). The unvegetated to vegetated ratio (UVVR) of marsh vegetation within these sites, specifically the 100 m^2 area surrounding the SET stations, ranged from 0.94, which indicates nearly complete unvegetated marsh, to 0.001, indicating near ubiquitous vegetated marsh (Table 3).

At each of these salt marsh sites, two surface elevation monuments (SETs) were installed to monitor elevation changes driven by SLR with the exception of FB8 and BW7 where four SETs each were installed, which is distinguished through the addition of A or D after the site identification labels (Table 3). SET stations are comprised of a deep rod SET marker that is installed deep into wetland soils until reaching refusal to which a receiver is attached. Off of this receiver, the SET arm can be affixed and then rotated to four of eight permanent positions on the receiver. The SET is a portable device that provides repeatable, high-precision measurements of relative elevation change at consistent locations within coastal wetlands. This portable instrument extends horizontally over the marsh surface and from this extended arm, approximately seven or eight pins at fixed points along the instrument are dropped to marsh surface and the height of those pins above the arm is measured. At the next measurement event, these pins reoccupy the same location on the wetland surface and are measured again. This repetitive measurement monitored through time examines changes to marsh surface elevation. Pin lengths are not measured if the marsh surface is obstructed, such as by wrack deposits or ice deposits. See Lynch, Hensel and Cahoon (2015) for extended details about SET instrumentation.

Most SET stations were installed in 2005 with the first measurement taken between July to September of 2005, except for SX, GM, and RC, which were installed in 2006 and were first sampled in March and May of 2006. All SETs were monitored with the same frequency for at least 13.5 years with collection dates occurring within 1-2 months of each other across the sites. SETs were measured at least twice yearly until 2008 after which SETs were measured once per year until 2019. SET stations were mostly installed above the site specific mean high water, except for the two SETs at BW7 which were 0.28 to 0.11 m below mean high water and, as sites, had limited land above mean high water. When installed, the dominant vegetation at most sites were either *Spartina patens*, *Distichlis spicata*, or *Schoenoplectus americanus* except for at RC where one SET was located within *Glaux maritima* (Table 3). Vegetation density and changes to both density and species were not recorded through time.

Traditional Vulnerability Metrics

Elevation change is calculated by averaging the rate of elevation change for each pin (n=28-32) within a SET through time. Cumulative elevation trends are regressed at the pin level to increase precision and to consider serial autocorrelation. This method results in approximately 30 estimates of linear trends that are then averaged to the entire station to get one, average rate of elevation change. Comparison of surface elevation change rates to the rate of local SLR allows for the calculation of the elevation change deficit (Cahoon, Reed and Day, 1995). Since the 1990s, elevation change deficits have been the benchmark for determining submergence potentials of wetland ecosystems (Cahoon, Reed and Day, 1995; Cahoon *et al.*, 2006; Cahoon, 2015; Lovelock *et al.*, 2015; Saintilan *et al.*, 2022; Steinmuller *et al.*, 2022). The general equation for elevation change deficit is:

$E_{def}=E_c-SLR$

Where E_c is the rate of elevation change (mm y^{-1}) and *SLR* is the local rate of SLR (SI Table 1). We utilized the 50-year averaged rate of SLR (mm y^{-1}) because it was found to be the greatest predictor of vertical accretion (Saintilan *et al.*, 2022). Rates of SLR were derived from the nearest NOAA tidal gauge with at least a 50-year record of sea level. Typically, a marsh is considered vulnerable if the elevation change deficit is negative, which indicates that the measured elevation change rate is less than the selected rate of SLR. However, it should be noted that the rate of SLR used can change vulnerability interpretation (Saintilan *et al.*, 2022). For example, because of general accelerations in eustatic SLR, using a rate of SLR averaged over more recent years will likely lower the elevation change deficit and increase the perceived vulnerability of the wetland.

Novel Microtopographic Vulnerability Metrics

Field measurements of microtopography consisted of pin length measurements taken along the SET arm. Our SET arm consists of 8 fixed points approximately 4 cm apart from which pins are lowered to the sediment surface and length is measured. The SET arm is rotated 90 degrees around the anchored center of the SET station and pin length is measured along the arm following each rotation resulting in approximately 32 measures of relative elevation (Figure 19). Microtopography was quantified using four index measures: random roughness (RR), tortuosity (T), elevation range (ΔH), and the surface area to map area ratio (SA:MA). Random roughness is the standard deviation of all pin readings at a point in time ($\sqrt{\frac{\sum(x_i - x_\mu)}{n-1}}$) and is the most suitable indicator of water storage in local depressions (Kamphorst *et al.*, 2000; Karstens *et al.*, 2016). For the two-dimensional path along each arm, the ratio of the over-surface distance to the corresponding straight-line path is referred to as “tortuosity” (Moser, Ahn and Noe, 2007; Karstens *et al.*, 2016; Smith *et al.*, 2022) and is defined as

$$\sum\sqrt{((x_2 - x_1)^2 + (y_2 - y_1)^2 + (z_2 - z_1)^2))/l)}$$

Where $(x_2 - x_1)$ and $(y_2 - y_1)$ are the respective distance in the x and y direction between adjacent pins, $(z_2 - z_1)$ is the difference in measured pin length, and *l* is the straight-line path length along the SET arm. This equation produces four tortuosity measurements per SET, one measure of tortuosity along each arm replication, which are then averaged to the plot level. The elevation range (ΔH) is calculated from the difference between the highest and lowest point measured at the SET during a sampling period. SA:MA is calculated in Matlab (version R2018b) by first using the *griddata* function. This function fits a surface to scattered elevation data by interpolating a surface so that it passes through the data points and interpolates intermediate values according to a triangulation-based natural neighbor interpolation. The interpolated surface consists of a square surface encompassing the extent of the area that the SET arm covers with 32 interpolated values along each edge of the square for a total of 1024 interpolated points fitted to the 32 loaded data points (Figure 19). The surface area of the interpolated surface is then measured in Matlab using the *delauney* function, which creates a 3-D Delauney triangulation from the points within the interpolated surface and returns the indices of the triangles. Using these indices, we then calculate the area of the individual triangles and the cumulative area of the interpolated surface. Finally, dividing the surface area of the interpolated surface to the footprint of the SET produces SA:MA. Tortuosity and SA:MA are both unitless ratios.

Microtopography of the marsh surface is likely to be variable between sites based off of local biotic and abiotic factors (Diamond *et al.*, 2021). Therefore, to relate microtopography to vulnerability, we focus on the change in microtopography (SI Figure 1). According to our hypothesis, we expect microtopographic variation to increase as a vulnerable system becomes more degraded. Therefore, we stipulate that these microtopographic metrics indicate

vulnerability if the linear change in microtopographic variation increases significantly during the study period. Linear regressions were fitted in Matlab and significance was tested using an F-statistic which tests the significance between two datasets – here the modeled linear relationship and a population showing a null hypothesis (i.e. stable microtopographic variation). Metrics that show significant changes in microtopographic variability are then cataloged in the Marsh Vulnerability Report Card (Table 4).

Results

Traditional Vulnerability Metrics

Elevation change data from the twenty SET stations indicated that rates of elevation change ranged from -7.83 to 5.95 mm y^{-1} over the duration of the records. Negative rates of elevation change, or elevation loss, were recorded at only two SETs, FB8D4 and BW7D4 (-7.83 and -0.94 mm y^{-1}, respectively). All other elevation change rates were greater than zero, indicating increasing elevation during the study period. Of these SETs, the average elevation change rate was 3.46 mm y^{-1} (± 1.22 mm y^{-1}, standard deviation) and was greatest at BH2 (5.95 mm y^{-1}) (SI Table 1). The elevation change deficit, the difference between elevation change and the 50-year averaged rate of local SLR (SI Table 1), ranged from -11.72 m y^{-1} (FB8D4) to 2.19 mm y^{-1} (BH2) (Figure 20). Of the twenty SETs, seven had elevation change deficits significantly less than zero (with an average of -3.90 ± 2.04 mm y^{-1}), seven SETs displayed elevation change deficits not significantly different than zero (-0.48 ± 0.56 mm y^{-1}), and six SETs had significantly positive elevation change deficits (1.52 ± 0.52 mm y^{-1}) (Figure 20). Based on these elevation change deficits, we then classify our set of SETs into three categories: “vulnerable”, where elevation change deficit is negative, “steady”, where the elevation change deficit is not

significantly different than zero, and "surplus" where the elevation change deficit is significantly positive (Figure 21).

Novel Microtopographic Vulnerability Metrics

Initial measurements of microtopography indicated significant differences between SETs. For example, RR was highest at BW7D (1.20 mm), approximately 2.5 times rougher than the site with the lowest RR (SX4, 0.46 mm). However, an insignificant relationship was found between initial variability and change in microtopographic variation across all metrics (p-value =.42). Sites where microtopographic variability increased significantly were categorized as vulnerable. RR increased at a rate significantly greater than zero across 12 SETs and was the microtopographic metric that identified the greatest number of sites as vulnerable (Figure 21a; Table 4). Tortuosity increased at a significant rate at 8 SETs, all of which were also indicated as vulnerable by RR (Figure 21b; Table 4). At 11 SETs, ΔH increased at a significant rate. However, two of these SETs (HI2 and HI3) were not indicated as vulnerable according to either the tortuosity or RR metrics (Figure 21c; Table 4). Finally, SA:MA increased at a significant rate at 6 SETs (Figure 19; Figure 21d; Table 4). These SETs were indicated as vulnerable by all aforementioned microtopographic variation metrics. Across all of these microtopographic metrics, positive rates of change are associated with a marsh surface that is increasing in roughness generally.

Discussion

Microtopographic Change as an Early Indicator of Ecosystem Vulnerability

"Critical slowing down", is an early warning signal for impending state changes, where the time required for a system to recover from a disturbance lengthens as the magnitude of

stressor applied increases, and typically results in an increase in spatial heterogeneity and stochasticity under applied stress (van Nes and Scheffer, 2007; Dakos *et al.*, 2008; van Belzen *et al.*, 2017). In coastal wetlands, vegetation recovery to disturbance slows with increasing inundation, thereby increasing the risk of marsh degradation (van Belzen *et al.*, 2017). Ponds and stable wetlands display a markedly bimodal elevation distribution with a low proportion of transitional, intermediary states within the marsh landscape, and with little potential for unvegetated ponds to become revegetated (Wang and Temmerman, 2013; Watson *et al.*, 2017; Schepers, Brennand, *et al.*, 2020). Given the feedbacks that maintain ponds and marshes at their respective stable equilibria, ponds and wetlands have been proposed to reflect alternative ecosystem states, where early warning signals are critical for forecasting impending state changes prior to landscape-scale changes.

While landscape heterogeneity encapsulates the degree of ecosystem degradation, changes in microtopographic variation potentially precede state change because microtopography is highly sensitive to the abiotic and biotic drivers that experience critical slowing down (van Belzen *et al.*, 2017; Diamond *et al.*, 2021). In wetlands, as vegetation recovery rates decrease with increased inundation stress from rising sea levels, a greater proportion of the marsh platform is likely in or near a lower elevation degraded state following disturbances (van Belzen *et al.*, 2017; Schepers, Kirwan, *et al.*, 2020). Therefore, microtopographic variation is expected to increase with inundation, making microtopography a potential leading indicator of landscape-scale ecosystem state change. While similar fundamental biophysical interactions between vegetation and morphology have been used to examine mechanisms that stabilize marsh resilience to SLR (Kirwan and Megonigal, 2013), this study presents the novel idea that changes in sub-meter scale topography can be used as an early

indicator of looming state change that can be detected prior to large scale state changes that would be captured with traditional approaches to assessing wetland vulnerability.

Traditional analyses of wetland vulnerability utilizing SET data emphasize elevation change deficits, the difference between the rates of elevation change and local SLR, as a primary indicator of wetland vulnerability (van Wijnen and Bakker, 2001; Cahoon *et al.*, 2006; Kirwan and Temmerman, 2009; Cahoon and Guntenspergen, 2010; Cahoon, 2015). According to this traditional metric, 7 of the SETs in this study are highly vulnerable to SLR while the other SETs are keeping pace with SLR (7 SETs) or increasing in elevation faster than the rate of SLR (6 SETs) (Figure 20, Figure 21, SI Table 1). The collated novel metrics of changing microtopographic variation examined indicated similar results: 6 of the SETs are vulnerable according to all four metrics, 8 were categorized as vulnerable by one, two, or three metrics, and 6 were identified as stable ecosystems (Table 4). While a limited sample size prevents the application of significant statistical regressions between the novel and traditional vulnerability metrics, 6 out of the 7 SETs indicated by traditional metrics as highly vulnerable were positively identified as vulnerable by all novel microtopographic metrics (Figure 22). This suggests that microtopographic variation can be used to assess vulnerability in those wetlands that are at high risk of drowning from SLR. Of the SETs where the elevation change was approximately equal to the 50-year averaged rate of SLR, 5 out of the 7 SETs were indicated as vulnerable by at least one microtopographic metric (Figure 21, Figure 22). This could indicate that while these sites are keeping up with historic rates of SLR, modern rates may be exceeding marsh stability and increasing ecosystem degradation. Of the 6 sites with positive elevation change deficits and not considered vulnerable to SLR, 2 SETs were categorized as vulnerable by at least one microtopographic metric (Figure 22).

Without additional information regarding biomass density or vegetation shifts, it is impossible to determine if these indicators are false positives or indicators of a hidden vulnerability not captured in the elevation change deficit. For example, because microtopography is greatly affected by vegetation morphology and density, changing microtopography could be driven by SLR induced recovery time reductions or by independent changes in plant community (Bertness, Gough and Shumway, 1992; Diamond *et al.*, 2021). Additionally, abiotic drivers like wrack deposition and sediment accumulation can both increase variance or homogenize the marsh surface (Werner and Zedler, 2002). The limitations of this dataset prevent the examination of these co-occurring drivers, but the general congruence between microtopographic and traditional wetland vulnerability metrics indicates that microtopographic changes can be used as a proxy for wetland vulnerability. A holistic model that integrates both traditional and novel microtopographic metrics as well as information regarding changes in vegetation density and species that affect both metrics may best encapsulate wetland vulnerability. Additionally, examining these changes in SET records that span the entire transition from the vegetated to ponded ecosystem states would better reveal how early microtopography can detect decreased vulnerability and therefore further resolve some of these potential false positives.

Temporal and Spatial Scaling of Microtopography

Microtopography is driven directly by abiotic and biotic drivers that are influenced by climate forcing (Diamond *et al.*, 2021). Because of this cascading relationship, changes in microtopographic variation may be more sensitive to alterations to the climate than processes like elevation change, which is a factor of dynamic biophysical feedbacks that operate at the decadal scale (Törnqvist *et al.*, 2021). Low-magnitude early indicators of abrupt ecosystem state changes may be homogenized in the decadal sediment record (Fagherazzi *et al.*, 2012). In

contrast to this, high resolution microtopography responds directly to biotic and abiotic changes that portend ecosystem state change, such as slower plant recovery or decreased belowground biomass, and may be valid as an early indicator of ecosystem degradation (Stribling, Cornwell and Glahn, 2007; van Belzen *et al.*, 2017; Diamond *et al.*, 2021). However, the high sensitivity of microtopography to these factors creates noise even under stable conditions (Stribling, Cornwell and Glahn, 2007; Harman *et al.*, 2014). Therefore, similar to elevation trends measured using SETs, equilibration time is likely required to assess the magnitude of background fluctuations associated with a naturally variable living marsh surface (Lynch, Hensel and Cahoon, 2015; Blum *et al.*, 2021). Ultimately, the extended application of these microtopographic vulnerability metrics described herein to regional and global SET datasets could potentially strengthen the use of microtopography as an early indicator of state change.

Elevation change deficits calculated at SET stations have been scaled-up to represent vulnerability of entire ecosystems and regions (Cahoon *et al.*, 2002; Wasson *et al.*, 2019). The spatial dependent nature of microtopographic measurements prevents similar direct scaling, but spatial heterogeneity can be measured at the landscape scale using LIDAR based digital elevation models (or DEMs) (Doughty *et al.*, 2021). For the past 20 years, many studies have used LIDAR to remotely sense ground elevation over large areas, but salt marsh vegetation structure and instrument error make it difficult to detect meaningful differences in elevation across the landscape at the microtopographic scale (Hladik and Alber, 2012). While recent advances in error correction can reduce error – for example reducing mean error from 0.16 m to 0.004 m (McClure *et al.*, 2015) – centimeter-scale horizontal resolutions homogenize across the millimeter-scale topography of the marsh surface that SETs quantify. The ratio of unvegetated to vegetated marsh (UVVR) has been suggested as an indicator of marsh health where wetland

complexes are stable below UVVR values of 0.10 to 0.15 (Wasson *et al.*, 2019; Ganju *et al.*, 2022). UVVR is quantified independently of SLR, similar to microtopographic variation (Ganju *et al.*, 2017). However, the sensing of UVVR at the landscape scale necessitates imagery with a coarse horizontal resolution (from 3-30 m), which neglects ponds below this detection threshold (Ganju *et al.*, 2022). While the presence of larger ponds does have implications about ecosystem-scale functions and vulnerability, the formation of large ponds follows rather than precedes ecosystem state change (Duran Vinent *et al.*, 2021). Because of this temporal difference, there is a lack of correlation between UVVR and the novel microtopographic vulnerability metrics (SI Figure 2). However, as the temporal resolution of UVVR datasets improves and we assess the spatiotemporal UVVR dynamics, comparisons of changing landscape heterogeneity with changing microtopographic variability may support insights into the spatial scaling of microtopographic vulnerability metrics.

Applying Microtopographic Vulnerability Metrics

While this study only reviewed SET records across 10 sites along the U.S. mid-Atlantic, the novel metrics described can be easily applied to existing SET data records without requiring additional data collection or leveraged external variables, such as SLR. Because traditional metrics rely on rates of SLR, the time frame over which SLR is calculated can greatly change the perceived vulnerability of wetlands (Saintilan *et al.*, 2022). Microtopography data collected from SETs can be analyzed within the context of previous wetland conditions thereby making vulnerability relative to historical conditions of the marsh surface rather than to external drivers. Additionally, while this study only examined coastal marshes, SETs are widely used in a number of coastal ecosystems, such as mangrove forests (Lovelock *et al.*, 2015), tidal freshwater forests (Krauss et al., *in review*), and mud flats (Marion, Anthony and Trentesaux, 2009), to quantify

ecosystem vulnerability and could be implemented in peatlands where microtopographic formations arise from climate induced feedbacks (Harris, Roulet and Moore, 2020). The magnitude of microtopographic variation will differ among the various associated root structures, plant morphologies, and substrate compositions between ecological settings (Diamond *et al.*, 2021), but the parabolic change in microtopography examined herein will likely still apply to ecosystem state transitions within these systems. In general, microtopography will be altered if biotic or abiotic conditions change making this framework widely applicable to other transitions such as fronts associated with the migration of primary consumers (Vu and Pennings, 2021), barrier island transgression over back-barrier marshes (FitzGerald *et al.*, 2018), and warming driven vegetation shifts (i.e. shrubification (Mekonnen *et al.*, 2021) and mangrove encroachment into marshes (Osland *et al.*, 2017)). While microtopographic heterogeneity is a seldom used tool to predict or assess vulnerability, it can serve as an ecosystem vulnerability metric that directly reflects key aspects of ecological theory that operate across ecosystem and transition types.

Conclusions and Implications

While traditional applications of SET data have been used to assess wetland vulnerability using a single vertical response parameter (van Wijnen and Bakker, 2001; Cahoon *et al.*, 2002, 2006; Kirwan and Temmerman, 2009; Cahoon and Guntenspergen, 2010; Cahoon, 2015), marsh vulnerability should not be determined by a single indicator (Kirwan, Temmerman, *et al.*, 2016; Ganju *et al.*, 2017; Wasson *et al.*, 2019). More recent vulnerability indexes synthesize multiple vertical and horizontal stability metrics into a holistic assessment (Raposa *et al.*, 2016; Defne *et al.*, 2020; Ganju *et al.*, 2022), however the spatial scale of these assessments homogenize the marsh surface at the microtopographic scale. Our results indicate a correlation between increasing microtopographic variation and traditional wetland vulnerability metrics (Figure 22),

suggesting that metrics of microtopography could serve as early indicators of marsh degradation. These novel metrics could be applied to the catalog of existing SET data records, which includes globally dispersed datasets that extend up to 30 years into the past (Blum *et al.*, 2021; Saintilan *et al.*, 2022). This application would reveal if changing microtopographic variability can be used as an early indicator of degradation generally. Early detection of marsh vulnerability to SLR is critical to predict imminent ecosystem state change and to take management measures before irreversible degradation of these valuable coastal ecosystems occurs.

Summary

The following one-sentence summaries emphasize the critical findings and implications of the respective, preceding chapters.

1. While marsh migration does result in the net loss of carbon during the transition from forest to marsh, accumulating marsh soils in the newly formed marsh can compensate and replace that lost carbon at the centennial scale.
2. Moderate warming maximizes marsh stability and carbon storage, but continued warming exacerbates marsh and carbon loss as the thermal optima for marsh function is exceeded.
3. Compensatory mechanisms at the landscape scale largely preserve ecosystem extents and can quickly compensate for carbon lost, even at the decadal scale.
4. Increasing microtopography can be used as an early indicator of critical ecosystem transition in salt marsh communities before widespread marsh degradation.

Overall, this dissertation presents four separate, yet connected chapters that demonstrate developments to coastal carbon dynamics in the face of climate driven ecosystem transitions. Through these studies we show that climate driven ecosystem transitions are complex interactions that can critically alter coastal carbon dynamics, but are relatively understudied within the field of coastal carbon research. However, I believe that studies like these exemplify how the interactions between ecology, biogeochemistry, climate, and geomorphology drive the coastal carbon engine.

Figures and Tables

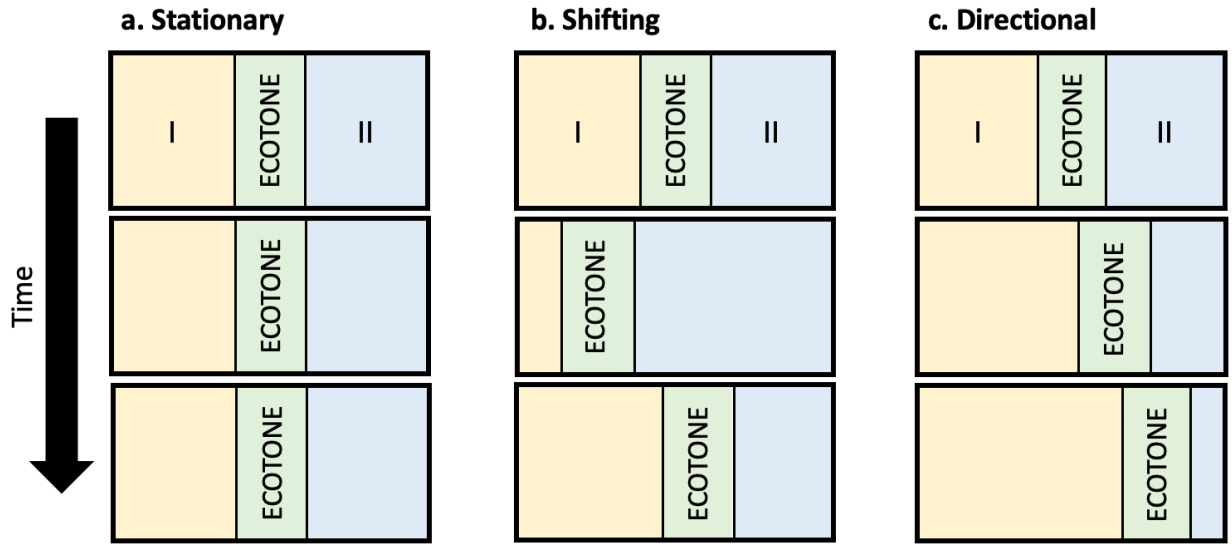

Figure 1 Schematic of (a) stationary, (b) shifting, and (c) directional ecotone movement over time where I and II are the ecosystems adjacent to the ecotone

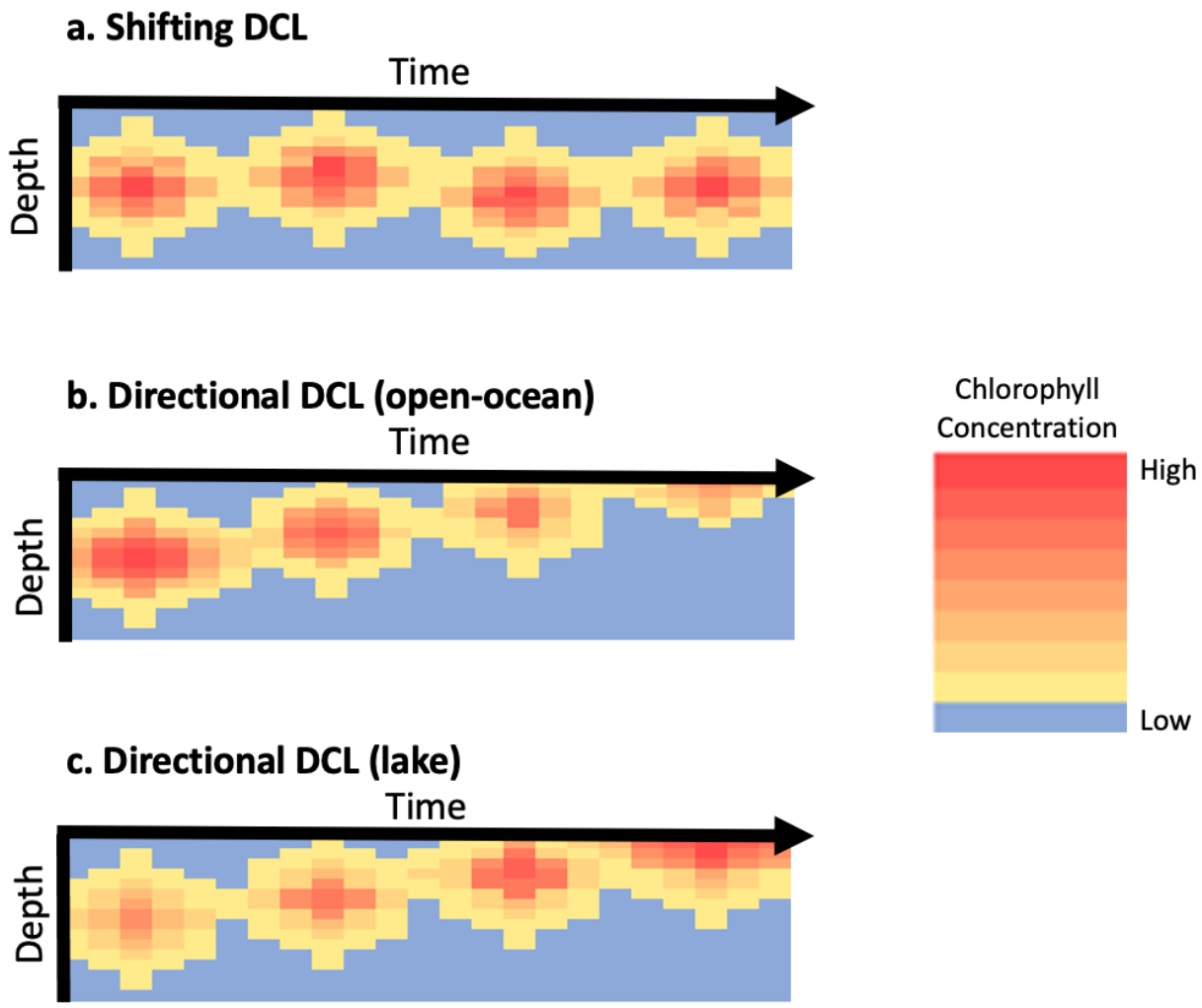

Figure 2 Conceptual diagram depicting (a) shifting ecotone movement of the DCL where depth is relatively maintained over time despite seasonal variation (b) directional shoaling and decreasing chlorophyll concentrations in open-ocean systems, and (c) directional shoaling and increasing chlorophyll concentrations in lake systems

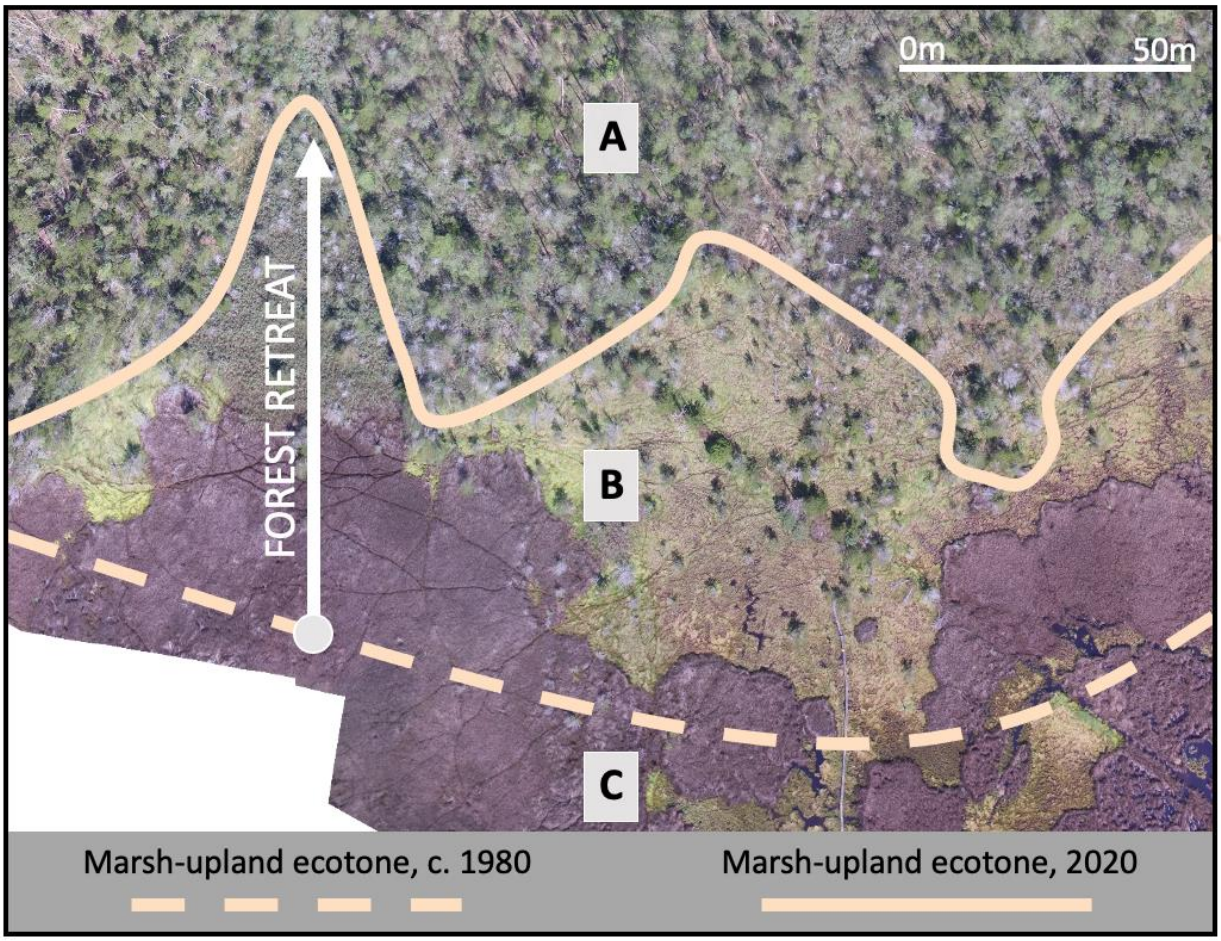

Figure 3 Aerial, true-color image from Brownsville Preserve (Virginia, USA) showing upland movement of the directional marsh-upland ecotone as tidal marsh migrates into space previously occupied by coastal forest. The tan lines represent the approximate locations of the marsh-upland ecotone in 1980 (dashed) and 2020 (solid), while the white line shows the direction and extent of forest retreat between 1980 and 2020. Letters represent zones of (A) forest, (B) new marsh formed since 1980, and (C) marsh older than 40 years. Data from Smith and Kirwan (2021)

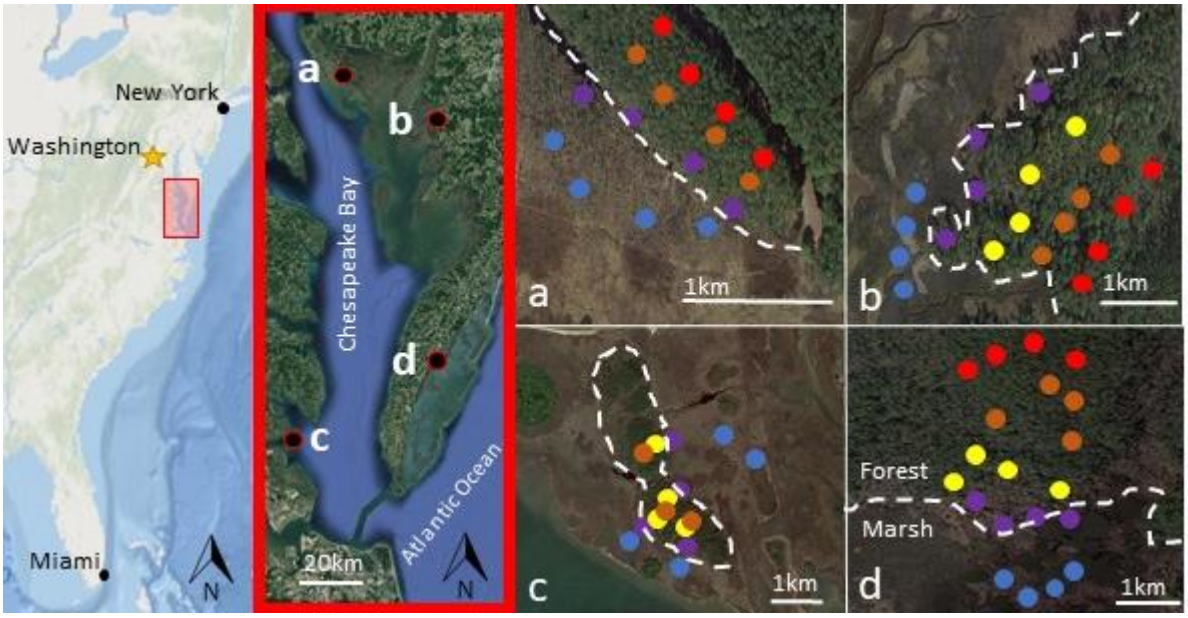

Figure 4 A general map of the Chesapeake Bay in Virginia and Maryland (United States of America) showing the region's location along the mid-Atlantic seaboard, site locations, and four inset maps showing transects across the marsh forest boundary at each site (**a**: Moneystump Swamp, **b**: Monie Bay, **c**: Goodwin Island, **d**: Phillips Creek) with individual sampling locations marked. The vegetation zones are differentiated by the color of the symbol. High marsh is blue, transition zone is purple, low forest is yellow, mid forest is orange, and high forest is red. The dashed line delineates the general forested ecosystem from the high marsh.

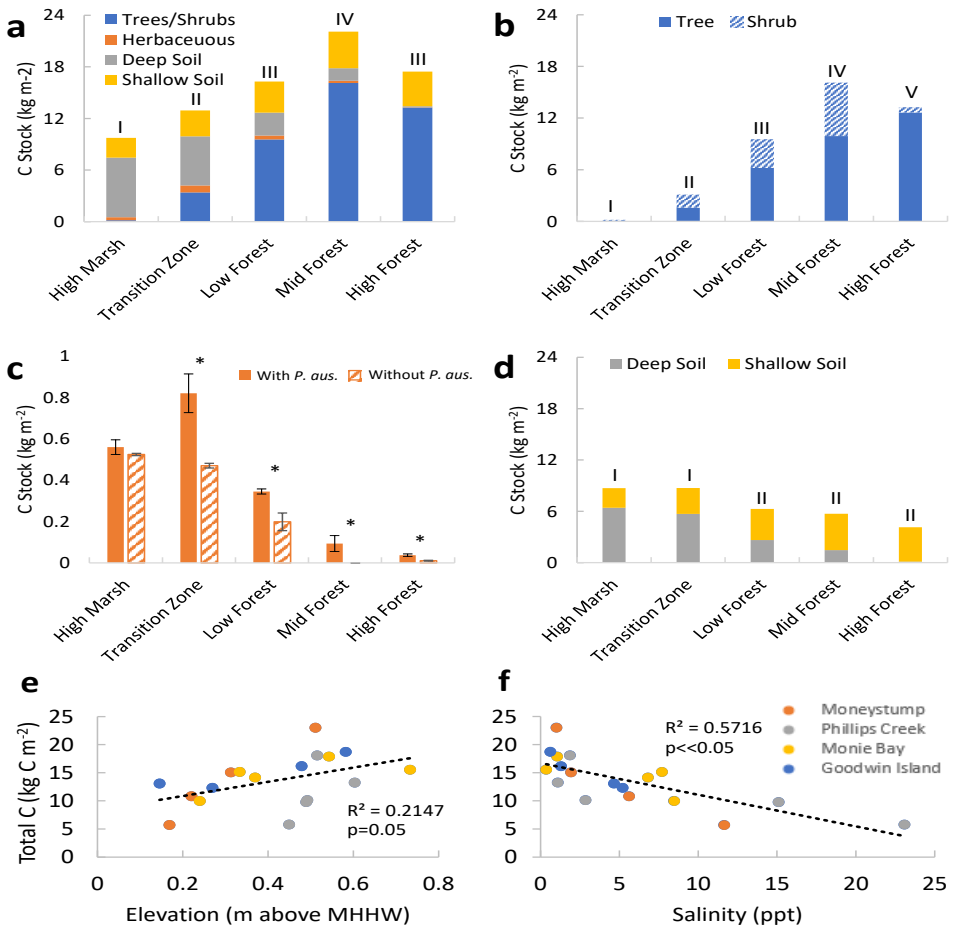

Figure 5 The C stock of distinct pools across the high forest to high marsh gradient, where the C stock refers to the average stock of four sites in the Chesapeake Bay. (**a**) Cumulative average C stocks by pool, (**b**) woody C partitioned into C stored in trees and shrubs, (**c**) herbaceous C separated into sites with *P. australis* and the site managed for *P. australis* removal (Moneystump Swamp), (**d**) soil C in upper 10 cm ("shallow") and from 10 cm to the depth of parent material ("deep"). Relationships between total C stock and elevation (**e**) and soil salinity (**f**) for each site and vegetation zone. The black dashed lines indicate the linear regression between total carbon stock and elevation (**e**, y=12.63x+8.323) and between total carbon stock and salinity (**f**, y=-0.563x+16.706). Simple projections based on the elevation of vegetation zones and a regionally averaged rate of sea level rise suggest conversion of high forest to high marsh in approximately 90 years. Roman numerals in **a**, **b**, and **d** represent statistically significant differences between vegetation zones while asterisks (*) in **c** represent statistically significant differences between sites with and without *P. australis*.

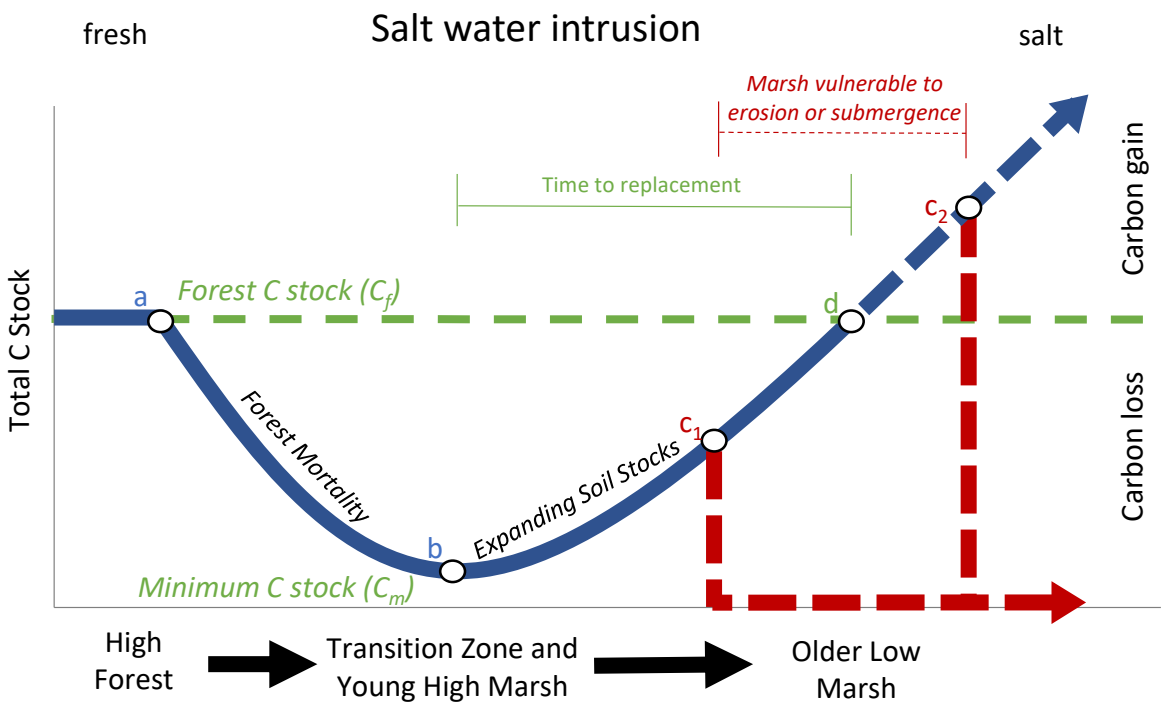

Figure 6 Conceptual diagram of the changing total C stock associated with salt water intrusion and the transition from forest to marsh. The total carbon stock in the forest (C_f) decreases through time following salt water intrusion (a) in response to forest mortality. Carbon stocks reach a minimum (C_m) when forests are first replaced by marshes (b), but then increase through time as developing marsh soils accumulate carbon. Carbon stocks increase with sea level rise and salt water intrusion until marshes submerge (c), potentially compensating for the loss of forest carbon (d). Variable times to submergence (c_1, c_2) relative to the time to replacement (d) suggest that complete replacement of forest carbon is tenuous.

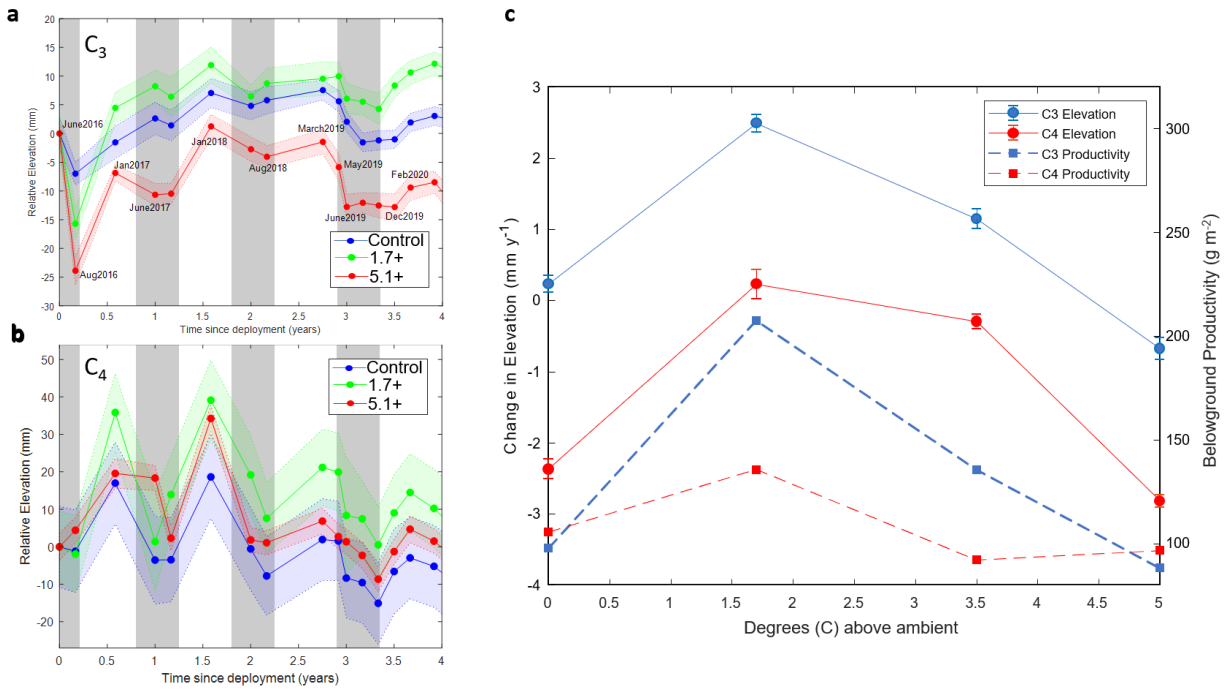

Figure 7 Elevation trends through time in response to warming in the C_3 (a) and C_4 (b) plant communities. Shaded regions correspond to the standard error in elevation associated with each treatment. Gray areas represent the approximate growing season (April to September). For clarity, the +3.4 °C treatment is not shown, but tracks with similar seasonal trends as the displayed treatments (SI Figure 3). Relative elevation measurements were averaged across plots and replications (*n*=3). (c) Average elevation change rate (mm y^{-1}) of triplicate replications in the C_3 and C_4 community averaged through time under the four temperature treatments. Regression analyses were applied to individual pins and then averaged between plots and treatments (n=~120). Belowground productivity data is from Noyce et al.[19], updated with an additional two years of data to encompass 2018-2020.

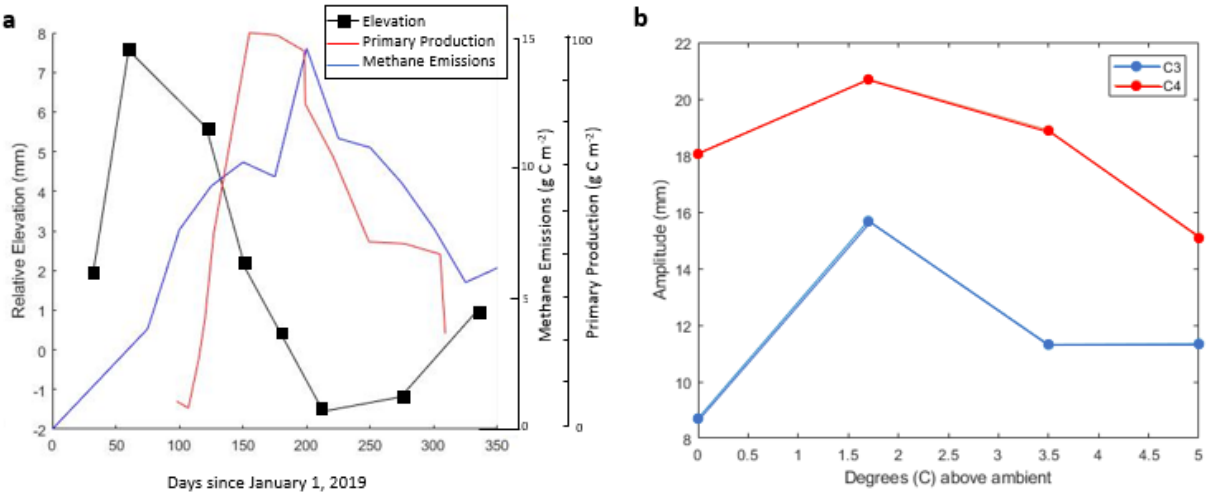

Figure 8 (a) Seasonal patterns in marsh elevation, productivity, and decomposition. Relative elevation (black), primary production (red) and methane emissions (blue) from March 2019 to

Feb 2020. Primary production is measured as changes in total green biomass relative to total green biomass during peak productivity. Methane emissions are measured monthly using static chambers and act as a proxy for organic matter decomposition. Relative elevation is the average elevation of the C_3 community only at ambient temperatures. (b) Average amplitude (mm) of the seasonal variability between the highest and lowest average elevations over the year-long intensive sampling period.

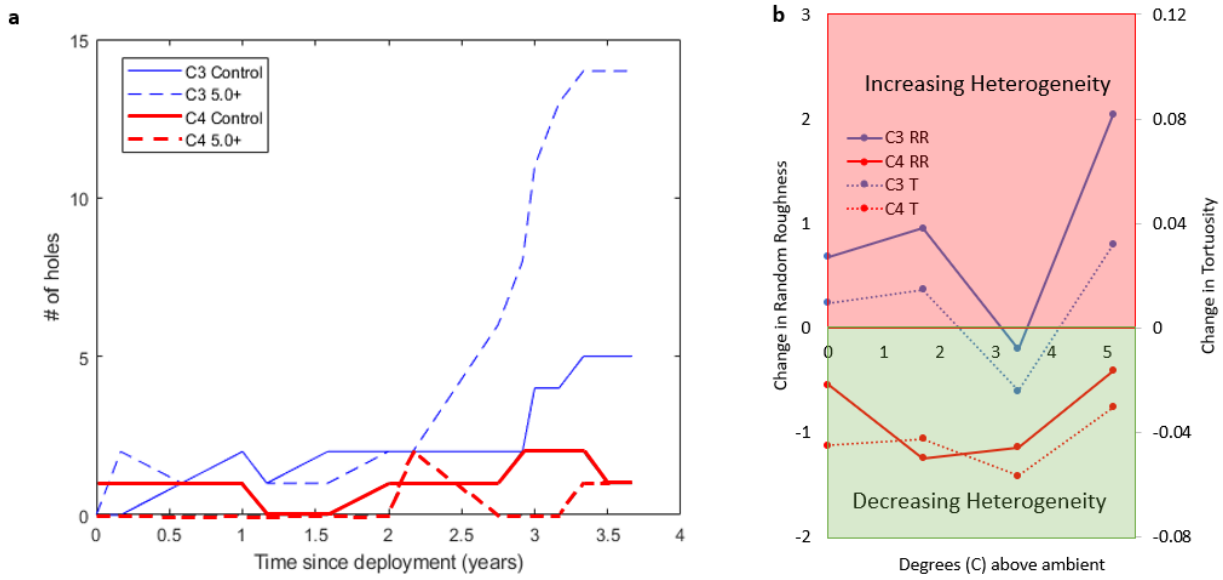

Figure 9 (a) Changes in heterogeneity across temperature treatments and plant community as represented by the number of holes in a given year. Holes were defined as locations with a difference in adjacent elevation measurements of greater than 20 mm. Adjacent pins were approximately 4.5 mm apart. (b) The average change in random roughness (RR) and tortuosity (T) over the duration of this experiment. Positive values indicate an increase in heterogeneity, which we associate with a decrease in marsh resilience, while negative values indicate a decrease in heterogeneity, where the marsh surface becomes less variable.

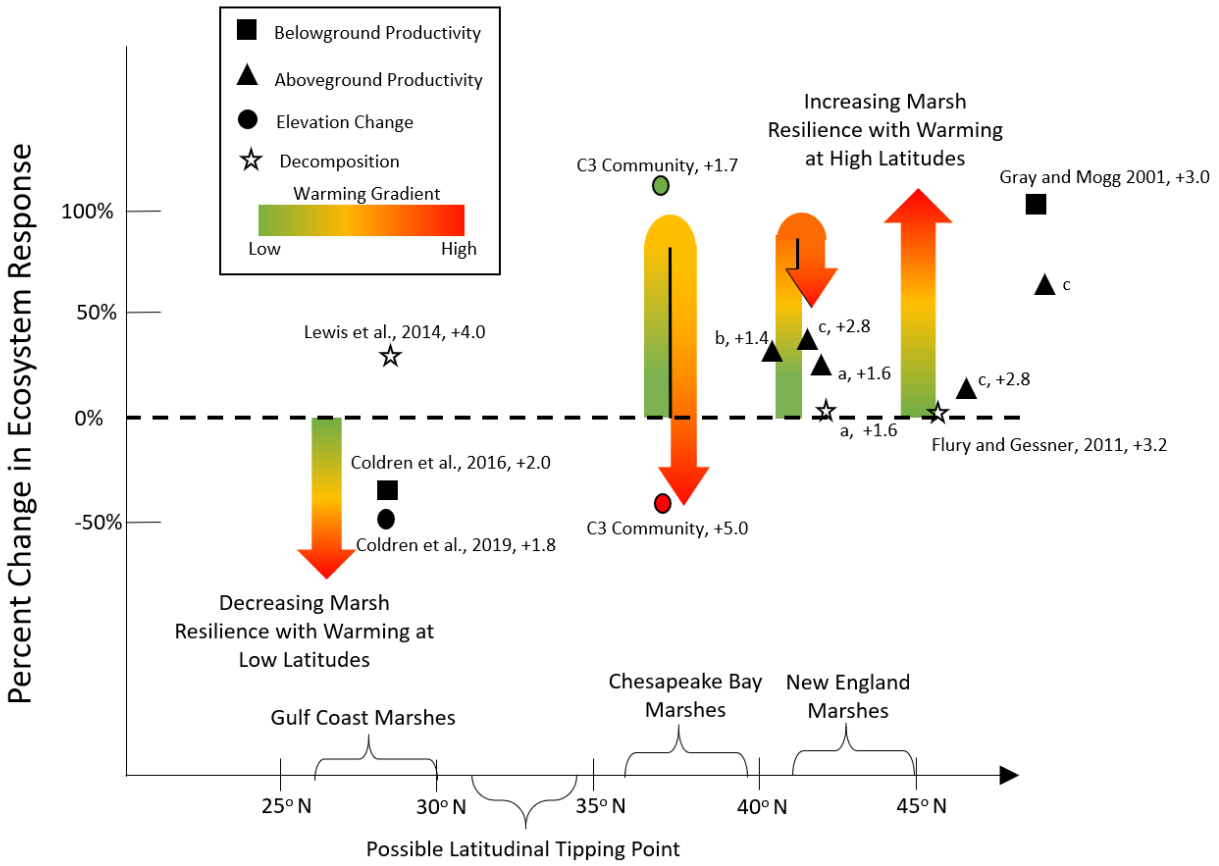

Figure 10 Meta-analysis and conceptual diagram showing that the effect of warming on ecosystem response will vary with latitude in the United States. Colors of the arrows represent degree of warming where green represents slight increases above ambient temperatures and red represents extreme warming. In low-latitude marshes, ambient temperatures are above metabolic optima, so that warming will lead to decreased marsh resilience. In high-latitude marshes, warming increases marsh resilience. The possible latitudinal tipping point represents a range of potential latitudes along the North American Atlantic seaboard below which any degree of warming is expected to decrease resilience. Squares, triangles, circles, and stars in the figure represent percent changes in belowground productivity, aboveground productivity, elevation change, and decomposition measured in prior warming experiments, where the numbers to the right of the citation indicate the magnitude of warming treatment (°C). Symbols a, b, and c represent data from Charles and Dukes[9], Gedan and Bertness[8], and Baldwin et al.,[60]. The red and green points near the middle of the figure represent the results of our warming experiment in the C3 community, where elevation gain is enhanced +1.7 °C and reduced at +5.1 °C, demonstrating a switch from positive to negative effects on marsh resilience.

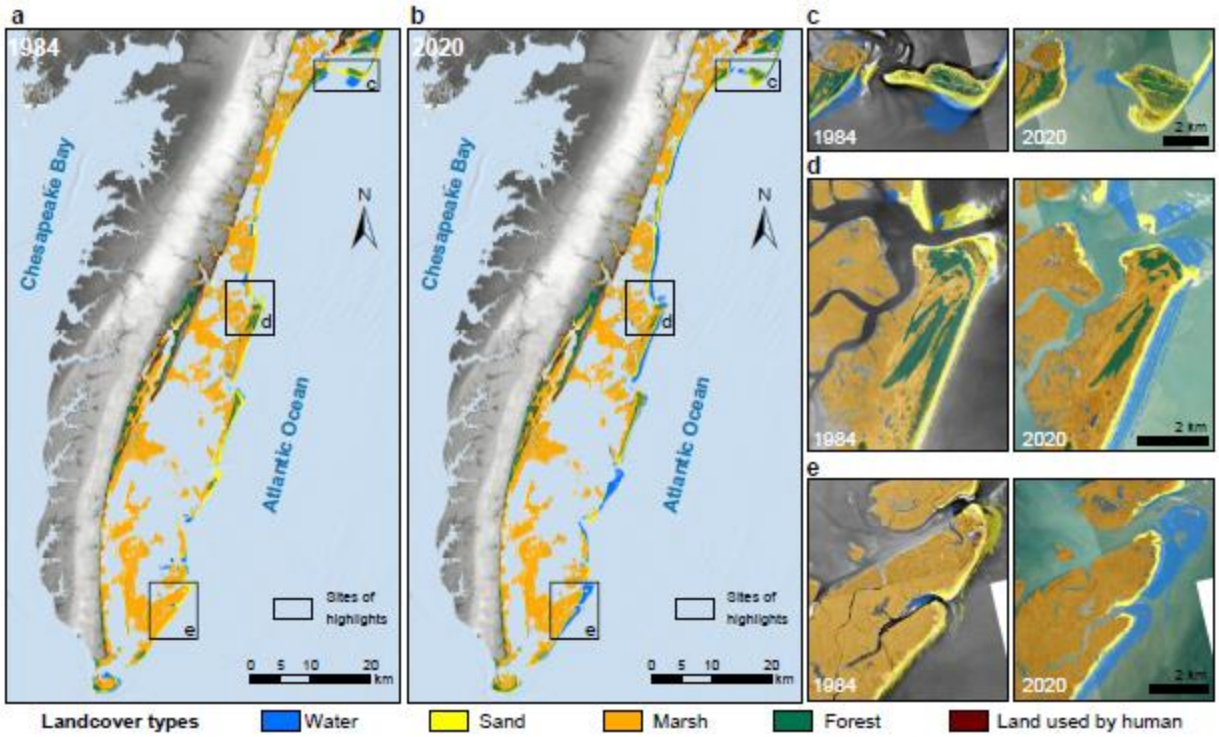

Figure 11 Landcover maps of the study area, the Virginia Coastal Reserve, on the Delmarva Peninsula in 1984 (**a**) and 2020 (**b**) (base map in **a** and **b** ArcGIS v10.7). Black boxes in **a** and **b** indicate locations of representative ecosystem transitions common throughout the Virginia Coastal Reserve: barrier island expansion (**c**), barrier island erosion and coastal forest reduction (**d**), and barrier island retreat over back barrier marshes (**e**). The landcover maps in panels **c-d** were plotted on top of high-resolution aerial images acquired around 1984 from the U.S. Bureau of Land Management (displayed in black and white) and 2020 from the National Agriculture Imagery Program (displayed in color) with respective landcover classifications superimposed atop the imagery.

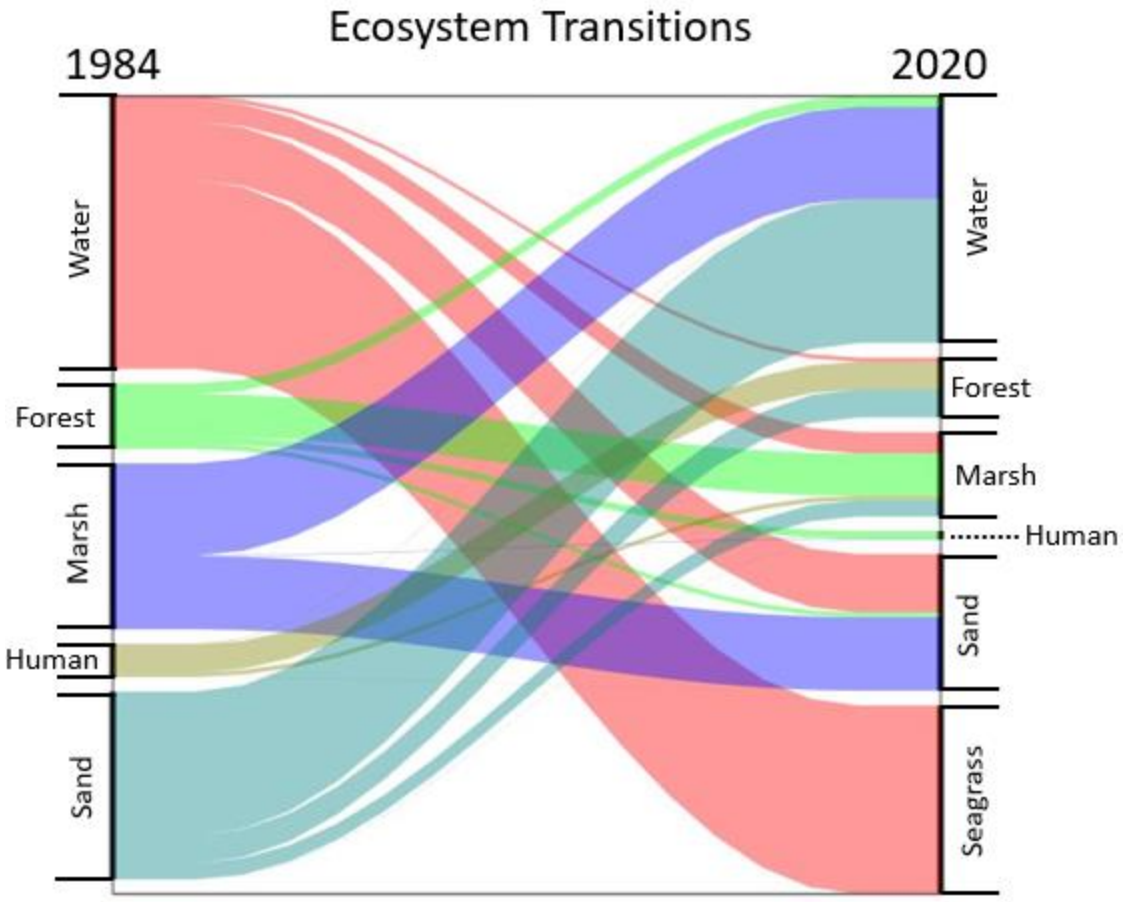

Figure 12 Sankey diagram showing ecosystem transition between two time intervals, 1984 and 2020, within the VCR coastal network. Stable pixels – pixels within the landscape that did not change land cover —are excluded from this visualization for clarity as stable pixels comprise ~80% of the coastal landscape.

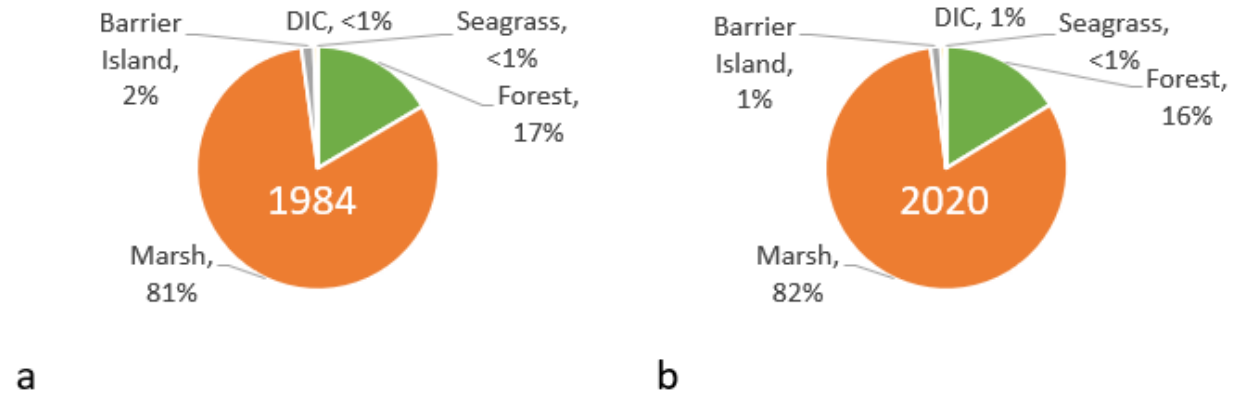

Figure 13 Pie charts indicating the contribution of the coastal ecosystem's carbon stocks (marshes, coastal forests, barrier islands, seagrass, and DIC in the water column) to the regional carbon budget in 1984 (**a**) and 2020 (**b**).

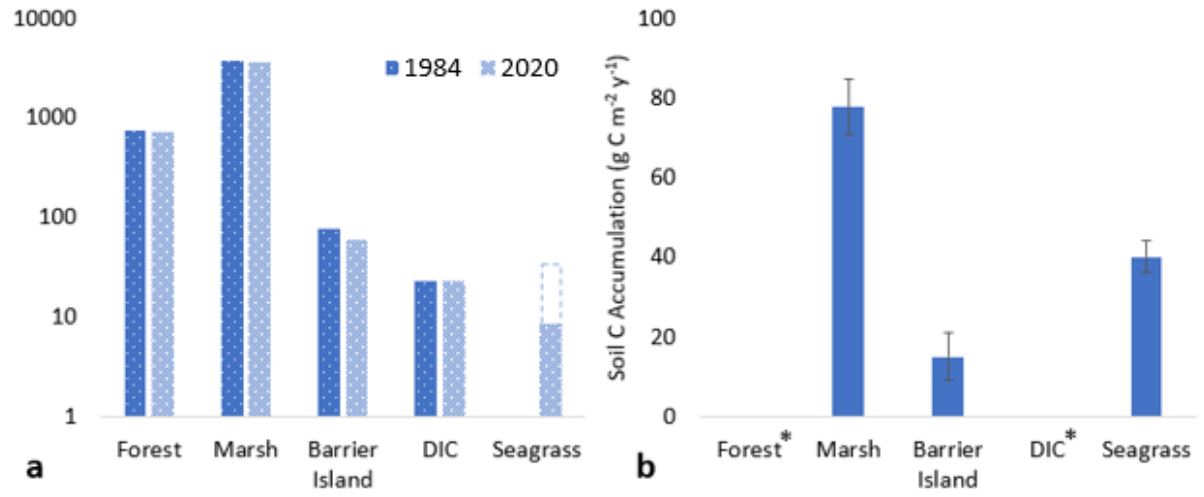

Figure 14 (**a**) The carbon stocks (Gg C) of individual coastal ecosystems in 1984 and 2020. Note the data is presented on a log scale. The dashed box above the seagrass stock represents the potential increase in seagrass carbon stock if soils were able to accumulate carbon to comparable depths (i.e. 40 cm) (**b**) Soil carbon accumulation rates (g C m^{-2} y^{-1}) of coastal ecosystems (mean ± standard error). *While we assume negligible rates for these ecosystems, we recognize that there may be some depositional accumulation of carbon.

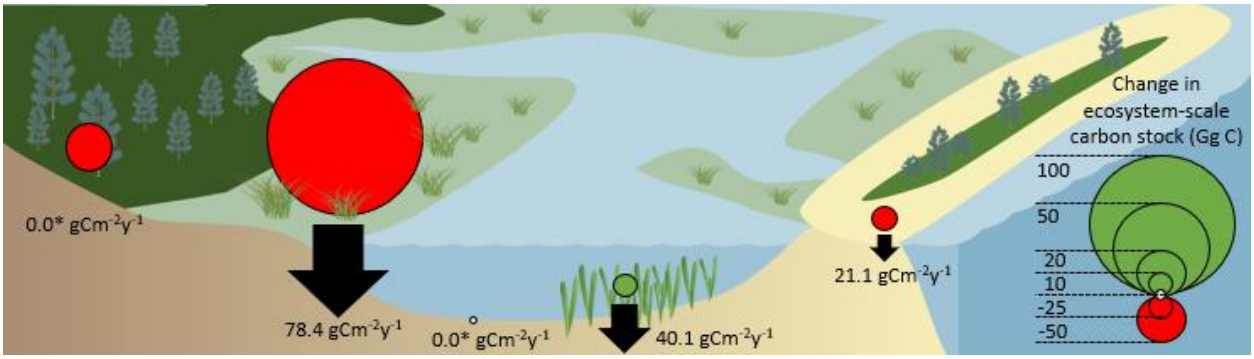

Figure 15 Changes in ecosystem carbon stocks in the coastal landscape from 1984 to 2020: forests (dark green), marshes (light green), DIC (blue; note no change in carbon stock), seagrass (benthic grass icons), and barrier islands (beige surrounding dark green). The size of the circle superimposed on each ecosystem indicates the magnitude of carbon stock change (Gg C) from 1984 to 2020 while the color of the circle portrays positive (green) or negative (red) changes. Arrows and the accompanying numbers represent the soil carbon accumulation rates measured in each of these ecosystems and follow the same size scale as the circles. *While we assume negligible rates of soil carbon accumulation by the forest and DIC pools, we recognize that there may be some depositional accumulation of carbon.

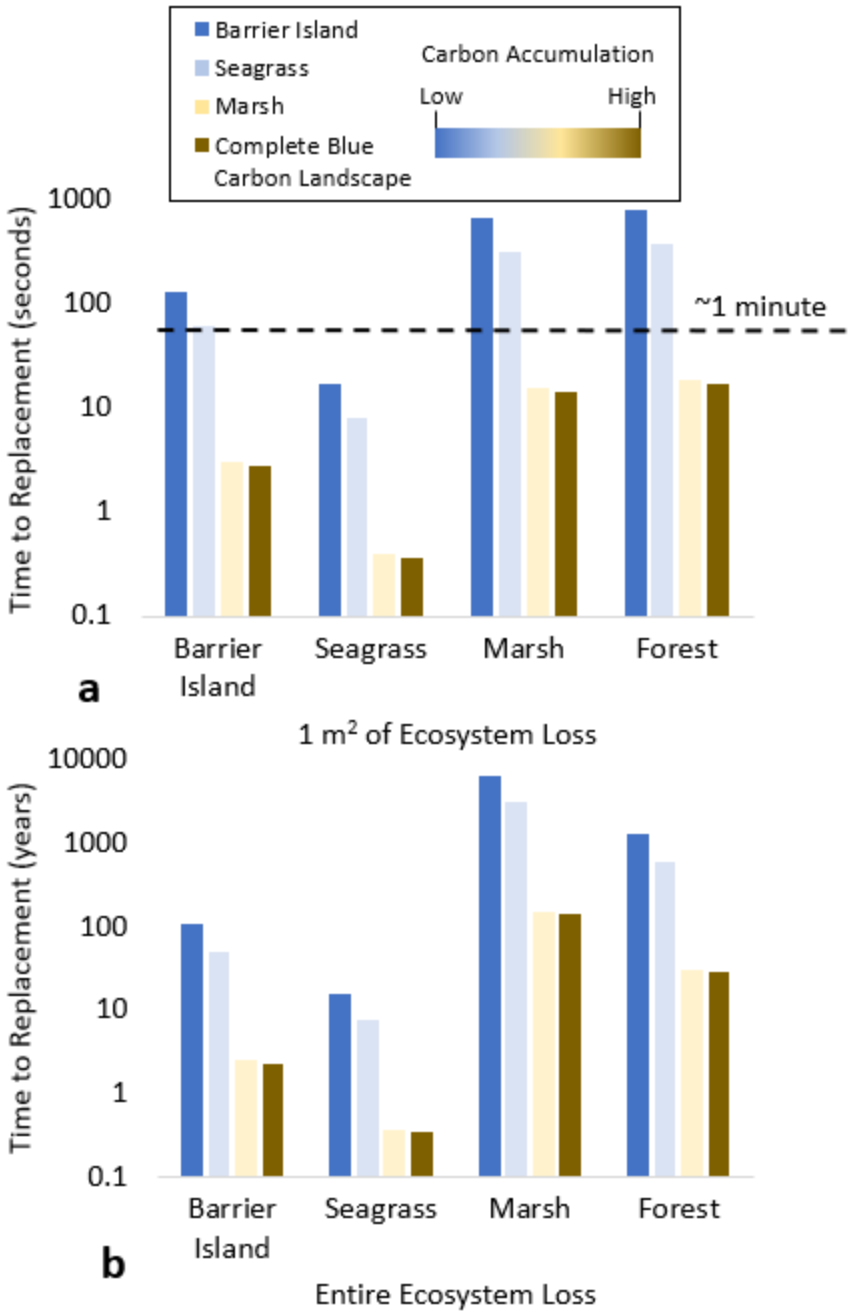

Figure 16 (**a**) The time to replacement (seconds) of carbon lost from the reduction of 1.0 m^2 of the respective ecosystem on the horizontal axis and replaced by the entire carbon accumulating power of the respective ecosystem or landscape in the legend. Ecosystems are plotted along the horizontal axis in order from least to greatest carbon density (g C m^{-2}). This increase in carbon density drives the increase in time to replacement. Meanwhile, the magnitude of carbon accumulation rates, which is smallest in the barrier islands and largest at the coastal landscape scale, decreases time to replacement within a categorical bin. (**b**) The time to replacement (years) of carbon lost from the entire loss of the respective ecosystem across the VCR on the horizontal

axis and replaced by the entire carbon accumulating power of the respective ecosystem or landscape in the legend.

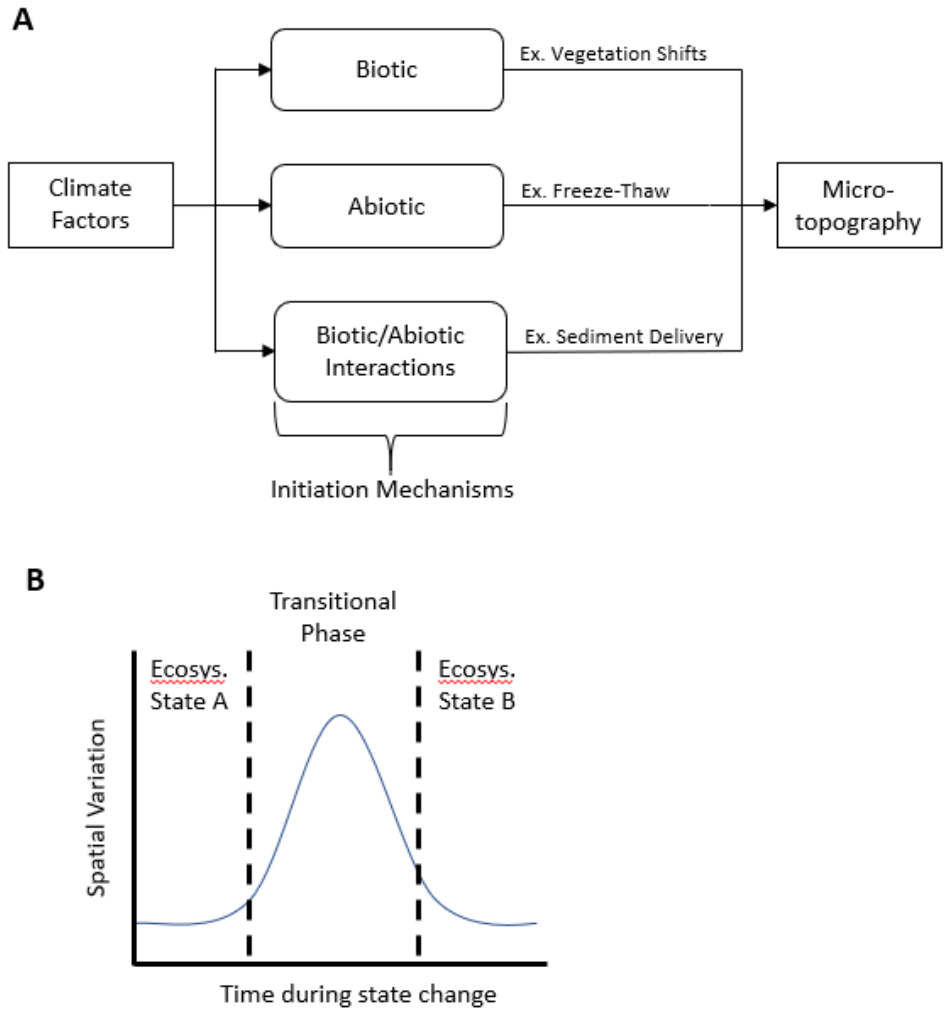

Figure 17 (a) Conceptual diagram of the influence of climate on microtopographic initiation in wetlands (adapted from Diamond et al. (2020)). Initiation mechanisms create small-scale variation in soil elevation. These mechanisms can be modulated by climate factors, such as elevated atmospheric CO_2 concentrations, warming, and enhanced productivity, that affect biotic and abiotic drivers of microtopography. (b) Conceptual diagram of increased spatial variation associated with the transition between two alternative stable states. As a stable ecosystem (Ecosys. State A) approaches the critical threshold of a state change, spatial variation (e.g. microtopographic variation, landscape heterogeneity, etc.) is expected to increase and is maximized during the transitional phase when the reference frame is a mosaic of either alternative states. As the alternative state (Ecosys. State B) dominates the reference frame, spatial variation is expected to decrease to the state's equilibrium conditions.

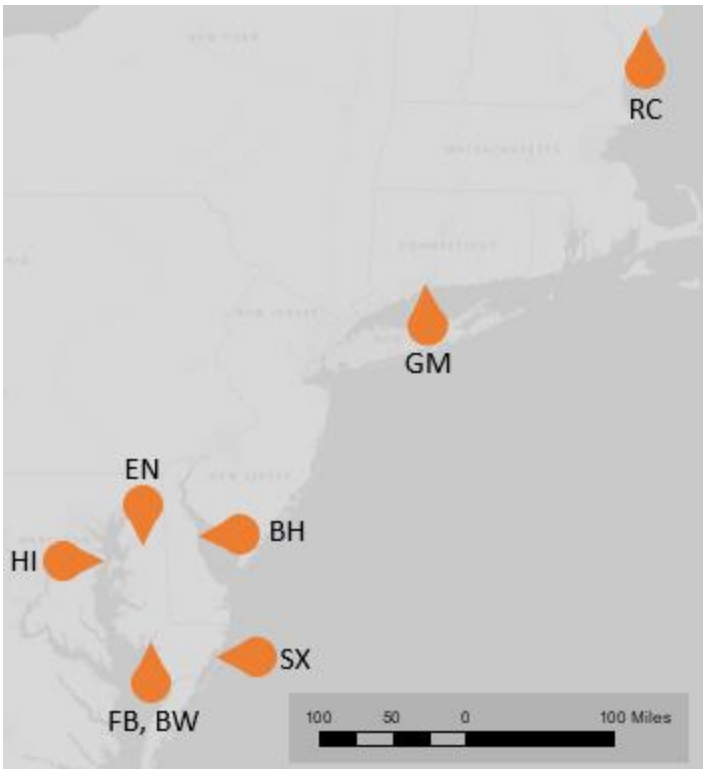

Figure 18 A general map of the mid-Atlantic region of North America showing site names and locations. The southernmost site is in Virginia (SX, Saxis Wildlife Management Area), six sites are located in Maryland (FB8, Fishing Bay Wildlife Management Area; BW7, Blackwater National Wildlife Refuge; HI, Hog Island at the Smithsonian Environmental Research Center; EN, Eastern Neck National Wildlife Refuge), and one site is located in Delaware (BH, Bombay Hook National Wildlife Refuge), Connecticut (GM, Great Meadows National Wildlife Refuge), and Maine (RC, Rachel Carbon National Wildlife Refuge). Each site contains two SET stations, except for FB8 and BW7, which contain four SET stations each.

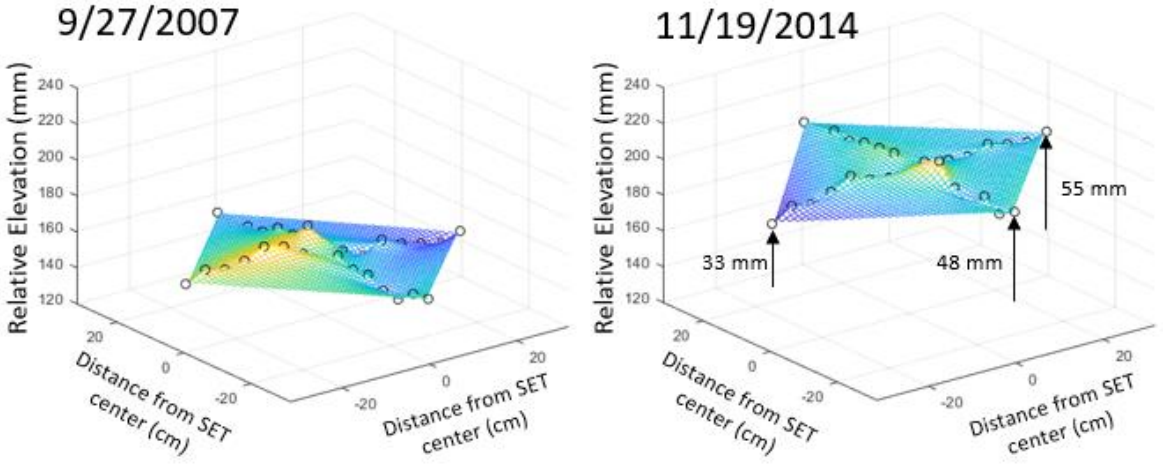

Figure 19 Interpolated mesh-grid of the marsh surface at BH2 (Bombay Hook National Wildlife Rescue, SET 2) on September 27th, 2007 and November 19th, 2014. These interpolated surfaces were created for all SETs during all measurement collections and serve as the surface utilized in

the SA:MA microtopographic variability metric. The color of the grid is relative to the height extremes of the marsh surface during each sampling period with the highest point in yellow and the lowest point in blue. The black open circles represent the SET derived measurements from the respective dates that were used to interpolate the surface. Arrows demarcate the change in elevation of identical locations in the marsh surface measured between the two time points.

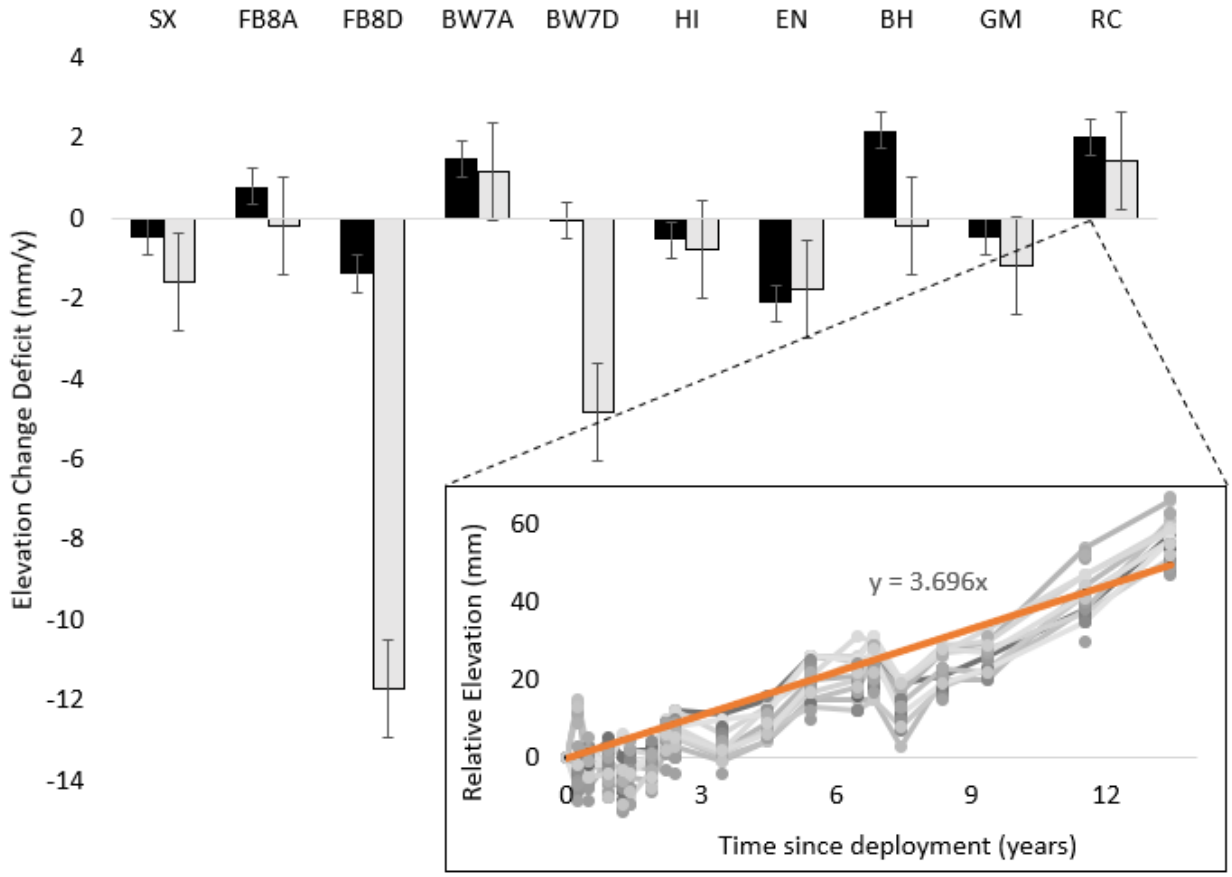

Figure 20 The elevation change deficits (mm y^{-1}) calculated from the SETs reviewed in this study. SETs are grouped by site with the respective site abbreviation above the paired stations. These are then organized from left to right in order of increasing latitude. The gray and black colors of the bar differentiate the SET stations present within each site and are not representative of any treatment or applied condition. Elevation change deficit is the difference between elevation change (mm y^{-1}) and 50-year average rate of SLR (mm y^{-1}). Elevation change at each SET was determined by averaging the rate of elevation change of each individual pin (n=~30) across the time period, exemplified by the inset of SET pin trajectories at RC1 shown in grays with the calculated average elevation change shown in orange. Error bars within the bar chart represent the standard deviation of the average elevation change deficit.

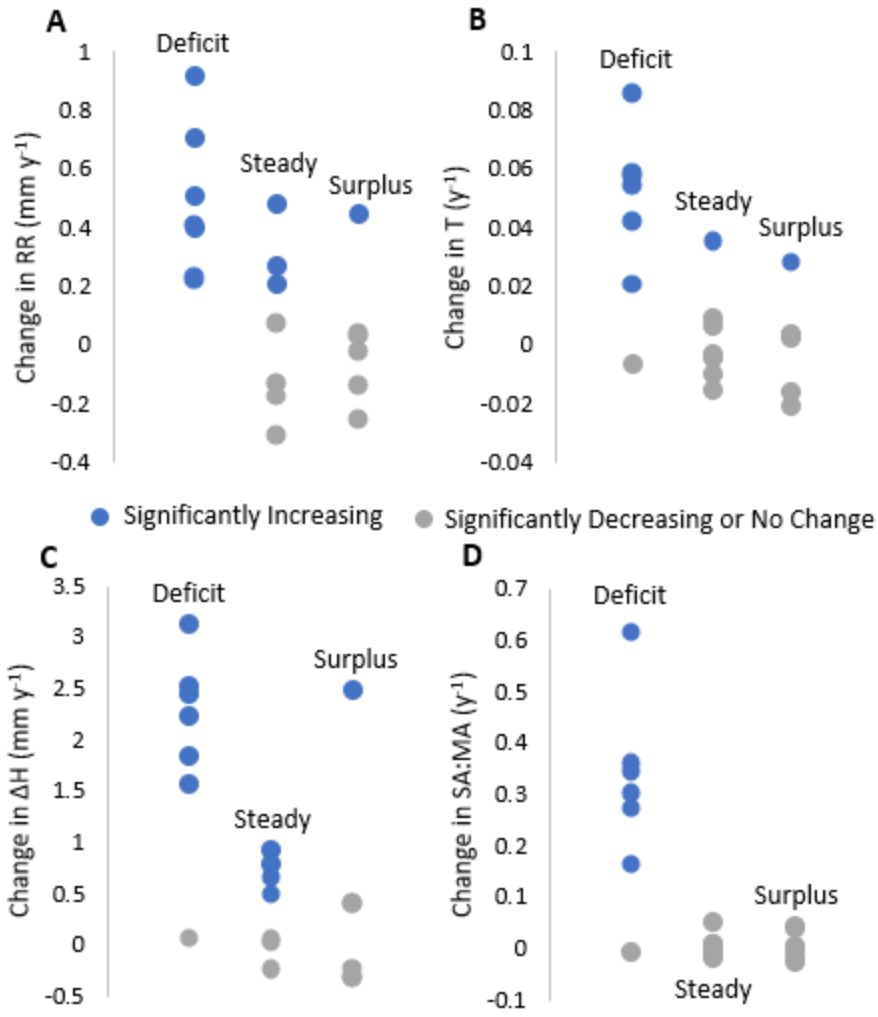

Figure 21 Categorical scatterplots of rates of changes of the four microtopographic variability metrics, (a) random roughness (RR), (b) tortuosity (T), (c) elevation range (ΔH), (d) the surface area to map area ratio (SA:MA), grouped according to traditional metrics of vulnerability (i.e. elevation change deficits). The "Deficit" category refers to SETs where the elevation change was less than the 50-year averaged rate of local SLR, while the "steady" and "surplus" categories indicate SETs where the elevation change was not different or significantly less than the rate of local SLR. The color of the datapoint represents whether the linear regression calculated for the respective vulnerability metrics is either significantly increasing through time (blue) or decreasing or not significantly changing (both in gray).

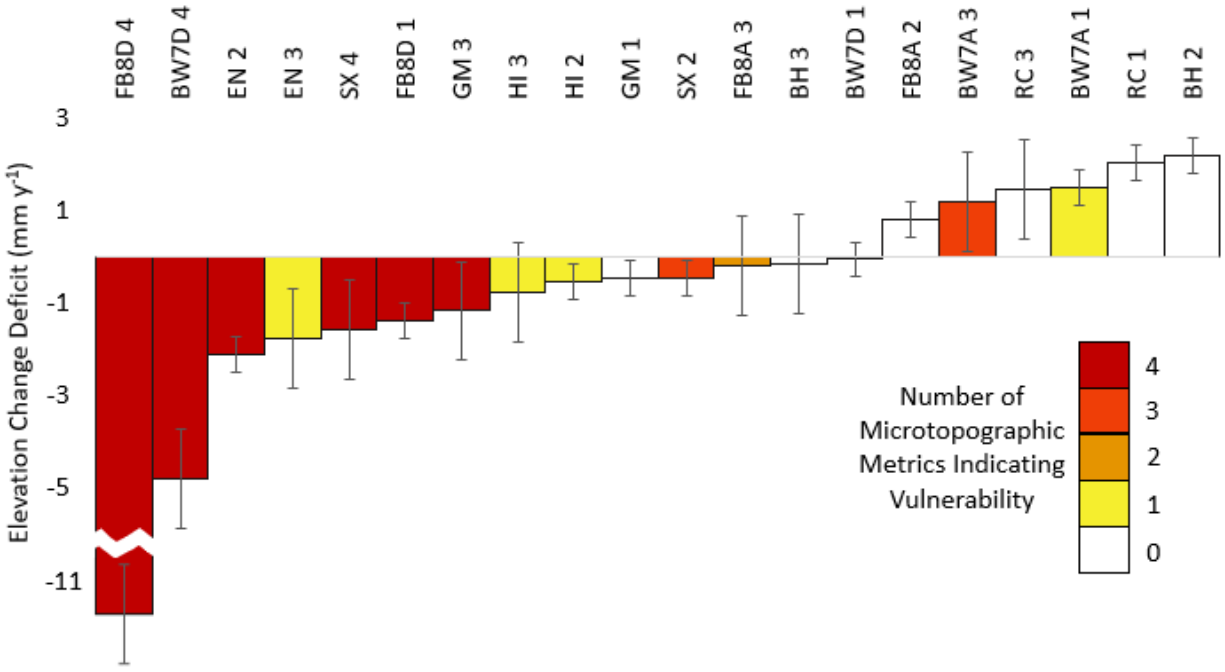

Figure 22 Comparison of traditional vulnerability metrics (elevation change deficit) with the novel microtopographic vulnerability metrics. Elevation change deficit data is the same data displayed in Figure 20, but arranged from lowest to highest elevation change deficit with the respective SET label displayed above. The color of the bars is determined by the number of microtopographic metrics that indicated vulnerability (Table 2). From this, we can see that six of the seven most vulnerable sites identified by traditional metrics are also identified as vulnerable according to every novel microtopographic vulnerability metric. Error bars represent standard error.

Table 1. Cross tabulation matrix for the landcover change map (Figure 11c) from 1984 to 2020 showing the extent of land cover category persistence and change (km^2) during the time interval. *Indicates that the change in seagrass extent was quantified using the VIMS seagrass database.

		Landcover in 1984 (km^2)						
		Water	Forest	Marsh	Human	Sand	Seagrass*	**Gains**
Landcover in 2020 (km^2)	Water	14.7	1.68	14.3	0.09	22.3	0	38.3
	Forest	0.66	43.9	0.0	4.33	4.33	0	7.16
	Marsh	3.35	6.58	292	0.70	2.52	0	13.1
	Human	0.01	1.14	0.10	16.4	0.05	0	1.29
	Sand	9.07	0.76	11.4	0.04	7.82	0	20.2
	Seagrass*	29.3	0	0	0	0	0	29.3
	Losses	12.2	10.1	25.8	5.12	27.0	0	
	Net Change	26.2	-3.00	-12.6	-3.84	-6.78	29.3	

Table 2. The spatial extent (km^2) of landcover classes and ecosystem carbon storage (Gg C) in 1984 and 2020 and the change between these dates. *Indicates that there were no detectable seagrass meadows within the study area in 1984. N/A indicates that no carbon stock data was collected for agricultural or urban areas.

Landcover Classification	1984 (km^2)	2020 (km^2)	Percent Change (%)	1984 (Gg C)	2020 (Gg C)	Carbon Storage Change (Gg C)
Water	26.7	53.0	98	23	23	0
Marsh	318.0	305.4	-4	3711	3564	-147
Human	21.5	17.7	-18	N/a	N/a	N/a
Forest	54.1	51.1	-5	754	712	-41
Seagrass	0*	29.3	>100	0*	8.66	+8.66
Sand/Barrier Islands	34.8	28.0	-20	75.9	59.4	-16.5
			Total:	**4563.9**	**4366.9**	**-196.9**

Table 3. Environmental characteristics at the site and SET level. Every SET is accompanied with elevation data of the marsh surface in m in NAVD88 and D, the dimensionless position within the tidal frame where positive values indicate an elevation greater than mean high water, and the dominant vegetation surrounding the plot at the point of installation. Site level characteristics include regional 50-year averaged rates of SLR (mm y^{-1}) (NOAA Sea Level Trends, 2023), porewater salinity (ppt) measured in April to May of 2006, and the ratio of unvegetated to vegetated marsh surface (UVVR) within 10 ha patches including both SETs at each site.

State	SET Label	Elevation (m, NAVD88)	D (m)	SLR (mm y^{-1})	Salinity (ppt)	UVVR	Dominant Vegetation
VA	SX2	0.452	-0.68	4.00	17.4	0.07	S. patens
	SX4	0.379	-0.68				D. spicata
MD	FB8A2	0.487	-0.77	3.89	11.4	0.09	S. patens
	FB8A3	0.461	-0.81				S. americanus
	FB8D1	0.402	-1.09	3.89	10.8	0.09	S. patens
	FB8D4	0.413	-0.99				S. patens
	BW7A1	0.169	0.11	3.89	10.6	0.94	S. americanus
	BW7A3	0.136	0.23				S. americanus

	BW7D1	0.122	0.28	3.89	9.6	0.94	S. americanus
	BW7D4	0.123	0.27				S. alterniflora
	HI2	0.344	-0.55	3.73	8.9	0.001	S. americanus
	HI3	0.337	-0.52				S. americanus
	EN2	0.308	-0.42	3.73	11.2	0.15	S. americanus
	EN3	0.416	-0.45				S. americanus
DE	BH2	0.914	-0.03	3.76	13.6	0.16	D. spicata
	BH3	0.823	0.02				S. Patens
CT	GM1	1.329	-0.18	3.14	16.0	0.42	S. americanus
	GM3	1.379	-0.2				S. americanus
ME	RC1	1.369	-0.06	1.90	19.9	0.24	D. spicata
	RC3	1.348	-0.04				G. maritima

Table 4. Marsh Vulnerability Report Card. A summary table of traditional and microtopographic vulnerability metrics. The calculated elevation change deficit (E_{def}, mm y^{-1}) is written out while the table depicts in red if a microtopographic metric (random roughness (RR), Tortuosity (T), elevation range (ΔH), or surface area to map area ratio (SA:MA)) detected vulnerability. SETs are grouped within their respective states and ordered latitudinally from left to right.

	VA		MD											DE		CT		ME	
	SX2	SX4	FBA2	FBA3	FBD1	FBD4	BWA1	BWA3	BWD1	BWD4	HI2	HI3	EN2	EN3	BH2	BH3	GM1	GM3	RC1	RC3
E_{def}	-0.453	-1.58	0.802	-0.201	-1.375	-11.7	1.49	1.19	-0.056	-4.83	-0.533	-0.762	-2.12	-1.78	2.19	-0.163	-0.467	-1.17	2.01	1.45
RR																				
T																				
ΔH																				
SA: MA																				
Total	3	4	0	2	4	4	1	3	1	4	1	1	4	1	0	0	0	4	0	0

References

Abbott, M.R. *et al.* (1984) 'Mixing and the dynamics of the deep chlorophyll maximum in Lake Tahoe', *Limnol Oceanogr*, 29, pp. 862–878. Available at: https://doi.org/10.4319/lo.1984.29.4.0862.

Aguilos, M. *et al.* (2021) 'Millennial-Scale Carbon Storage in Natural Pine Forests of the North Carolina Lower Coastal Plain: Effects of Artificial Drainage in a Time of Rapid Sea Level Rise', *Land*, 10(12), p. 1294.

Allen, C.D. and Breshears, D.D. (1998) 'Drought-induced shift of a forest–woodland ecotone: rapid landscape response to climate variation', *Proc Natl Acad Sci*, 95, pp. 14839–14842. Available at: https://doi.org/10.1073/pnas.95.25.14839.

Anderson, R.C. (2006) 'Evolution and origin of the central grassland of North America: climate, fire, and mammalian grazers', *J Torrey Bot Soc*, 133, pp. 626–647. Available at: https://doi.org/10.3159/1095-5674(2006)133.

Anisfeld, S., Cooper, K. and Kemp, A. (2017) 'Upslope development of a tidal marsh as a function of upland land use', *Glob Chang Biol*, 23, pp. 755–766. Available at: https://doi.org/10.1111/gcb.13398.

Aoki, L.R. *et al.* (2021) 'Seagrass Recovery Following Marine Heat Wave Influences Sediment Carbon Stocks', *Frontiers in Marine Science*, 7. Available at: https://www.frontiersin.org/articles/10.3389/fmars.2020.576784 (Accessed: 7 February 2023).

Appleby, P.G. and Oldfield, F. (1978) *Catena*, 5, pp. 1–8.

Archer, A., SR *et al.* (2017) 'Woody plant encroachment: causes and consequences', in D. Briske (ed.) *Rangeland systems*. Cham: Springer, pp. 25–84. Available at: https://doi.org/10.1007/978-3-319-46709-2_2.

Ardón, M., Helton, A.M. and Bernhardt, E.S. (2018) 'Salinity effects on greenhouse gas emissions from wetland soils are contingent upon hydrologic setting: a microcosm experiment', *Biogeochemistry*, 140, pp. 217–232.

Arias-Ortiz, A. *et al.* (2018) 'A marine heatwave drives massive losses from the world's largest seagrass carbon stocks', *Nature Climate Change*, 8(4), pp. 338–344.

Arias-Ortiz, A. (2018) 'Reviews and syntheses: 210 Pb-derived sediment and carbon accumulation rates in vegetated coastal ecosystems - Setting the record straight', *Biogeosciences*, 15, pp. 6791–6818.

Auer, M.T. and Powell, K.D. (2004) 'Heterotrophic bacterioplankton dynamics at a site off the southern shore of Lake Superior', *J Great Lakes Res*, 30, pp. 214–229. Available at: https://doi.org/10.1016/S0380-1330(04)70387-1.

Baldwin, A.H., Jensen, K. and Schönfeldt, M. (2014) 'Warming increases plant biomass and reduces diversity across continents, latitudes, and species migration scenarios in experimental wetland communities', *Global change biology*, 20(3), pp. 835–850.

Barbiero, R.P. and Tuchman, M.L. (2004) 'The deep chlorophyll maximum in Lake Superior', *J Great Lakes Res*, 30, pp. 256–268.

Bashan, Y. *et al.* (2013) 'Restoration and recovery of hurricane-damaged mangroves using the knickpoint retreat effect and tides as dredging tools', *Journal of environmental management*, 116, pp. 196–203.

Baustian, J.J., Mendelssohn, I.A. and Hester, M.W. (2012) 'Vegetation's importance in regulating surface elevation in a coastal salt marsh facing elevated rates of sea level rise', *Global Change Biology*, 18(11), pp. 3377–3382. Available at: https://doi.org/10.1111/j.1365-2486.2012.02792.x.

van Belzen, J. *et al.* (2017) 'Vegetation recovery in tidal marshes reveals critical slowing down under increased inundation', *Nature Communications*, 8(1), p. 15811. Available at: https://doi.org/10.1038/ncomms15811.

Berg, P. *et al.* (2019) 'Dynamics of benthic metabolism, O2, and pCO2 in a temperate seagrass meadow', *Limnology and Oceanography*, 64(6), pp. 2586–2604. Available at: https://doi.org/10.1002/lno.11236.

Bernhardt, J.R. and Leslie, H.M. (2013) 'Resilience to climate change in coastal marine ecosystems', *Annual review of marine science*, 5, pp. 371–392.

Bertness, M.D., Gough, L. and Shumway, S.W. (1992) 'Salt Tolerances and The Distribution of Fugitive Salt Marsh Plants', *Ecology*, 73(5), pp. 1842–1851. Available at: https://doi.org/10.2307/1940035.

Bestelmeyer, B.T., Khalil, N.I. and Peters, D.P. (2007) 'Does shrub invasion indirectly limit grass establishment via seedling herbivory? A test at grassland-shrubland ecotones', *J Veg Sci*, 18, pp. 363–371. Available at: https://doi.org/10.1111/j.1654-1103.2007.tb02548.x.

Bird, D.F. and Kalff, J. (1989) 'Phagotrophic sustenance of a metalimnetic phytoplankton peak', *Limnol Oceanogr*, 34, pp. 155–162. Available at: https://doi.org/10.4319/lo.1989.34.1.0155.

Blum, L.K. *et al.* (2021) 'Processes Influencing Marsh Elevation Change in Low- and High-Elevation Zones of a Temperate Salt Marsh', *Estuaries and Coasts*, 44(3), pp. 818–833. Available at: https://doi.org/10.1007/s12237-020-00796-z.

Bopp, L. *et al.* (2001) 'Potential impact of climate change on marine export production', *Global Biogeochem Cycles*, 15, pp. 81–99. Available at: https://doi.org/10.1029/1999GB001256.

Bormann, F.H. and Likens, G.E. (2012) *Pattern and process in a forested ecosystem: disturbance, development and the steady state based on the Hubbard Brook ecosystem study*. Springer Science & Business Media.

Brinson, M.M., D., B.H. and JONES, M.N. (1985) 'Transitions in forested wetlands along gradients of salinity and hydroperiod', *Journal of the Elisha Mitchell Scientific Society*, 101, pp. 76–94.

Brinson, M.M., R., C.R. and K, B.L. (1995) 'Multiple states in the sea-level induced transition from terrestrial forest to estuary', *Estuaries*, 18, pp. 648–659.

Brown, C.D. and Johnstone, J.F. (2011) 'How does increased fire frequency affect carbon loss from fire? A case study in the northern boreal forest', *International Journal of Wildland Fire*, 20(7), pp. 829–837.

Burns, C.J., Alexander, C.R. and Alber, M. (2021) 'Assessing long-term trends in lateral salt-marsh shoreline change along a US east coast latitudinal gradient', *Journal of Coastal Research*, 37(2), pp. 291–301.

Cahoon, D.R. *et al.* (2002) 'High-Precision Measurements of Wetland Sediment Elevation: II. The Rod Surface Elevation Table', *Journal of Sedimentary Research*, 72(5), pp. 734–739. Available at: https://doi.org/10.1306/020702720734.

Cahoon, D.R. *et al.* (2006) 'Coastal Wetland Vulnerability to Relative Sea-Level Rise: Wetland Elevation Trends and Process Controls', in J.T.A. Verhoeven et al. (eds) *Wetlands and Natural Resource Management*. Berlin, Heidelberg: Springer (Ecological Studies), pp. 271–292. Available at: https://doi.org/10.1007/978-3-540-33187-2_12.

Cahoon, D.R. *et al.* (2011) 'Elevation trends and shrink–swell response of wetland soils to flooding and drying', *Estuarine, Coastal and Shelf Science*, 91(4), pp. 463–474. Available at: https://doi.org/10.1016/j.ecss.2010.03.022.

Cahoon, D.R. (2015) 'Estimating Relative Sea-Level Rise and Submergence Potential at a Coastal Wetland', *Estuaries and Coasts*, 38(3), pp. 1077–1084. Available at: https://doi.org/10.1007/s12237-014-9872-8.

Cahoon, D.R. and Guntenspergen, G.R. (2010) 'Climate Change, Sea-Level Rise, and Coastal Wetlands', 32(1).

Cahoon, D.R., Reed, D.J. and Day, J.W. (1995) 'Estimating shallow subsidence in microtidal salt marshes of the southeastern United States: Kaye and Barghoorn revisited', *Marine Geology*, 128(1), pp. 1–9. Available at: https://doi.org/10.1016/0025-3227(95)00087-F.

Callaway, J.C., Cahoon, D.R. and Lynch, J.C. (2013) 'The Surface Elevation Table–Marker Horizon Method for Measuring Wetland Accretion and Elevation Dynamics', in *Methods in Biogeochemistry of Wetlands*. John Wiley & Sons, Ltd, pp. 901–917. Available at: https://doi.org/10.2136/sssabookser10.c46.

Caputi, N. *et al.* (2013) 'The impact of climate change on exploited lobster stocks', in B.F. Phillips (ed.) *Lobsters: biology, management, aquaculture and fisheries*, pp. 84–112. Available at: https://doi.org/10.1002/9781118517444.ch4.

Cavanaugh, K.C. *et al.* (2019) 'Climate-driven regime shifts in a mangrove–salt marsh ecotone over the past 250 years', *Proceedings of the National Academy of Sciences*, 116(43), pp. 21602–21608.

Chambers, L.G. (2014) 'Biogeochemical effects of simulated sea level rise on carbon loss in an everglades mangrove peat soil', *Hydrobiologia*, 726, pp. 195–211.

Chambers, L.G., R., R.K. and Z, O.T. (2011) 'Short-term response of carbon cycling to salinity pulses in a freshwater wetland', *Soil Science Society of America Journal*, 75, pp. 2000–2007.

Charles, H. and Dukes, J.S. (2009) 'Effects of warming and altered precipitation on plant and nutrient dynamics of a New England salt marsh', *Ecological Applications*, 19, pp. 1758–1773.

Chen, Y. and Kirwan, M.L. (2022) 'A phenology- and trend-based approach for accurate mapping of sea-level driven coastal forest retreat', *Remote Sensing of Environment*, 281, p. 113229. Available at: https://doi.org/10.1016/j.rse.2022.113229.

Chmura, G.L. *et al.* (2003) 'Global carbon sequestration in tidal, saline wetland soils', *Global Biogeochemical Cycles*, 17(4), p. n/a-n/a. Available at: https://doi.org/10.1029/2002GB001917.

Chojnacky, D.C., Heath, L.S. and Jenkins, J.C. (2014) 'Updated generalized biomass equations for North American tree species', *Forestry*, 87, 1, pp. 129–151.

Clark, A.I. and Schroeder, J.G. (1985) 'Weight, volume, and physical properties of major hardwood species in the southern Appalachian mountains', in *Res. Pap. SE-253*. Asheville, NC: US Department of Agriculture, Forest Service, Southeastern Forest Experiment Station, pp. 63, 253.

Coldren, G.A. *et al.* (2016) 'Chronic warming stimulates growth of marsh grasses more than mangroves in a coastal wetland ecotone', *Ecology*, 97(11), pp. 3167–3175.

Coldren, G.A. *et al.* (2018) 'Warming accelerates mangrove expansion and surface elevation in a subtropical wetland', *J Ecol*, 107, pp. 79–90. Available at: https://doi.org/10.1111/1365-2745.13049.

Coldren, G.A. *et al.* (2019) 'Warming accelerates mangrove expansion and surface elevation gain in a subtropical wetland', *Journal of Ecology*, 107(1), pp. 79–90.

Connell, L.C., Scasta, J.D. and Porensky, L.M. (2018) 'Prairie dogs and wildfires shape vegetation structure in a sagebrush grassland more than does rest from ungulate grazing', *Ecosphere*, 9:e02390. Available at: https://doi.org/10.1002/ecs2.2390.

Connor, R. and Chmura, G.L. (2000) 'Dynamics of above-and belowground organic matter in a high latitude macrotidal saltmarsh', *Marine Ecology Progress Series*, 204, pp. 101–110.

Conti, G. (2019) 'Developing allometric models to predict the individual aboveground biomass of shrubs worldwide', *Global Ecology and Biogeography*, 28, pp. 961–975.

Couto, T. *et al.* (2014) 'Modelling the effects of global temperature increase on the growth of salt marsh plants', *Applied Ecology and Environmental Research*, 12(3), pp. 753–764.

Craft, C. *et al.* (1999) 'Twenty-Five Years of Ecosystem Development of Constructed Spartina Alterniflora (loisel) Marshes', *Ecological Applications*, 9(4), pp. 1405–1419. Available at: https://doi.org/10.1890/1051-0761(1999)009[1405:TFYOED]2.0.CO;2.

Craft, C. (2000) 'Co-development of wetland soils and benthic invertebrate communities following salt marsh creation', *Wetlands Ecology and Management*, 8, pp. 197–207.

Craft, C. *et al.* (2009) 'Forecasting the effects of accelerated sea-level rise on tidal marsh ecosystem services', *Frontiers in Ecology and the Environment*, 7(2), pp. 73–78. Available at: https://doi.org/10.1890/070219.

Craft, C.B., Seneca, E.D. and Broome, S.W. (1991) 'Loss on ignition and Kjeldahl digestion for estimating organic carbon and total nitrogen in estuarine marsh soils: calibration with dry combustion', *Estuaries*, 14, pp. 175–179.

Crosby, S.C. *et al.* (2016) 'Salt marsh persistence is threatened by predicted sea-level rise', *Estuarine, Coastal and Shelf Science*, 181, pp. 93–99. Available at: https://doi.org/10.1016/j.ecss.2016.08.018.

Cullen, J.J. (1982) 'The deep chlorophyll maximum: comparing vertical profiles of chlorophyll a', *Can J Fish Aquat Sci*, 39, pp. 791–803. Available at: https://doi.org/10.1139/f82-108.

Cullen, J.J. (2015) 'Subsurface chlorophyll maximum layers: enduring enigma or mystery solved?', *Ann Rev Mar Sci*, 7, pp. 207–239. Available at: https://doi.org/10.1146/annurev-marine-010213-135111.

Dakos, V. *et al.* (2008) 'Slowing down as an early warning signal for abrupt climate change', *Proceedings of the National Academy of Sciences*, 105(38), pp. 14308–14312. Available at: https://doi.org/10.1073/pnas.0802430105.

Darby, F.A. and Turner, R.E. (2008) 'Below-and aboveground Spartina alterniflora production in a Louisiana salt marsh', *Estuaries and Coasts*, 31(1), pp. 223–231.

Deaton, C.D., Hein, C.J. and Kirwan, M.L. (2017) 'Barrier island migration dominates ecogeomorphic feedbacks and drives salt marsh loss along the Virginia Atlantic Coast, USA', *Geology*, 45(2), pp. 123–126. Available at: https://doi.org/10.1130/G38459.1.

Defne, Z. *et al.* (2020) 'A geospatially resolved wetland vulnerability index: Synthesis of physical drivers', *PLOS ONE*, 15(1), p. e0228504. Available at: https://doi.org/10.1371/journal.pone.0228504.

DeLaune, R.D., Nyman, J.A. and Jr., W.H.P. (1994) 'Peat Collapse, Ponding and Wetland Loss in a Rapidly Submerging Coastal Marsh', *Journal of Coastal Research*, 10(4), pp. 1021–1030.

Delcourt, P.A. and Delcourt, H.R. (1992) 'Ecotone dynamics in space and time', in A.J. Hansen and F. Castri (eds) *Landscape boundaries*. New York: Springer, pp. 19–54. Available at: https://doi.org/10.1007/978-1-4612-2804-2_2.

Diamond, J.S. *et al.* (2021) 'A little relief: Ecological functions and autogenesis of wetland microtopography', *WIREs Water*, 8(1), p. e1493. Available at: https://doi.org/10.1002/wat2.1493.

D'Odorico, P. *et al.* (2010) 'Positive feedback between microclimate and shrub encroachment in the northern Chihuahuan desert', *Ecosphere*, 1, pp. 1–11. Available at: https://doi.org/10.1890/ES10-00073.1.

Doney, S.C. *et al.* (2012) 'Climate change impacts on marine ecosystems', *Annual review of marine science*, 4, pp. 11–37.

Donnelly, J.P. and Bertness, M.D. (2001) 'Rapid shoreward encroachment of salt marsh cordgrass in response to accelerated sea-level rise', *Proc Natl Acad Sci*, 98, pp. 14218–14223. Available at: https://doi.org/10.1073/pnas.251209298.

Dontis, E.E. *et al.* (2020) *Carbon Storage Increases with Site Age as Created Salt Marshes Transition to Mangrove Forests in Tampa*. Bay, Florida (USA: ESTUARIES AND COASTS.

Doody, J.P. (2013) 'Coastal squeeze and managed realignment in southeast England, does it tell us anything about the future?', *Ocean & coastal management*, 79, pp. 34–41.

Doughty, C.L. *et al.* (2016) 'Mangrove Range Expansion Rapidly Increases Coastal Wetland Carbon Storage', *Estuaries and Coasts*, 39(2), pp. 385–396. Available at: https://doi.org/10.1007/s12237-015-9993-8.

Doughty, C.L. *et al.* (2021) 'Characterizing spatial variability in coastal wetland biomass across multiple scales using UAV and satellite imagery', *Remote Sensing in Ecology and Conservation*, 7(3), pp. 411–429. Available at: https://doi.org/10.1002/rse2.198.

Doyle, T.W. (2010) 'Predicting the retreat and migration of tidal forests along the northern Gulf of Mexico under sea-level rise', *Forest Ecology and Management*, 259(4), pp. 770–777.

Duarte, C.M., Middelburg, J.J. and Caraco, N. (2005) 'Major role of marine vegetation on the oceanic carbon cycle', *Biogeosciences*, 2, pp. 1–8.

Duniway, M.C., Snyder, K.A. and Herrick, J.E. (2010) 'Spatial and temporal patterns of water availability in a grass–shrub ecotone and implications for grassland recovery in arid environments', *Ecohydrology*, 3, pp. 55–67. Available at: https://doi.org/10.1002/eco.94.

Duran Vinent, O. *et al.* (2021) 'Onset of runaway fragmentation of salt marshes', *One Earth*, 4(4), pp. 506–516. Available at: https://doi.org/10.1016/j.oneear.2021.02.013.

E, M. (1990) 'Ecotones and ecoclines are different', *J Veg Sci*, 1, pp. 135–138. Available at: https://doi.org/10.2307/3236065.

Elsey-Quirk, T. *et al.* (2011) 'Salt marsh carbon pool distribution in a mid-Atlantic lagoon, USA: sea level rise implications', *Wetlands*, 31(1), pp. 87–99.

Enwright, N.M., Griffith, K.T. and Osland, M.J. (2016) 'Barriers to and opportunities for landward migration of coastal wetlands with sea-level rise', *Frontiers in Ecology and the Environment*, 14(6), pp. 307–316. Available at: https://doi.org/10.1002/fee.1282.

Estrada, M. *et al.* (1993) 'Variability of deep chlorophyll maximum characteristics in the Northwestern Mediterranean', *Mar Ecol Prog Ser*, 92, pp. 289–300. Available at: https://doi.org/10.3354/meps092289.

Ewers Lewis, C.J. *et al.* (2019) 'Impacts of land reclamation on tidal marsh "blue carbon" stocks', *Science of The Total Environment*, 672, pp. 427–437. Available at: https://doi.org/10.1016/j.scitotenv.2019.03.345.

Fagherazzi, S. *et al.* (2012) 'Numerical models of salt marsh evolution: Ecological, geomorphic, and climatic factors', *Reviews of Geophysics*, 50(1). Available at: https://doi.org/10.1029/2011RG000359.

Fagherazzi, S. *et al.* (2019) 'Sea level rise and the dynamics of the marsh-upland boundary', *Front Environ Sci*, 7, pp. 1–18. Available at: https://doi.org/10.3389/fenvs.2019.00025.

Fagherazzi, S. *et al.* (2020) 'Salt marsh dynamics in a period of accelerated sea level rise', *Journal of Geophysical Research: Earth Surface*, 125(8), p. 2019 005200.

Faunce, K.E. and Rapp, J.L. (2020) 'Topobathymetric Digital Elevation Model (TBDEM) of the Eastern Shore Peninsula of Virginia and adjacent parts of Maryland with a horizontal resolution of 1 meter and vertical resolution of 1 centimeter: U.S', *Geological Survey data release* [Preprint]. Available at: https://doi.org/10.5066/P9F5CV1Y.

Fee, E.J. (1976) 'The vertical and seasonal distribution of chlorophyll in lakes of the Experimental Lakes Area, northwestern Ontario: Implications for primary production estimates', *Limnol Oceanogr*, 21, pp. 767–783. Available at: https://doi.org/10.4319/lo.1976.21.6.0767.

Fenster, M.S., Dolan, R. and Smith, J.J. (2016) 'Grain-size distributions and coastal morphodynamics along the southern Maryland and Virginia barrier islands', *Sedimentology*, 63(4), pp. 809–823. Available at: https://doi.org/10.1111/sed.12239.

Field, C.R., Gjerdrum, C. and Elphick, C.S. (2016) 'Forest resistance to sea-level rise prevents landward migration of tidal marsh', *Biological Conservation*, 201, pp. 363–369.

FitzGerald, D.M. *et al.* (2018) 'Runaway Barrier Island Transgression Concept: Global Case Studies', in L.J. Moore and A.B. Murray (eds) *Barrier Dynamics and Response to Changing Climate*. Cham: Springer International Publishing, pp. 3–56. Available at: https://doi.org/10.1007/978-3-319-68086-6_1.

FitzGerald, D.M. and Hughes, Z. (2019) 'Marsh processes and their response to climate change and sea-level rise', *Annual Review of Earth and Planetary Sciences*, 47, pp. 481–517.

Flester, J.A. and Blum, L.K. (2020) 'Rates of mainland marsh migration into uplands and seaward edge erosion are explained by geomorphic type of salt marsh in Virginia coastal lagoons', *Wetlands*, 40(6), pp. 1703–1715.

Folke, C. *et al.* (2004) 'Regime shifts, resilience, and biodiversity in ecosystem management', *Annu. Rev. Ecol. Evol. Syst*, 35, pp. 557–581.

Forman, R.T. (2014) 'Land Mosaics: The ecology of landscapes and regions'.

Forman, R.T. and Moore, P.N. (1992) 'Theoretical foundations for understanding boundaries in landscape mosaics', in A.J. Hansen and F. Castri (eds) *Landscape boundaries*. New York: Springer, pp. 236–258. Available at: https://doi.org/10.1007/978-1-4612-2804-2_11.

Fourqurean, J.W. *et al.* (2012) 'Seagrass ecosystems as a globally significant carbon stock', *Nature Geoscience*, 5(7), pp. 505–509. Available at: https://doi.org/10.1038/ngeo1477.

Friedrichs, C.T. and Perry, J.E. (2001) 'Tidal Salt Marsh Morphodynamics: A Synthesis', *Journal of Coastal Research*, pp. 7–37.

Fryer, J. and Williams, I.D. (2021) 'Regional carbon stock assessment and the potential effects of land cover change', *Science of The Total Environment*, 775, p. 145815.

Fuhlendorf, S.D. *et al.* (2006) 'Should heterogeneity be the basis for conservation? Grassland bird response to fire and grazing', *Ecol Appl*, 16, pp. 1706–1716. Available at: https://doi.org/10.1890/1051-0761(2006)016.

Gamache, I. and Payette, S. (2005) 'Latitudinal response of subarctic tree lines to recent climate change in eastern Canada', *Journal of Biogeography*, 32(5), pp. 849–862.

Ganju, N.K. *et al.* (2017) 'Spatially integrative metrics reveal hidden vulnerability of microtidal salt marshes', *Nature Communications*, 8(1), p. 14156. Available at: https://doi.org/10.1038/ncomms14156.

Ganju, N.K. *et al.* (2022) 'Development and Application of Landsat-Based Wetland Vegetation Cover and UnVegetated-Vegetated Marsh Ratio (UVVR) for the Conterminous United States', *Estuaries and Coasts*, 45(7), pp. 1861–1878. Available at: https://doi.org/10.1007/s12237-022-01081-x.

Ganju, N.K., Nidzieko, N.J. and Kirwan, M.L. (2013) 'Inferring tidal wetland stability from channel sediment fluxes: Observations and a conceptual model', *Journal of Geophysical Research: Earth Surface*, 118(4), pp. 2045–2058. Available at: https://doi.org/10.1002/jgrf.20143.

Gardner, L.R. and Reeves, H.W. (2002) 'Spatial patterns in soil water fluxes along a forest-marsh transect in the southeastern United States', *Aquatic Sciences*, 64, pp. 141–155.

Garrard, S.L. and Beaumont, N.J. (2014) 'The effect of ocean acidification on carbon storage and sequestration in seagrass beds; a global and UK context', *Marine Pollution Bulletin*, 86(1–2), pp. 138–146.

Gedan, K. and Fernández-Pascual, E. (2019) 'Salt marsh migration into salinized agricultural fields: a novel assembly of plant communities', *J Veg Sci*, 30, pp. 1007–1016. Available at: https://doi.org/10.1111/jvs.12774.

Gedan, K.B. and Bertness, M.D. (2009) 'Experimental warming causes rapid loss of plant diversity in New England salt marshes', *Ecology Letters*, 12(8), pp. 842–848.

Gedan, K.B. and Bertness, M.D. (2010) 'How will warming affect the salt marsh foundation species Spartina patens and its ecological role?', *Oecologia*, 164(2), pp. 479–487.

Gehman, A.M. *et al.* (2018) 'Effects of small-scale armoring and residential development on the salt marsh-upland ecotone', *Estuaries Coast*, 41:S54-S67. Available at: https://doi.org/10.1007/s12237-017-0300-8.

Ghedini, G., Russell, B.D. and Connell, S.D. (2015) 'Trophic compensation reinforces resistance: herbivory absorbs the increasing effects of multiple disturbances', *Ecology Letters*, 18(2), pp. 182–187.

Giurgevich, J.R. and Dunn, E.L. (1979) 'Seasonal patterns of CO 2 and water vapor exchange of the tall and short height forms of Spartina alterniflora Loisel in a Georgia salt marsh', *Oecologia*, 43(2), pp. 139–156.

Goldblum, D. and Rigg, L.S. (2005) 'Tree growth response to climate change at the deciduous boreal forest ecotone, Ontario, Canada', *Can J For Res*, 35, pp. 2709–2718. Available at: https://doi.org/10.1139/x05-185.

Gonneea, M.E. *et al.* (2019) 'Salt marsh ecosystem restructuring enhances elevation resilience and carbon storage during accelerating relative sea-level rise', *Estuarine, Coastal and Shelf Science*, 217, pp. 56–68. Available at: https://doi.org/10.1016/j.ecss.2018.11.003.

Gonzalez, A. and Loreau, M. (2009) 'The Causes and Consequences of Compensatory Dynamics in Ecological Communities', *Annual Review of Ecology, Evolution, and Systematics*, 40(1), pp. 393–414. Available at: https://doi.org/10.1146/annurev.ecolsys.39.110707.173349.

Gonzalez, P. *et al.* (2010) 'Global patterns in the vulnerability of ecosystems to vegetation shifts due to climate change', *Glob Ecol Biogeogr*, 19, pp. 755–768. Available at: https://doi.org/10.1111/j.1466-8238.2010.00558.x.

Gosz, J. (1993) 'Ecological hierarchies', *Ecol Appl*, 3, pp. 369–376. Available at: https://doi.org/10.2307/1941905.

Greiner, J.T. *et al.* (2013) 'Seagrass restoration enhances "blue carbon" sequestration in coastal waters', *PloS one*, 8(8), p. 72469.

Guimond, J.A. *et al.* (2020) 'Using hydrological-biogeochemical linkages to elucidate carbon dynamics in coastal marshes subject to relative sea level rise', *Water Resources Research*, 56(2), p. 2019 026302.

Hamilton, S.E. and Friess, D.A. (2018) 'Global carbon stocks and potential emissions due to mangrove deforestation from 2000 to 2012', *Nat. Clim. Change*, 8, pp. 240–244.

Hanson, P.J. *et al.* (2020) 'Rapid net carbon loss from a whole-ecosystem warmed Peatland', *AGU Advances*, 1(3), p. 2020 000163.

Hardie, M. and Doyle, R. (2012) 'Measuring soil salinity', *Methods Mol. Biol*, 913, pp. 415–25.

Harman, C.J. *et al.* (2014) 'Spatial patterns of vegetation, soils, and microtopography from terrestrial laser scanning on two semiarid hillslopes of contrasting lithology', *Journal of Geophysical Research: Biogeosciences*, 119(2), pp. 163–180. Available at: https://doi.org/10.1002/2013JG002507.

Harris, L.I., Roulet, N.T. and Moore, T.R. (2020) 'Mechanisms for the Development of Microform Patterns in Peatlands of the Hudson Bay Lowland', *Ecosystems*, 23(4), pp. 741–767. Available at: https://doi.org/10.1007/s10021-019-00436-z.

Hartig, E.K. *et al.* (2002) 'Anthropogenic and climate-change impacts on salt marshes of Jamaica Bay, New York City', *Wetlands*, 22(1), pp. 71–89.

Hayden, B.P. *et al.* (1991) 'Long-term research at the Virginia Coast Reserve', *BioScience*, 41(5), pp. 310–318.

He, C. *et al.* (2016) 'Assessing the potential impacts of urban expansion on regional carbon storage by linking the LUSD-urban and InVEST models', *Environmental Modelling & Software*, 75, pp. 44–58.

He, Y. *et al.* (2012) 'Evaluation of 1: 5 soil to water extract electrical conductivity methods', *Geoderma*, 185, pp. 12–17.

Helmuth, B. *et al.* (2010) 'Organismal climatology: analyzing environmental variability at scales relevant to physiological stress', *Journal of Experimental Biology*, 213(6), pp. 995–1003.

Heras M, M., L, T. and J, W. (2016) 'Seed-bank structure and plant-recruitment conditions regulate the dynamics of a grassland-shrubland Chihuahuan ecotone', *Ecology*, 97, pp. 2303–2318. Available at: https://doi.org/10.1002/ecy.1446.

Herbert, E.R., J., S.-B. and Craft, C.B. (2018) 'Differential effects of chronic and acute simulated seawater intrusion on tidal freshwater marsh carbon cycling', *Biogeochemistry*, 138, pp. 137–154.

Herbert, E.R., Windham-Myers, L. and Kirwan, M.L. (2021) 'Sea-level rise enhances carbon accumulation in United States tidal wetlands', *One Earth*, 4(3), pp. 425–433. Available at: https://doi.org/10.1016/j.oneear.2021.02.011.

van Heuven, S. (2011) *MATLAB Program Developed for CO2 System Calculations. ORNL/CDIAC-105b. Carbon Dioxide Information Analysis Center, Oak Ridge National Laboratory, U.S. Department of Energy, Oak Ridge, Tennessee.* Available at: https://www.eea.europa.eu/data-and-maps/indicators/ocean-acidification-3/van-heuven-s-d-pierrot (Accessed: 15 March 2023).

Hladik, C. and Alber, M. (2012) 'Accuracy assessment and correction of a LIDAR-derived salt marsh digital elevation model', *Remote Sensing of Environment*, 121, pp. 224–235. Available at: https://doi.org/10.1016/j.rse.2012.01.018.

Hoegh-Guldberg, O. *et al.* (2007) 'Coral reefs under rapid climate change and ocean acidification', *science*, 318(5857), pp. 1737–1742.

Holmquist, J.R. *et al.* (2018) 'Accuracy and Precision of Tidal Wetland Soil Carbon Mapping in the Conterminous United States', *Scientific Reports*, 8(1), p. 9478. Available at: https://doi.org/10.1038/s41598-018-26948-7.

Hopkinson, C.S., Cai, W.-J. and Hu, X. (2012) 'Carbon sequestration in wetland dominated coastal systems—a global sink of rapidly diminishing magnitude', *Current Opinion in Environmental Sustainability*, 4(2), pp. 186–194. Available at: https://doi.org/10.1016/j.cosust.2012.03.005.

Horton, B.P. *et al.* (2018) 'Predicting marsh vulnerability to sea-level rise using Holocene relative sea-level data', *Nature Communications*, 9(1), p. 2687. Available at: https://doi.org/10.1038/s41467-018-05080-0.

Horváth, A., March, I.J. and Wolf, J.H. (2001) 'Rodent diversity and land use in Montebello, Chiapas, Mexico', *Stud Neotrop Fauna Environ*, 36, pp. 169–176. Available at: https://doi.org/10.1076/snfe.36.3.169.2130.

Houlahan, J.E. *et al.* (2007) 'Compensatory dynamics are rare in natural ecological communities', *Proceedings of the National Academy of Sciences*, 104(9), pp. 3273–3277.

Huisman, J. *et al.* (2006) 'Reduced mixing generates oscillations and chaos in the oceanic deep chlorophyll maximum', *Nature*, 439, pp. 322–325. Available at: https://doi.org/10.1038/nature04245.

Hussein, A.H. (2009) 'Modeling of sea-level rise and deforestation in submerging coastal utisols of Chesapeake Bay', *Soil Sci. Soc. Of America Journal*, 73(1), pp. 185–196.

Jankowski, K.L., Törnqvist, T.E. and Fernandes, A.M. (2017) 'Vulnerability of Louisiana's coastal wetlands to present-day rates of relative sea-level rise', *Nature Communications*, 8(1), p. 14792. Available at: https://doi.org/10.1038/ncomms14792.

Jenkins, J.C. *et al.* (2003) 'National-scale biomass estimators for United States tree species', *Forest Sci*, 49, pp. 12–35.

Johnston, C.A. (1991) 'Sediment and nutrient retention by freshwater wetlands: effects on surface water quality', *Crit Rev Environ Sci Technol*, 21, pp. 491–565. Available at: https://doi.org/10.1080/10643389109388425.

Jordan, T.E. and Correll, D.L. (1991) 'Continuous automated sampling of tidal exchanges of nutrients by brackish marshes', *Estuarine, Coastal and Shelf Science*, 32(6), pp. 527–545.

Jorgensen, E.E., Demarais, S. and Monasmith, T. (2000) 'Rodent habitats in a Chihuahuan Desert/desert plains grassland ecotone', *Tex J Sci*, 52, pp. 303–312.

Junior, N.A. *et al.* (2015) 'Microbial community diversity and physical–chemical features of the Southwestern Atlantic Ocean', *Arch Microbiol*, 197, pp. 165–179. Available at: https://doi.org/10.1007/s00203-014-1035-6.

Kamphorst, E.C. *et al.* (2000) 'Predicting Depressional Storage from Soil Surface Roughness', *Soil Science Society of America Journal*, 64(5), pp. 1749–1758. Available at: https://doi.org/10.2136/sssaj2000.6451749x.

Karstens, S. *et al.* (2016) 'Dynamics of surface elevation and microtopography in different zones of a coastal Phragmites wetland', *Ecological Engineering*, 94, pp. 152–163. Available at: https://doi.org/10.1016/j.ecoleng.2016.05.049.

Kashian, D.M. *et al.* (2006) 'Carbon storage on landscapes with stand-replacing fires', *Bioscience*, 56(7), pp. 598–606.

Kearney, M.S. and Turner, R.E. (2016) 'Microtidal marshes: Can these widespread and fragile marshes survive increasing climate–sea level variability and human action?', *Journal of Coastal Research*, 32(3), pp. 686–699.

Kéfi, S. *et al.* (2007) 'Spatial vegetation patterns and imminent desertification in Mediterranean arid ecosystems', *Nature*, 449(7159), pp. 213–217.

Kefi, S. *et al.* (2014) 'Early warning signals of ecological transitions: methods for spatial patterns', *PloS one*, 9(3), p. 92097.

Kelleway, J.J. *et al.* (2016) 'Sedimentary factors are key predictors of carbon storage in SE Australian saltmarshes', *Ecosystems*, 19(5), pp. 865–880.

Kimor, B., Berman, T. and Schneller, A. (1987) 'Phytoplankton assemblages in the deep chlorophyll maximum layers off the Mediterranean coast of Israel', *J Plankton Res*, 9, pp. 433–443. Available at: https://doi.org/10.1093/plankt/9.3.433.

Kirschbaum, M.U. (1995) 'The temperature dependence of soil organic matter decomposition, and the effect of global warming on soil organic C storage', *Soil Biology and biochemistry*, 27(6), pp. 753–760.

Kirwan, M. and Temmerman, S. (2009) 'Coastal marsh response to historical and future sea-level acceleration', *Quaternary Science Reviews*, 28(17), pp. 1801–1808. Available at: https://doi.org/10.1016/j.quascirev.2009.02.022.

Kirwan, M.L., Temmerman, S., *et al.* (2016) 'Overestimation of marsh vulnerability to sea level rise', *Nature Climate Change*, 6(3), pp. 253–260. Available at: https://doi.org/10.1038/nclimate2909.

Kirwan, M.L., Walters, D.C., *et al.* (2016) 'Sea level driven marsh expansion in a coupled model of marsh erosion and migration', *Geophysical Research Letters*, 43(9), pp. 4366–4373. Available at: https://doi.org/10.1002/2016GL068507.

Kirwan, M.L. and Blum, L.K. (2011) 'Enhanced decomposition offsets enhanced productivity and soil carbon accumulation in coastal wetlands responding to climate change', *Biogeosciences*, 8(4), pp. 987–993.

Kirwan, M.L. and Gedan, K.B. (2019) 'Sea-level driven land conversion and the formation of ghost forests', *Nature Climate Change*, 9(6), pp. 450–457. Available at: https://doi.org/10.1038/s41558-019-0488-7.

Kirwan, M.L., Guntenspergen, G.R. and Langley, J.A. (2014) 'Temperature sensitivity of organic-matter decay in tidal marshes', *Biogeosciences*, 11(17), pp. 4801–4808.

Kirwan, M.L., Guntenspergen, G.R. and Morris, J.T. (2009) 'Latitudinal trends in Spartina alterniflora productivity and the response of coastal marshes to global change', *Global Change Biology*, 15(8), pp. 1982–1989.

Kirwan, M.L. and Megonigal, J.P. (2013) 'Tidal wetland stability in the face of human impacts and sea-level rise', *Nature*, 504(7478), pp. 53–60. Available at: https://doi.org/10.1038/nature12856.

Kirwan, M.L. and Mudd, S.M. (2012) 'Response of salt-marsh carbon accumulation to climate change', *Nature*, 489(7417), pp. 550–553. Available at: https://doi.org/10.1038/nature11440.

Kolasa, J. and Zalewski, M. (1995) 'Notes on ecotone attributes and functions', *Hydrobiologia*, 303, pp. 1–7. Available at: https://doi.org/10.1007/BF00034039.

Körner, C. (1998) 'A re-assessment of high elevation treeline positions and their explanation', *Oecologia*, 115, pp. 445–459. Available at: https://doi.org/10.1007/s004420050540.

Kozlowski, T. (1997) 'Responses of woody plants to flooding and salinity', *Tree Physiol. Monogr*, 17(490). Available at: https://doi.org/10.1093/treephys/17.7.490.

Krause, J.R. *et al.* (2022) 'Beyond habitat boundaries: Organic matter cycling requires a system-wide approach for accurate blue carbon accounting', *Limnology and Oceanography*, 67(S2), pp. S6–S18. Available at: https://doi.org/10.1002/lno.12071.

Krauss, K.W. *et al.* (2018) 'The Role of the Upper Tidal Estuary in Wetland Blue Carbon Storage and Flux', *Global Biogeochemical Cycles*, 32(5), pp. 817–839. Available at: https://doi.org/10.1029/2018GB005897.

Krauss, K.W., L., C.J. and Creech, D. (2007) *Selection for salt tolerance in tidal freshwater swamp species: advances using baldcypress as a model for restoration. Ecology of tidal freshwater forested wetlands of the southeastern United States*. Springer, Dordrech.

Kupfer, J.A. and Cairns, D.M. (1996) 'The suitability of montane ecotones as indicators of global climatic change', *Prog Phys Geogr*, 20, pp. 253–272. Available at: https://doi.org/10.1177/030913339602000301.

Langley, J.A. *et al.* (2009) 'Elevated CO2 stimulates marsh elevation gain, counterbalancing sea-level rise', *Proceedings of the National Academy of Sciences*, 106(15), pp. 6182–6186. Available at: https://doi.org/10.1073/pnas.0807695106.

Langston, A.K., Kaplan, D.A. and Putz, F.E. (2017) 'A casualty of climate change? Loss of freshwater forest islands on Florida's Gulf Coast', *Global Change Biology*, 23(12), pp. 5383–5397.

Letelier, R.M. *et al.* (2004) 'Light driven seasonal patterns of chlorophyll and nitrate in the lower euphotic zone of the North Pacific Subtropical Gyre', *Limnol Oceanogr*, 49, pp. 508–519. Available at: https://doi.org/10.4319/lo.2004.49.2.0508.

Lewis, E.R. and Wallace, D.W.R. (1998) 'Program developed for CO2 system calculations (No. cdiac: CDIAC-105', *Environmental System Science Data Infrastructure for a Virtual Ecosystem* [Preprint].

Liu, W. *et al.* (2016) 'Geographical variation in vegetative growth and sexual reproduction of the invasive Spartina alterniflora in China', *Journal of Ecology*, 104(1), pp. 173–181.

Liu, W. *et al.* (2020) 'Climate and geographic adaptation drive latitudinal clines in biomass of a widespread saltmarsh plant in its native and introduced ranges', *Limnology and Oceanography*, 65(6), pp. 1399–1409.

Lloyd, K.M. *et al.* (2000) 'Evidence on ecotone concepts from switch, environmental and anthropogenic ecotones', *J Veg Sci*, 11, pp. 903–910. Available at: https://doi.org/10.2307/3236560.

Long, S.P., Incoll, L.D. and Woolhouse, H.W. (1975) 'C 4 photosynthesis in plants from cool temperate regions, with particular reference to Spartina townsendii', *Nature*, 257(5527), pp. 622–624.

Longhurst, A. (2006) *Ecological geography of the sea*. 2nd edn. New York: Elsevier Science Publishers.

Loreau, M. and Mazancourt, C. (2013) 'Biodiversity and ecosystem stability: a synthesis of underlying mechanisms', *Ecology letters*, 16, pp. 106–115.

Lovelock, C.E. *et al.* (2015) 'The vulnerability of Indo-Pacific mangrove forests to sea-level rise', *Nature*, 526(7574), pp. 559–563. Available at: https://doi.org/10.1038/nature15538.

Lynch, J., Hensel, P. and Cahoon, D. (2015) 'The Surface Elevation Table and Marker Horizon Technique: A Protocol for Monitoring Wetland Elevation Dynamics', *(No. NPS/NCBN/NRR—2015/1078). National Park Service.* [Preprint].

MacArthur, R.H., Diamond, J.M. and Karr, J.R. (1972) 'Density compensation in island faunas', *Ecology*, 53(2), pp. 330–342.

Macías, D., Stips, A. and Garcia-Gorriz, E. (2014) 'The relevance of deep chlorophyll maximum in the open Mediterranean Sea evaluated through 3D hydrodynamic-biogeochemical coupled simulations', *Ecol Modell*, 281, pp. 26–37. Available at: https://doi.org/10.1016/j.ecolmodel.2014.03.002.

Macreadie, P.I. *et al.* (2017) 'Can we manage coastal ecosystems to sequester more blue carbon?', *Frontiers in Ecology and the Environment*, 15(4), pp. 206–213.

Maher, E.L., Germino, M.J. and Hasselquist, N.J. (2005) 'Interactive effects of tree and herb cover on survivorship, physiology, and microclimate of conifer seedlings at the alpine tree-line ecotone', *Canadian Journal of Forest Research*, 35(3), pp. 567–574.

Marion, C., Anthony, E.J. and Trentesaux, A. (2009) 'Short-term (≤2 yrs) estuarine mudflat and saltmarsh sedimentation: High-resolution data from ultrasonic altimetery, rod surface-elevation table, and filter traps', *Estuarine, Coastal and Shelf Science*, 83(4), pp. 475–484. Available at: https://doi.org/10.1016/j.ecss.2009.03.039.

Mariotti, G. (2016) 'Revisiting salt marsh resilience to sea level rise: Are ponds responsible for permanent land loss?: SALT MARSH PONDS', *Journal of Geophysical Research: Earth Surface*, 121(7), pp. 1391–1407. Available at: https://doi.org/10.1002/2016JF003900.

Mariotti, G. (2020) 'Beyond marsh drowning: The many faces of marsh loss (and gain)', *Advances in Water Resources*, 144, p. 103710. Available at: https://doi.org/10.1016/j.advwatres.2020.103710.

Mariotti, G. *et al.* (2020) 'Modeling the spatial dynamics of marsh ponds in New England salt marshes', *Geomorphology*, 365, p. 107262. Available at: https://doi.org/10.1016/j.geomorph.2020.107262.

Mariotti, G. and Carr, J. (2014) 'Dual role of salt marsh retreat: Long-term loss and short-term resilience', *Water Resources Research*, 50(4), pp. 2963–2974. Available at: https://doi.org/10.1002/2013WR014676.

Mariotti, G. and Fagherazzi, S. (2013) 'Critical width of tidal flats triggers marsh collapse in the absence of sea-level rise', *Proceedings of the National Academy of Sciences*, 110(14), pp. 5353–5356. Available at: https://doi.org/10.1073/pnas.1219600110.

Mariotti, G. and Hein, C.J. (2022) 'Lag in response of coastal barrier-island retreat to sea-level rise', *Nature Geoscience*, 15(8), pp. 633–638. Available at: https://doi.org/10.1038/s41561-022-00980-9.

Martin, J.G. *et al.* (1998) 'Aboveground biomass and nitrogen allocation of ten deciduous southern Appalachian tree species', *Canadian Journal of Forest Research*, 28(11), pp. 1648–1659.

Martinez, M. (2021) *State Changes in Coastal Wetlands: Anticipating Transitions and Evaluating the Role of Ghost Forests in Regional Greenhouse Gas Emissions*. (Doctoral dissertation,. North Carolina State University.

Martínez-Soto, K.S. and Johnson, D.S. (2020) 'The density of the Atlantic marsh fiddler crab (Minuca pugnax, Smith, 1870)(Decapoda: Brachyura: Ocypodidae) in its expanded range in the Gulf of Maine', *USA. J Crustac Biol*, 40, pp. 544–548. Available at: https://doi.org/10.1093/jcbiol/ruaa049.

Masubelele, M.L. *et al.* (2014) 'A 50 year study shows grass cover has increased in shrublands of semi-arid South Africa', *J Arid Environ*, 104, pp. 43–51. Available at: https://doi.org/10.1016/j.jaridenv.2014.01.011.

May, S.K., Dolan, R. and Hayden, B.P. (1983) 'Erosion of US shorelines', *Eos, Transactions American Geophysical Union*, 64(35), pp. 521–523.

McClure, A. *et al.* (2015) 'Evaluation of Error Reduction Techniques on a LIDAR-Derived Salt Marsh Digital Elevation Model', *Journal of Coastal Research*, 32(2), pp. 424–433. Available at: https://doi.org/10.2112/JCOASTRES-D-14-00185.1.

McElligot, K.M. and Bragg, D.C. (2013) 'Deriving biomass models for small-diameter loblolly pine on the Crossett Experimental Forest', *Journal of the Arkansas Academy of Science*, 67(1), pp. 94–102.

McGlathery, K.J. *et al.* (2013) 'Nonlinear dynamics and alternate stable states in shallow coastal systems', *Oceanography*, 26(3), pp. 220-231,. Available at: https://doi.org/10.5670/oceanog.2013.66.

McGranahan, D.A. *et al.* (2012) 'Spatial heterogeneity across five rangelands managed with pyric-herbivory', *J Appl Ecol*, 49, pp. 903–910. Available at: https://doi.org/10.1111/j.1365-2664.2012.02168.x.

Mcleod, E. *et al.* (2011) 'A blueprint for blue carbon: toward an improved understanding of the role of vegetated coastal habitats in sequestering CO2', *Frontiers in Ecology and the Environment*, 9(10), pp. 552–560. Available at: https://doi.org/10.1890/110004.

McLoughlin, S.M. *et al.* (2015) 'Rates and Forcing of Marsh Edge Erosion in a Shallow Coastal Bay', *Estuaries and Coasts*, 38(2), pp. 620–638. Available at: https://doi.org/10.1007/s12237-014-9841-2.

McTigue, N. (2019) 'Sea level rise explains changing carbon accumulation rates in a salt marsh over the past two millennia', *Journal of Geophysical Research: Biogeosciences*, 124, pp. 2945–2957.

Mekonnen, Z.A. *et al.* (2021) 'Arctic tundra shrubification: a review of mechanisms and impacts on ecosystem carbon balance', *Environmental Research Letters*, 16(5), p. 053001. Available at: https://doi.org/10.1088/1748-9326/abf28b.

Melillo, J.M. (2017) 'Long-term pattern and magnitude of soil carbon feedback to the climate system in a warming world', *Science*, 358, pp. 101–105.

Merecí-Guamán, J. *et al.* (2021) 'Impact of Shrimp Ponds on Mangrove Blue Carbon Stocks in Ecuador', *Forests*, 12(7), p. 816. Available at: https://doi.org/10.3390/f12070816.

Minchinton, T.E. and Bertness, M.D. (2003) 'Disturbance-mediated competition and the spread of Phragmites australis in a coastal marsh', *Ecol Appl*, 13, pp. 1400–1416. Available at: https://doi.org/10.1890/02-5136.

Mokany, K., Raison, R.J. and Prokushkin, A.S. (2006) 'Critical analysis of root: shoot ratios in terrestrial biomes', *Global Change Biology*, 12(1), pp. 84–96.

Molino, G.D. *et al.* (2021) 'Quantifying slopes as a driver of forest to marsh conversion using geospatial techniques: application to chesapeake bay coastal-plain, United States', *Frontiers in Environmental Science*, 9, p. 149.

Morris, J.T. *et al.* (2012) 'Assessment of Carbon Sequestration Potential in Coastal Wetlands', in R. Lal et al. (eds) *Recarbonization of the Biosphere: Ecosystems and the Global Carbon Cycle*. Dordrecht: Springer Netherlands, pp. 517–531. Available at: https://doi.org/10.1007/978-94-007-4159-1_24.

Morris, J.T. *et al.* (2016) 'Contributions of organic and inorganic matter to sediment volume and accretion in tidal wetlands at steady state', *Earth's Future*, 4(4), pp. 110–121. Available at: https://doi.org/10.1002/2015EF000334.

Morton, R.A. (2008) *National assessment of shoreline change: Part 1: Historical shoreline changes and associated coastal land loss along the US Gulf of Mexico*. Diane Publishing.

Moser, K., Ahn, C. and Noe, G. (2007) 'Characterization of microtopography and its influence on vegetation patterns in created wetlands', *Wetlands*, 27(4), pp. 1081–1097. Available at: https://doi.org/10.1672/0277-5212(2007)27[1081:COMAII]2.0.CO;2.

Mudd, S.M., D'Alpaos, A. and Morris, J.T. (2010) 'How does vegetation affect sedimentation on tidal marshes? Investigating particle capture and hydrodynamic controls on biologically mediated sedimentation', *Journal of Geophysical Research: Earth Surface*, 115(F3). Available at: https://doi.org/10.1029/2009JF001566.

Mueller, P. *et al.* (2020) 'Plant species determine tidal wetland methane response to sea level rise', *Nature Communications*, 11(1), p. 5154. Available at: https://doi.org/10.1038/s41467-020-18763-4.

Mueller, P., Jensen, K. and Megonigal, J.P. (2016) 'Plants mediate soil organic matter decomposition in response to sea level rise', *Global Change Biology*, 22(1), pp. 404–414. Available at: https://doi.org/10.1111/gcb.13082.

Muñoz-Rodríguez, A.F. *et al.* (2017) 'Germination syndromes in response to salinity of Chenopodiaceae halophytes along the intertidal gradient', *Aquat Bot*, 139, pp. 48–56. Available at: https://doi.org/10.1016/j.aquabot.2017.02.003.

Nahlik, A.M. and Fennessy, M. (2016) 'Carbon storage in US wetlands', *Nature Communications*, 7(1), pp. 1–9.

Naiman, R.J. *et al.* (1988) 'The potential importance of boundaries of fluvial ecosystems', *J North Am Benthol Soc*, 7, pp. 289–306. Available at: https://doi.org/10.2307/1467295.

Naito, A.T. and Cairns, D.M. (2011) 'Patterns and processes of global shrub expansion', *Prog Phys Geogr*, 35, pp. 423–442. Available at: https://doi.org/10.1177/0309133311403538.

Najjar, R.G. *et al.* (2000) 'The potential impacts of climate change on the mid-Atlantic coastal region', *Climate Research*, 14(3), pp. 219–233.

Neilson, R.P. (1993) 'Transient ecotone response to climatic change: some conceptual and modelling approaches', *Ecol Appl*, 3, pp. 385–395. Available at: https://doi.org/10.2307/1941907.

van Nes, E.H. and Scheffer, M. (2007) 'Slow Recovery from Perturbations as a Generic Indicator of a Nearby Catastrophic Shift.', *The American Naturalist*, 169(6), pp. 738–747. Available at: https://doi.org/10.1086/516845.

Noble, I.R. (1993) 'A model of the responses of ecotones to climate change', *Ecol Appl*, 3, pp. 396–403. Available at: https://doi.org/10.2307/1941908.

Norris, M.D. *et al.* (2001) 'Assessing changes in biomass, productivity, and C and N stores following Juniperus virginiana forest expansion into tallgrass prairie', *Canadian Journal of Forest Research*, 31(11), pp. 1940–1946.

Norwood, M.J. *et al.* (2020) *J. P. Coastal Forest Seawater Exposure Increases Stem Methane Concentration. Journal of Geophysical Research: Biogeosciences*, e2020JG005915.

Novellie, P.A. and Bezuidenhout, H. (1994) 'The influence of rainfall and grazing on vegetation changes in the Mountain Zebra National Park', *Afr J Wildl Res*, 24, pp. 60–71.

Noyce, G.L. *et al.* (2019) 'Asynchronous nitrogen supply and demand produce nonlinear plant allocation responses to warming and elevated CO2', *Proceedings of the National Academy of Sciences*, 116(43), pp. 21623–21628. Available at: https://doi.org/10.1073/pnas.1904990116.

Noyce, G.L. and Megonigal, J.P. (2021) 'Biogeochemical and plant trait mechanisms drive enhanced methane emissions in response to whole-ecosystem warming', *Biogeosciences*, 18(8), pp. 2449–2463. Available at: https://doi.org/10.5194/bg-18-2449-2021.

O'Connor, T.G. and Roux, P.W. (1995) 'Vegetation changes (1949-71) in a semi-arid, grassy dwarf shrubland in the Karoo, South Africa: influence of rainfall variability and grazing by sheep', *J Appl Ecol*, 32, pp. 612–626. Available at: https://doi.org/10.2307/2404657.

Oreska, M.P., McGlathery, K.J. and Porter, J.H. (2017) 'Seagrass blue carbon spatial patterns at the meadow-scale', *PloS one*, 12(4), p. 0176630.

Orr, J.C. *et al.* (2018) 'Routine uncertainty propagation for the marine carbon dioxide system', *Marine Chemistry*, 207, pp. 84–107.

Orr, J.C., Epitalon, J.M. and Gattuso, J.P. (2015) 'Comparison of ten packages that compute ocean carbonate chemistry', *Biogeosciences*, 12(5), pp. 1483–1510.

Orth, R.J. *et al.* (2020) 'Restoration of seagrass habitat leads to rapid recovery of coastal ecosystem services', *Science Advances*, 6(41), p. eabc6434. Available at: https://doi.org/10.1126/sciadv.abc6434.

Orth, R.J. and McGlathery, K.J. (2012) 'Eelgrass recovery in the coastal bays of the Virginia Coast Reserve, USA', *Marine Ecology Progress Series*, 448, pp. 173–176.

Osland, M.J. *et al.* (2017) 'Climatic controls on the global distribution, abundance, and species richness of mangrove forests', *Ecological Monographs*, 87(2), pp. 341–359. Available at: https://doi.org/10.1002/ecm.1248.

O'sullivan, O.S. *et al.* (2017) 'Thermal limits of leaf metabolism across biomes', *Global Change Biology*, 23(1), pp. 209–223.

Palinkas, C.M. and Engelhardt, K.A. (2019) 'Influence of inundation and suspended-sediment concentrations on spatiotemporal sedimentation patterns in a tidal freshwater marsh', *Wetlands*, 39(3), pp. 507–520.

Pan, Y. (2011) 'A large and persistent carbon sink in the world's forests', *Science*, 333, pp. 988–993.

Pennings, S. and Callaway, R. (1992) 'Salt marsh plant zonation: the relative importance of competition and physical factors', *Ecology*, 73, pp. 681–690. Available at: https://doi.org/10.2307/1940774.

Peteet, D.M. *et al.* (2018) 'Sediment starvation destroys New York City marshes' resistance to sea level rise', *Proceedings of the National Academy of Sciences*, 115(41), pp. 10281–10286.

Peters, D.P.C. (2002) 'Plant species dominance at a grassland-shrubland ecotone: an individual-based gap dynamics model of herbaceous and woody species', *Ecol Modell*, 152, pp. 5–32. Available at: https://doi.org/10.1016/S0304-3800(01)00460-4.

Peters, D.P.C. *et al.* (2006) 'Integrating patch and boundary dynamics to understand and predict biotic transitions at multiple scales', *Landsc Ecol*, 21, pp. 19–33. Available at: https://doi.org/10.1007/s10980-005-1063-3.

Phillips, C.L. (2020) 'How Much Will Soil Warm?', *Journal of Geophysical Research: Biogeosciences*, 125(7), p. 2020 005668.

Pockman, W.T. and Small, E.E. (2010) 'The influence of spatial patterns of soil moisture on the grass and shrub responses to a summer rainstorm in a Chihuahuan Desert ecotone', *Ecosystems*, 13, pp. 511–525. Available at: https://doi.org/10.1007/s10021-010-9337-2.

Pollehne, F., Klein, B. and Zeitzschel, B. (1993) 'Low light adaptation and export production in the deep chlorophyll maximum layer in the northern Indian Ocean'. Available at: https://doi.org/10.1016/0967-0645(93)90055-R.

Pontee, N. (2013) 'Defining coastal squeeze: A discussion', *Ocean & coastal management*, 84, pp. 204–207.

Porensky, L.M. *et al.* (2016) 'Thresholds and gradients in a semi-arid grassland: long-term grazing treatments induce slow, continuous and reversible vegetation change', *J Appl Ecol*, 53, pp. 1013–1022. Available at: https://doi.org/10.1111/1365-2664.12630.

Prentice, C. *et al.* (2020) 'A Synthesis of Blue Carbon Stocks, Sources, and Accumulation Rates in Eelgrass (Zostera marina) Meadows in the Northeast Pacific', *Global Biogeochemical Cycles*, 34(2), p. e2019GB006345. Available at: https://doi.org/10.1029/2019GB006345.

Raposa, K.B. *et al.* (2016) 'Assessing tidal marsh resilience to sea-level rise at broad geographic scales with multi-metric indices', *Biological Conservation*, 204, pp. 263–275. Available at: https://doi.org/10.1016/j.biocon.2016.10.015.

Ratajczak, Z. *et al.* (2014) 'Fire dynamics distinguish grasslands, shrublands and woodlands as alternative attractors in the Central Great Plains of North America', *J Ecol*, 102, pp. 1374–1385. Available at: https://doi.org/10.1111/1365-2745.12311.

Reed, D.J. (1995) 'The response of coastal marshes to sea-level rise: Survival or submergence?', *Earth Surface Processes and Landforms*, 20(1), pp. 39–48. Available at: https://doi.org/10.1002/esp.3290200105.

Reinl, K.L., Sterner, R.W. and Austin, J.A. (2020) 'Seasonality and physical drivers of deep chlorophyll layers in Lake Superior, with implications for a rapidly warming lake', *J Great Lakes Res*, 46, pp. 1615–1624. Available at: https://doi.org/10.1016/j.jglr.2020.09.008.

Rhoades, J.D. (1992) 'Instrumental field methods of salinity appraisal. Advances in measurement of soil physical properties', *Bringing theory into practice*, 30, pp. 231–248.

Ribalet, F. *et al.* (2010) 'Unveiling a phytoplankton hotspot at a narrow boundary between coastal and offshore waters', *Proc Natl Acad Sci*, 107, pp. 16571–16576. Available at: https://doi.org/10.1073/pnas.1005638107.

Rietl, A.J. *et al.* (2021) 'Vegetation Type and Decomposition Priming Mediate Brackish Marsh Carbon Accumulation Under Interacting Facets of Global Change', *Geophysical Research Letters*, 48(8), p. e2020GL092051. Available at: https://doi.org/10.1029/2020GL092051.

Risser, P.G. (1995) 'The status of the science examining ecotones: a dynamic aspect of landscape is the area of steep gradients between more homogeneous vegetation associations', *BioScience*, 45, pp. 318–325. Available at: https://doi.org/10.2307/1312492.

Rogers, K. *et al.* (2019) 'Wetland carbon storage controlled by millennial-scale variation in relative sea-level rise', *Nature*, 567(7746), pp. 91–95. Available at: https://doi.org/10.1038/s41586-019-0951-7.

Rogers, K., Wilton, K.M. and Saintilan, N. (2006) 'Vegetation change and surface elevation dynamics in estuarine wetlands of southeast Australia', *Estuarine, Coastal and Shelf Science*, 66(3–4), pp. 559–569.

Roux, P.W. (1966) 'The effects of seasonal rainfall and grazing on mixed Karoo veld', *Afr J Range Forage Sci*, 1, pp. 103–110.

Rutherford, M.C., Powrie, L.W. and Husted, L.B. (2012) 'Plant diversity consequences of a herbivore-driven biome switch from Grassland to shrub steppe in South Africa', *Appl Veg Sci*, 15, pp. 14–25. Available at: https://doi.org/10.1111/j.1654-109X.2011.01160.x.

Safak, I. *et al.* (2015) 'Controls on residence time and exchange in a system of shallow coastal bays', *Continental Shelf Research*, 97, pp. 7–20.

Saintilan, N. *et al.* (2014) 'Mangrove expansion and salt marsh decline at mangrove poleward limits', *Global Change Biology*, 20(1), pp. 147–157. Available at: https://doi.org/10.1111/gcb.12341.

Saintilan, N. *et al.* (2020) 'Thresholds of mangrove survival under rapid sea level rise', *Science*, 368(6495), pp. 1118–1121. Available at: https://doi.org/10.1126/science.aba2656.

Saintilan, N. *et al.* (2022) 'Constraints on the adjustment of tidal marshes to accelerating sea level rise', *Science*, 377(6605), pp. 523–527. Available at: https://doi.org/10.1126/science.abo7872.

Sallenger, A.H., Doran, K.S. and Howd, P.A. (2012) 'Hotspot of accelerated sea-level rise on the Atlantic coast of North America', *Nature Climate Change*, 2(12), pp. 884–888.

Sanchez, B. and Parmenter, R. (2002) 'Patterns of shrub-dwelling arthropod diversity across a desert shrubland-grassland ecotone: a test of island biogeographic theory', *J Arid Environ*, 50, pp. 247–265. Available at: https://doi.org/10.1006/jare.2001.0920.

Sanchez-Cabeza, J.A. and Ruiz-Fernandez, A.C. (2012) 'Pb-210 sediment radiochronology: an integrated formulation and classification of dating models', *Geochim. Cosmochim. Acta*, 82, pp. 183–200.

Santelmann, M.V. *et al.* (2019) 'Relationships between salt marsh vegetation and surface elevation in Coos Bay Estuary, Oregon', *Northwest Sci*, 93, pp. 137–154. Available at: https://doi.org/10.3955/046.093.0205.

Scheffer, M. *et al.* (2001) 'Catastrophic shifts in ecosystems', *Nature*, 413(6856), pp. 591–596. Available at: https://doi.org/10.1038/35098000.

Schepers, L., Brennand, P., *et al.* (2020) 'Coastal Marsh Degradation Into Ponds Induces Irreversible Elevation Loss Relative to Sea Level in a Microtidal System', *Geophysical Research Letters*, 47(18), p. e2020GL089121. Available at: https://doi.org/10.1029/2020GL089121.

Schepers, L., Kirwan, M.L., *et al.* (2020) 'Evaluating indicators of marsh vulnerability to sea level rise along a historical marsh loss gradient', *Earth Surface Processes and Landforms*, 45(9), pp. 2107–2117. Available at: https://doi.org/10.1002/esp.4869.

Schieder, N.W. and Kirwan, M.L. (2019) 'Sea-level driven acceleration in coastal forest retreat', *Geology*, 47, pp. 1151–1155.

Schieder, N.W., Walters, D.C. and Kirwan, M.L. (2018) 'Massive Upland to Wetland Conversion Compensated for Historical Marsh Loss in Chesapeake Bay, USA', *Estuaries and Coasts*, 41(4), pp. 940–951. Available at: https://doi.org/10.1007/s12237-017-0336-9.

Schooley, R.L., Bestelmeyer, B.T. and Campanella, A. (2018) 'Shrub encroachment, productivity pulses, and core-transient dynamics of Chihuahuan Desert rodents', *Ecosphere*, 9:e02330. Available at: https://doi.org/10.1002/ecs2.2330.

Schulze, E.-D. and Mooney, H.A. (2012) *Biodiversity and Ecosystem Function*. Springer Science & Business Media.

Seneca, E.D. and Blum, U. (1984) 'Response to photoperiod and temperature by Spartina alterniflora (Poaceae) from North Carolina and Spartina foliosa from California', *American journal of botany*, 71(1), pp. 91–99.

Senft, A.R. (2009) 'Species diversity patterns at ecotones'. Available at: https://doi.org/10.17615/20k5-yb32.

Shepard, C.C., Crain, C.M. and Beck, M.W. (2011) 'The protective role of coastal marshes: a systematic review and meta-analysis', *PloS one*, 6(11), p. 27374.

Shiponeni, N. *et al.* (2011) 'Competitive interactions between grass and succulent shrubs at the ecotone between an arid grassland and succulent shrubland in the Karoo', *Plant Ecol*, 212, pp. 795–808. Available at: https://doi.org/10.1007/s11258-010-9864-0.

Siikamäki, J. *et al.* (2013) 'Blue carbon: coastal ecosystems, their carbon storage, and potential for reducing emissions', *Environment: Science and Policy for Sustainable Development*, 55(6), pp. 14–29.

Sirin, A.A. *et al.* (2020) 'Depth of peat burning and carbon loss during an underground forest fire', *Contemporary Problems of Ecology*, 13(7), pp. 769–779.

Smart, L.S. *et al.* (2020) 'Aboveground carbon loss associated with the spread of ghost forests as sea levels rise', *Environmental Research Letters*, 15(10), p. 104028. Available at: https://doi.org/10.1088/1748-9326/aba136.

Smart, L.S. *et al.* (2021) 'Quantifying Drivers of Coastal Forest Carbon Decline Highlights Opportunities for Targeted Human Interventions', *Land*, 10(7), p. 752.

Smith, A.J. *et al.* (2022) 'Temperature optimum for marsh resilience and carbon accumulation revealed in a whole-ecosystem warming experiment', *Global Change Biology*, 28(10), pp. 3236–3245. Available at: https://doi.org/10.1111/gcb.16149.

Smith, A.J. and Goetz, E.M. (2021) 'Climate change drives increased directional movement of landscape ecotones', *Landscape Ecology*, 36(11), pp. 3105–3116. Available at: https://doi.org/10.1007/s10980-021-01314-7.

Smith, A.J. and Kirwan, M.L. (2021) 'Sea Level-Driven Marsh Migration Results in Rapid Net Loss of Carbon', *Geophysical Research Letters*, 48(13), p. e2021GL092420. Available at: https://doi.org/10.1029/2021GL092420.

Smith, J.A. (2013) 'The role of phragmites australis in mediating inland salt marsh migration in a mid-Atlantic estuary', *PLoS ONE*, 8, e65091.

Smith, T.B. *et al.* (1997) 'A role for ecotones in generating rainforest biodiversity', *Science*, 276, pp. 1855–1857. Available at: https://doi.org/10.1126/science.276.5320.1855.

Smithwick, E.A.H. *et al.* (2009) 'Modeling the effects of fire and climate change on carbon and nitrogen storage in lodgepole pine (Pinus contorta) stands', *Global Change Biology*, 15(3), pp. 535–548.

Stagg, C.L. (2016) 'Processes contributing to resilience of coastal wetlands to sea-level rise', *Ecosystems*, 19, pp. 1445–1459.

Steinmuller, H.E. *et al.* (2022) 'Comparing Vertical Change in Riverine, Bayside, and Barrier Island Wetland Soils in Response to Acute and Chronic Disturbance in Apalachicola Bay, FL', *Estuaries and Coasts* [Preprint]. Available at: https://doi.org/10.1007/s12237-022-01131-4.

Stevenson, J.C., Kearney, M.S. and Pendleton, E.C. (1985) 'Sedimentation and erosion in a Chesapeake Bay brackish marsh system', *Marine Geology*, 67(3), pp. 213–235. Available at: https://doi.org/10.1016/0025-3227(85)90093-3.

Stribling, J.M., Cornwell, J.C. and Glahn, O.A. (2007) 'Microtopography in tidal marshes: Ecosystem engineering by vegetation?', *Estuaries and Coasts*, 30(6), pp. 1007–1015. Available at: https://doi.org/10.1007/BF02841391.

Sturchio, M.A. *et al.* (2021) *Temperature acclimation of leaf respiration differs between marsh and mangrove vegetation in a coastal wetland ecotone*. Global Change Biology.

Taylor, L. *et al.* (2020) 'Mapping sea level rise impacts to identify climate change adaptation opportunities in the Chesapeake and Delaware Bays, USA', *Wetlands Ecology and Management*, 28, pp. 527–541.

Temmerman, S. *et al.* (2003) 'Modelling long-term tidal marsh growth under changing tidal conditions and suspended sediment concentrations', *Scheldt estuary, Belgium. Marine Geology*, 193(1–2), pp. 151–169.

Temmerman, S. *et al.* (2013) 'Ecosystem-based coastal defence in the face of global change', *Nature*, 504(7478), pp. 79–83. Available at: https://doi.org/10.1038/nature12859.

Ter-Mikaelian, M.T. and Korzukhin, M.D. (1997) 'Biomass equations for sixty-five North American tree species', *Forest Ecology and Management*, 97(1), pp. 1–24.

Theuerkauf, E.J. and Rodriguez, A.B. (2017) 'Placing barrier-island transgression in a blue-carbon context', *Earth's Future*, 5(7), pp. 789–810.

Thomas, C.R. (2004) *Salt marsh biogeochemistry and sediment organic matter accumulation*. (Doctoral dissertation,. University of Virginia.

Torio, D.D. and Chmura, G.L. (2013) 'Assessing coastal squeeze of tidal wetlands', *Journal of Coastal Research*, 29(5), pp. 1049–1061.

Törnqvist, T.E. *et al.* (2021) 'Coastal Wetland Resilience, Accelerated Sea-Level Rise, and the Importance of Timescale', *AGU Advances*, 2(1), p. e2020AV000334. Available at: https://doi.org/10.1029/2020AV000334.

Traut, B. (2005) 'The role of coastal ecotones: a case study of the salt marsh/upland transition zone in California', *J Ecol*, 93, pp. 279–290. Available at: https://doi.org/10.1111/j.1365-2745.2005.00969.x.

Trevathan-Tackett, S.M. *et al.* (2018) 'Effects of small-scale, shading-induced seagrass loss on blue carbon storage: Implications for management of degraded seagrass ecosystems', *Journal of applied ecology*, 55(3), pp. 1351–1359.

Turner, M.G. (2010) ‘Disturbance and landscape dynamics in a changing world’, *Ecology*, 91(10), pp. 2833–2849.

Van de Broek, M. *et al.* (2018) ‘Long-term organic carbon sequestration in tidal marsh sediments is dominated by old-aged allochthonous inputs in a macrotidal estuary’, *Global Change Biology*, 24(6), pp. 2498–2512. Available at: https://doi.org/10.1111/gcb.14089.

Veldkornet, D.A., Adams, J.B. and Potts, A.J. (2015) ‘Where do you draw the line? Determining the transition thresholds between estuarine salt marshes and terrestrial vegetation’, *S Afr J Bot*, 101, pp. 153–159. Available at: https://doi.org/10.1016/j.sajb.2015.05.003.

Veraart, A.J. *et al.* (2012) ‘Recovery rates reflect distance to a tipping point in a living system’, *Nature*, 481(7381), pp. 357–359.

Vetter, S. (2009) ‘Drought, change and resilience in South Africa’s arid and semi-arid rangelands’, *S Afr J Sci*, 105, pp. 29–33. Available at: https://doi.org/10.4102/sajs.v105i1/2.35.

Vu, H.D. and Pennings, S.C. (2021) ‘Directional movement of consumer fronts associated with creek heads in salt marshes’, *Ecology*, 102(9), p. e03447. Available at: https://doi.org/10.1002/ecy.3447.

Wang, C. *et al.* (2021) ‘Different coastal marsh sites reflect similar topographic conditions under which bare patches and vegetation recovery occur’, *Earth Surface Dynamics*, 9(1), pp. 71–88. Available at: https://doi.org/10.5194/esurf-9-71-2021.

Wang, C. and Temmerman, S. (2013) ‘Does biogeomorphic feedback lead to abrupt shifts between alternative landscape states?: An empirical study on intertidal flats and marshes’, *Journal of Geophysical Research: Earth Surface*, 118(1), pp. 229–240. Available at: https://doi.org/10.1029/2012JF002474.

Wang, F. *et al.* (2019) ‘Tidal wetland resilience to sea level rise increases their carbon sequestration capacity in United States’, *Nature Communications*, 10(1), p. 5434. Available at: https://doi.org/10.1038/s41467-019-13294-z.

Wang, H. *et al.* (2020) ‘Acclimation of leaf respiration consistent with optimal photosynthetic capacity’, *Global Change Biology*, 26(4), pp. 2573–2583.

Ward, M.A. *et al.* (2021) ‘Blue carbon stocks and exchanges along the California coast’, *Biogeosciences*, 18(16), pp. 4717–4732. Available at: https://doi.org/10.5194/bg-18-4717-2021.

Ward, N.D. (2020) ‘Representing the function and sensitivity of coastal interfaces in Earth system models’, *Nature Communications*, 11(1), pp. 1–14.

Wasson, K. *et al.* (2019) ‘Understanding tidal marsh trajectories: evaluation of multiple indicators of marsh persistence’, *Environmental Research Letters*, 14(12), p. 124073. Available at: https://doi.org/10.1088/1748-9326/ab5a94.

Wasson, K., Woolfolk, A. and Fresquez, C. (2013) ‘Ecotones as indicators of changing environmental conditions: rapid migration of salt marsh-upland boundaries’, *Estuaries Coast*, 36, pp. 654–664. Available at: https://doi.org/10.1007/s12237-013-9601-8.

Watson, E.B. *et al.* (2017) 'Wetland Loss Patterns and Inundation-Productivity Relationships Prognosticate Widespread Salt Marsh Loss for Southern New England', *Estuaries and Coasts*, 40(3), pp. 662–681. Available at: https://doi.org/10.1007/s12237-016-0069-1.

Webb, E.L. *et al.* (2013) 'A global standard for monitoring coastal wetland vulnerability to accelerated sea-level rise', *Nature Climate Change*, 3(5), pp. 458–465. Available at: https://doi.org/10.1038/nclimate1756.

Werner, K.J. and Zedler, J.B. (2002) 'How sedge meadow soils, microtopography, and vegetation respond to Sedimentation', *Wetlands*, 22(3), pp. 451–466. Available at: https://doi.org/10.1672/0277-5212(2002)022[0451:HSMSMA]2.0.CO;2.

Więski, K. and Pennings, S. (2014) 'Latitudinal variation in resistance and tolerance to herbivory of a salt marsh shrub', *Ecography*, 37(8), pp. 763–769.

van Wijnen, H.J. and Bakker, J.P. (2001) 'Long-term Surface Elevation Change in Salt Marshes: a Prediction of Marsh Response to Future Sea-Level Rise', *Estuarine, Coastal and Shelf Science*, 52(3), pp. 381–390. Available at: https://doi.org/10.1006/ecss.2000.0744.

Williams, K., M., M. and Sternberg, L.D.S.L. (2003) 'Interactions of storm, drought, and sea-level rise on coastal forest: a case study', *Journal of Coastal Research*, 19, pp. 1116–1121.

Wilson, B.J. (2018) 'Salinity pulses interact with seasonal dry-down to increase ecosystem carbon loss in marshes of the Florida Everglades', *Ecological Applications*, 28, pp. 2092–2108.

Wilson, J.B. and Agnew, A.D.Q. (1992) 'Positive-feedback Switches in Plant Communities', in M. Begon and A.H. Fitter (eds) *Advances in Ecological Research*. Academic Press, pp. 263–336. Available at: https://doi.org/10.1016/S0065-2504(08)60149-X.

Woods, N.N., Tuley, P.A. and Zinnert, J.C. (2021) 'Long-term community dynamics reveal different trajectories on two mid-Atlantic coast maritime forests', *Forests*, 12, p. 1063.

Yando, E.S. *et al.* (2016) 'Salt marsh-mangrove ecotones: using structural gradients to investigate the effects of woody plant encroachment on plant–soil interactions and ecosystem carbon pools', *Journal of Ecology*, 104(4), pp. 1020–1031. Available at: https://doi.org/10.1111/1365-2745.12571.

Yeates, A.G. *et al.* (2020) 'Hurricane Sandy Effects on Coastal Marsh Elevation Change', *Estuaries and Coasts*, 43(7), pp. 1640–1657. Available at: https://doi.org/10.1007/s12237-020-00758-5.

Yvon-Durocher, G. *et al.* (2011) 'Warming alters the size spectrum and shifts the distribution of biomass in freshwater ecosystems', *Glob Chang Biol*, 17, pp. 1681–1694. Available at: https://doi.org/10.1111/j.1365-2486.2010.02321.x.

Zhang, C. *et al.* (2012) 'Impacts of urbanization on carbon balance in terrestrial ecosystems of the Southern United States', *Environmental Pollution*, 164, pp. 89–101.

Zhong, Q. *et al.* (2019) 'Responses of wetland soil carbon and nutrient pools and microbial activities after 7 years of experimental warming in the Yangtze Estuary', *Ecological Engineering*, 136, pp. 68–78.

Zinnert, J.C. *et al.* (2016) 'Spatio-temporal dynamics in barrier island upland vegetation: the overlooked coastal landscape', *Ecosystems*, 19, pp. 685–697.

Zinnert, J.C. *et al.* (2019) 'Connectivity in coastal systems: barrier island vegetation influences upland migration in a changing climate', *Global Change Biology*, 25, pp. 2419–2430.